# LECTURE 3 - Artificial Gauge Fields

**SSH model** - the simplest Topological Insulator

**Probing the Zak Phase in the SSH model**
- Bulk-Edge correspondence in 1d -

**'Aharonov Bohm' Interferometry for Measuring Band Geometry**

- Berry connection/Berry curvature
- pi-flux Singularity in Graphene
- Stückelberg Interferometry

(non-Abelian Berry connection, Wilson loops)

**Realizing Staggered Flux, Hofstadter & QSH Hamiltonian**

**Hall Response and Chern Number in Hofstadter Bands**

# Measuring the Zak-Berry's Phase of Topological Bands

M. Atala et al., Nature Physics (2013)

# Berry Phase in Quantum Mechanics

$$\Psi(R) \rightarrow e^{i(\varphi_{\text{Berry}}+\varphi_{\text{dyn}})}\ \Psi(R)$$

*Adiabatic evolution through closed loop*

$$\varphi_{\text{Berry}} = \oint_{\mathcal{C}} A_n(R) dR = i \oint_{\mathcal{C}} \langle n(R)|\nabla_R|n(R)\rangle\, dR$$

$$\varphi_{\text{Berry}} = \oint_{\mathcal{A}} \Omega_n(R)\, dA$$

**Berry Phase**

M.V. Berry, Proc. R. Soc. A (1984)

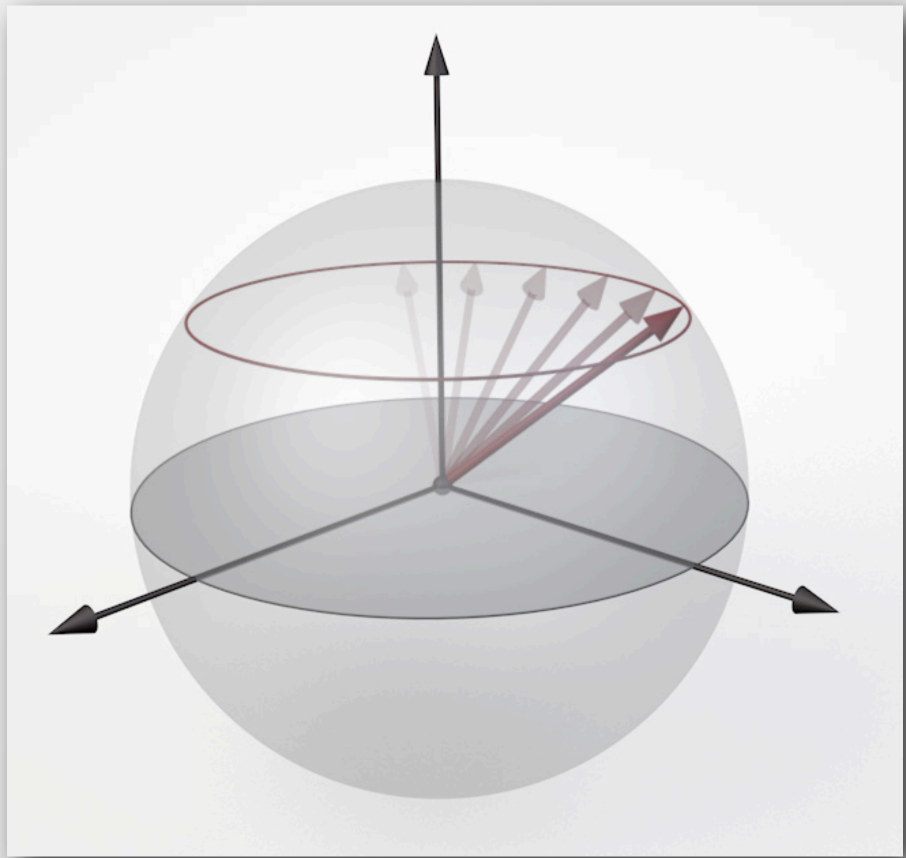

***Example:*** Spin-1/2 particle in magnetic field

**Berry connection**

$$A_n(R) = i\langle n(R)|\nabla_R|n(R)\rangle$$

**Berry curvature**

$$\Omega_{n,\mu\nu}(R) = \frac{\partial}{\partial R^\mu} A_{n,\nu} - \frac{\partial}{\partial R^\nu} A_{n,\mu}$$

# Berry Phase for Periodic Potentials

$$\Psi_k(\mathbf{r}) = e^{i\mathbf{k}\mathbf{r}} u_k(\mathbf{r})$$ Bloch wave in periodic potential

Adiabatic motion in momentum space generates Berry phase!

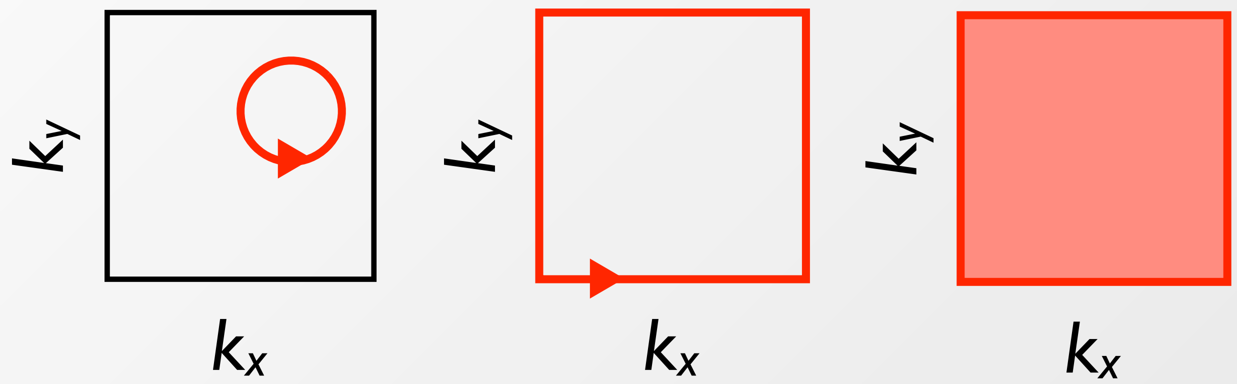


Berry phase is fundamental to characterize topology of energy bands

$$n_{\mathrm{Chern}} = \frac{1}{2\pi}\oint_{BZ} A_k dk = \frac{1}{2\pi}\int_{BZ} \Omega_k \, d^2k \quad \Longleftrightarrow \quad \sigma_{xy} = n_{\mathrm{Chern}}\, e^2/h$$

**Chern Number** (Topological Invariant) **Quantized Hall Conductance**

Thouless, Kohmoto, den Nijs, and Nightingale (TKNN), PRL 1982
Kohmoto Ann. of Phys. 1985

Mention Problem with going on a line is generally **NOT A LOOP IN PARAMETER SPACE!**

# Berry Phase for Periodic Potentials

$$\Psi_k(\mathbf{r}) = e^{i\mathbf{k}\mathbf{r}} u_k(\mathbf{r})$$ Bloch wave in periodic potential

Adiabatic motion in momentum space generates Berry phase!

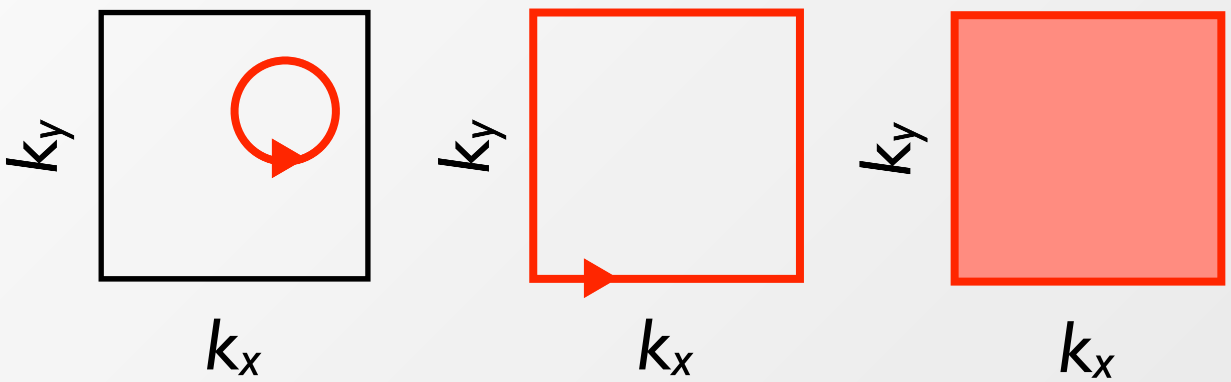


Berry phase is fundamental to characterize topology of energy bands

$$n_{\mathrm{Chern}} = \frac{1}{2\pi}\oint_{BZ} A_k dk = \frac{1}{2\pi}\int_{BZ} \Omega_k \, d^2k \quad \Leftrightarrow \quad \sigma_{xy} = n_{\mathrm{Chern}}\, e^2/h$$

**Chern Number** (Topological Invariant) **Quantized Hall Conductance**

Thouless, Kohmoto, den Nijs, and Nightingale (TKNN), PRL 1982
Kohmoto Ann. of Phys. 1985

What is the extension to 1D?

Mention Problem with going on a line is generally **NOT A LOOP IN PARAMETER SPACE!**

# Zak Phase

2D Brillouin Zone

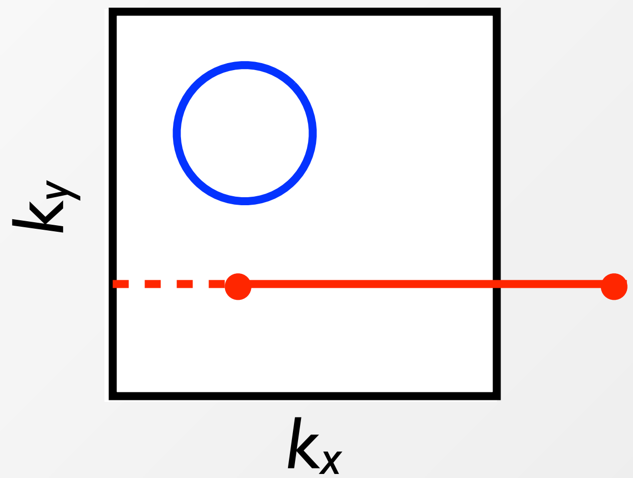


*going straight means going around!*

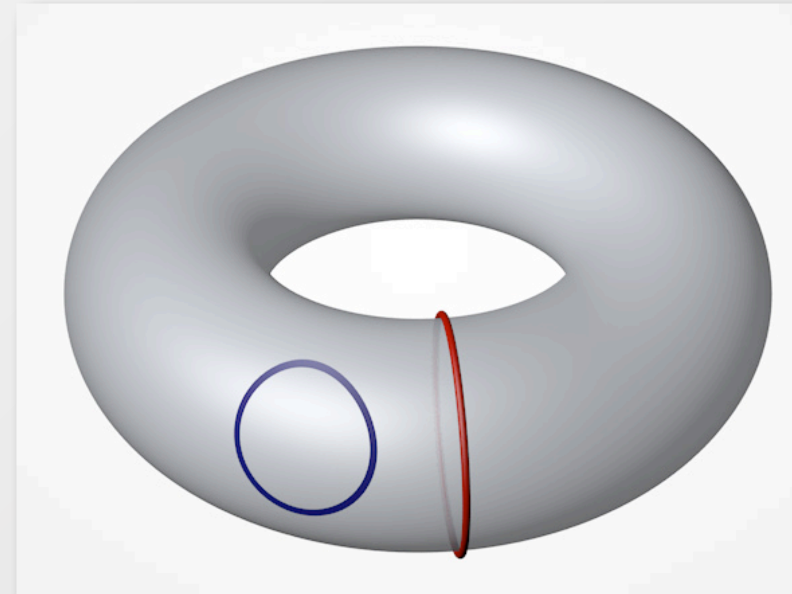

Band structure has torus topology!

# Zak Phase

2D Brillouin Zone

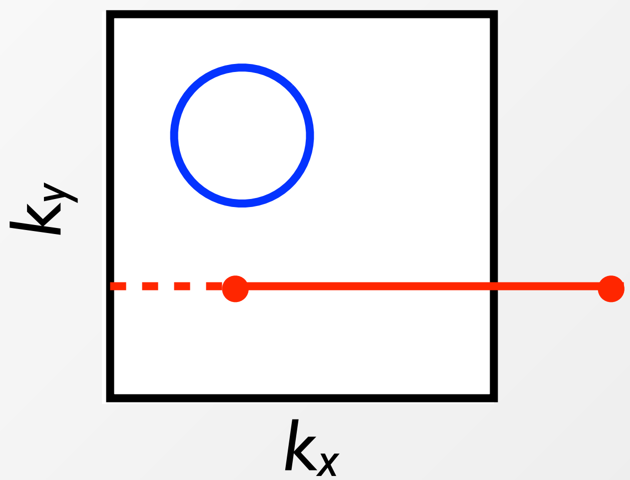


*going straight means going around!*

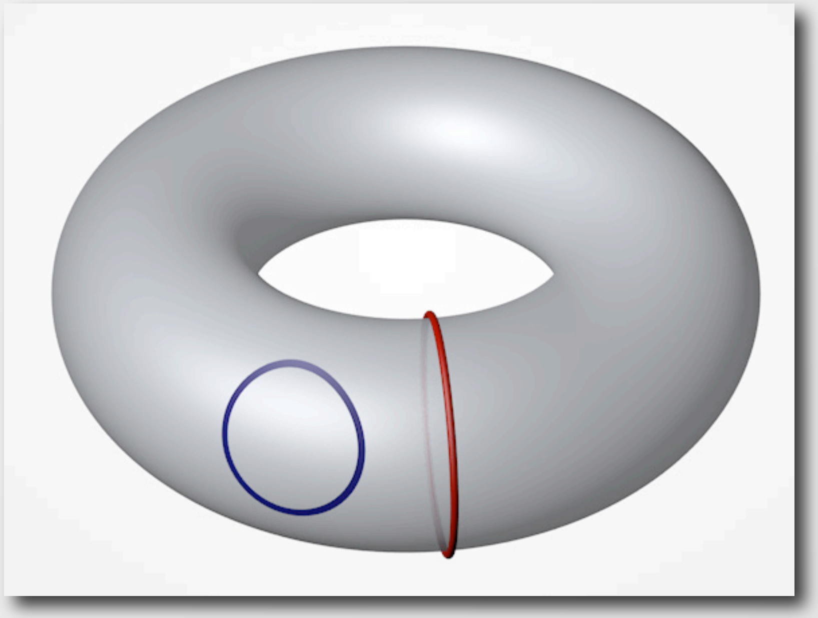

Band structure has torus topology!

$$\varphi_{Zak} = i \int_{k_0}^{k_0+G} \langle u_k | \partial_k | u_k \rangle \; dk$$

***Zak Phase -***
***the 1D Berry Phase***

J. Zak, Phys. Rev. Lett. **62**, 2747 (1989)

# Zak Phase

2D Brillouin Zone

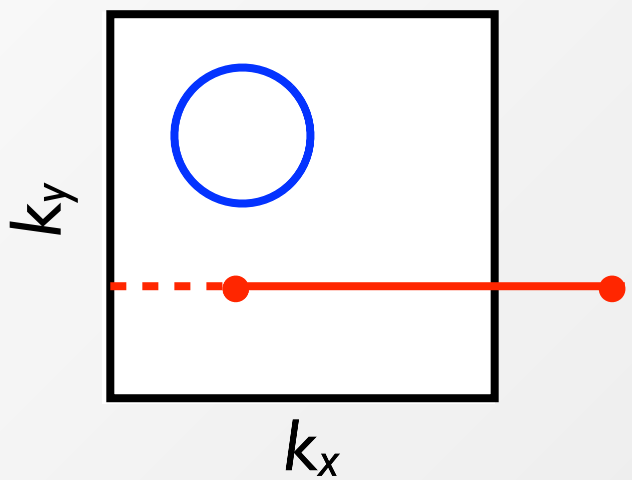


*going straight means going around!*

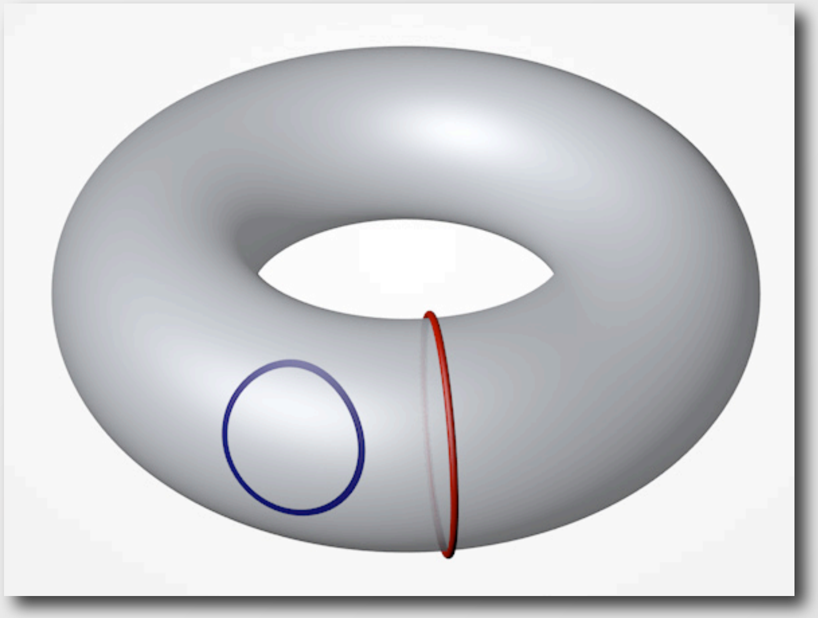

Band structure has torus topology!

$$\varphi_{Zak} = i \int_{k_0}^{k_0+G} \langle u_k | \partial_k | u_k \rangle \; dk$$

***Zak Phase - the 1D Berry Phase***

J. Zak, Phys. Rev. Lett. **62**, 2747 (1989)

Non-trivial Zak phase:

- Topological Band
- Edge States (for finite system)
- Domain walls with fractional quantum numbers
- Polarization of solids

R. Jackiw and C. Rebbi, Phys. Rev. D 13, 3398 (1976)
J. Goldstone and F. Wilczek, Phys. Rev. Lett. 47, 986 (1981)
R. King-Smith and D. Vanderbilt, Phys. Rev. B 46, 1651 (1993)

# Su-Shrieffer-Heeger Model (SSH)

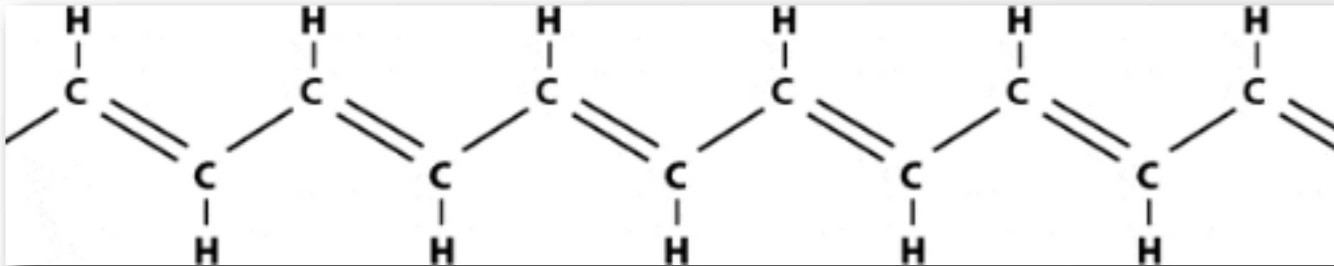

**Polyacetylene**

W. P. Su, J. R. Schrieffer & A. J. Heeger
Phys. Rev. Lett. 42, 1698 (1979).

$$H_{SSH} = -\sum_n \left\{ J \hat{a}_n^\dagger \hat{b}_n + J' \hat{a}_n^\dagger \hat{b}_{n-1} + \text{h.c.} \right\}$$

# Su-Shrieffer-Heeger Model (SSH)

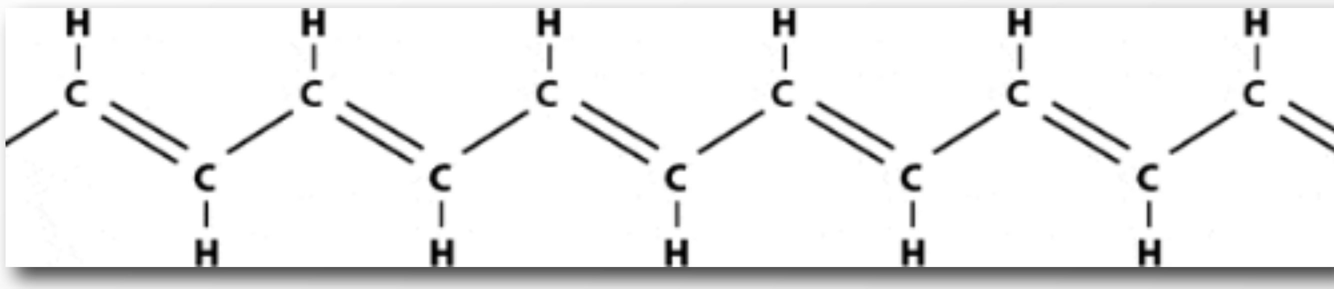


## Polyacetylene

W. P. Su, J. R. Schrieffer & A. J. Heeger
Phys. Rev. Lett. 42, 1698 (1979).

$$H_{SSH} = -\sum_n \left\{ J \hat{a}_n^\dagger \hat{b}_n + J' \hat{a}_n^\dagger \hat{b}_{n-1} + \text{h.c.} \right\}$$

Two topologically distinct phases:

**D1:** $J > J'$

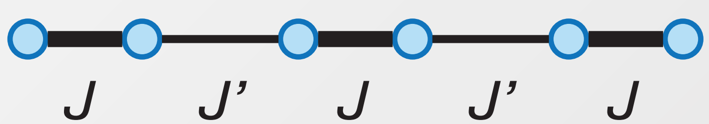


**D2:** $J' > J$

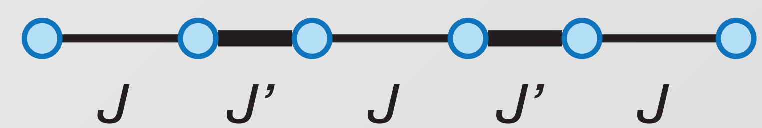

# Su-Shrieffer-Heeger Model (SSH)

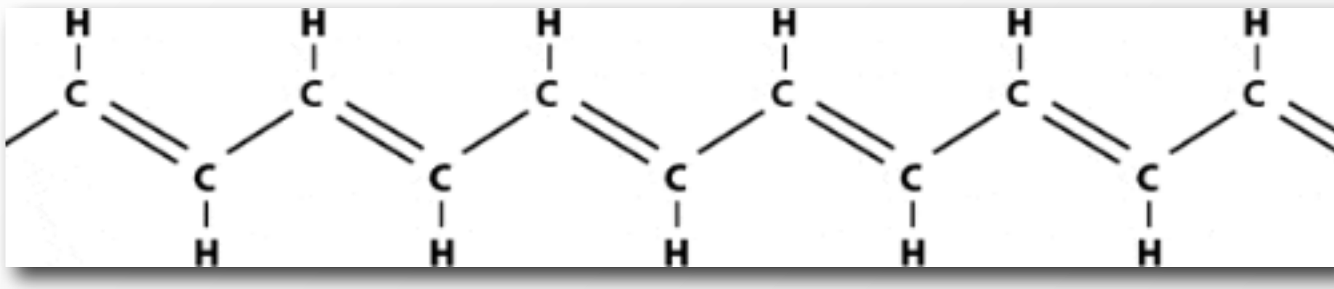


**Polyacetylene**

W. P. Su, J. R. Schrieffer & A. J. Heeger
Phys. Rev. Lett. 42, 1698 (1979).

$$H_{SSH} = -\sum_n \left\{ J \hat{a}_n^\dagger \hat{b}_n + J' \hat{a}_n^\dagger \hat{b}_{n-1} + \text{h.c.} \right\}$$

Two topologically distinct phases:

**D1:** $J > J'$

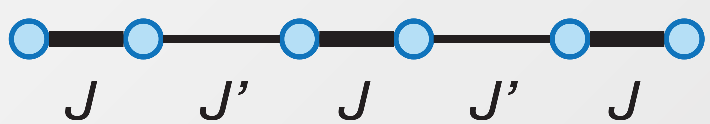


**D2:** $J' > J$

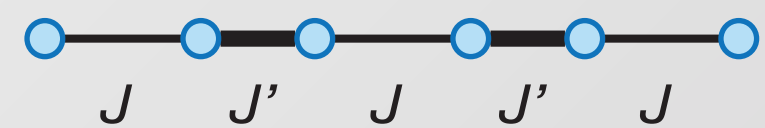


$$\delta\varphi_{Zak} = \varphi_{Zak}^{D1} - \varphi_{Zak}^{D2} = \pi$$

Topological properties:
domain wall features fractionalized excitations

Zak phase difference $\delta\varphi_{Zak}$ is gauge-invariant

# SSH Energy Bands - Eigenstates

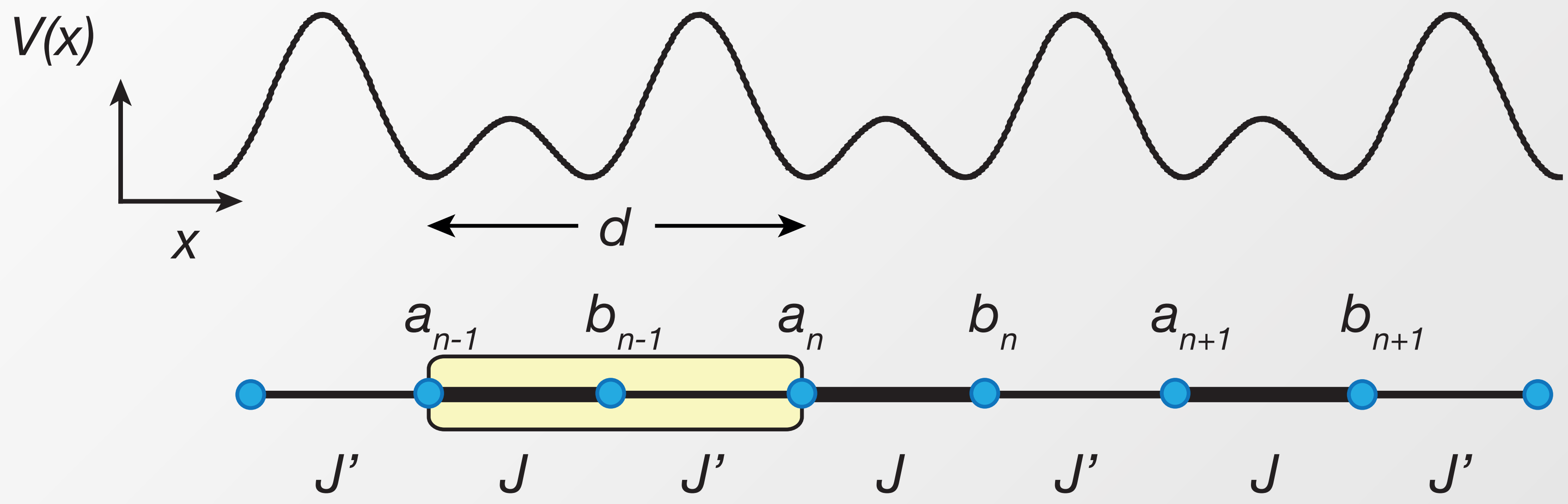

# SSH Energy Bands - Eigenstates

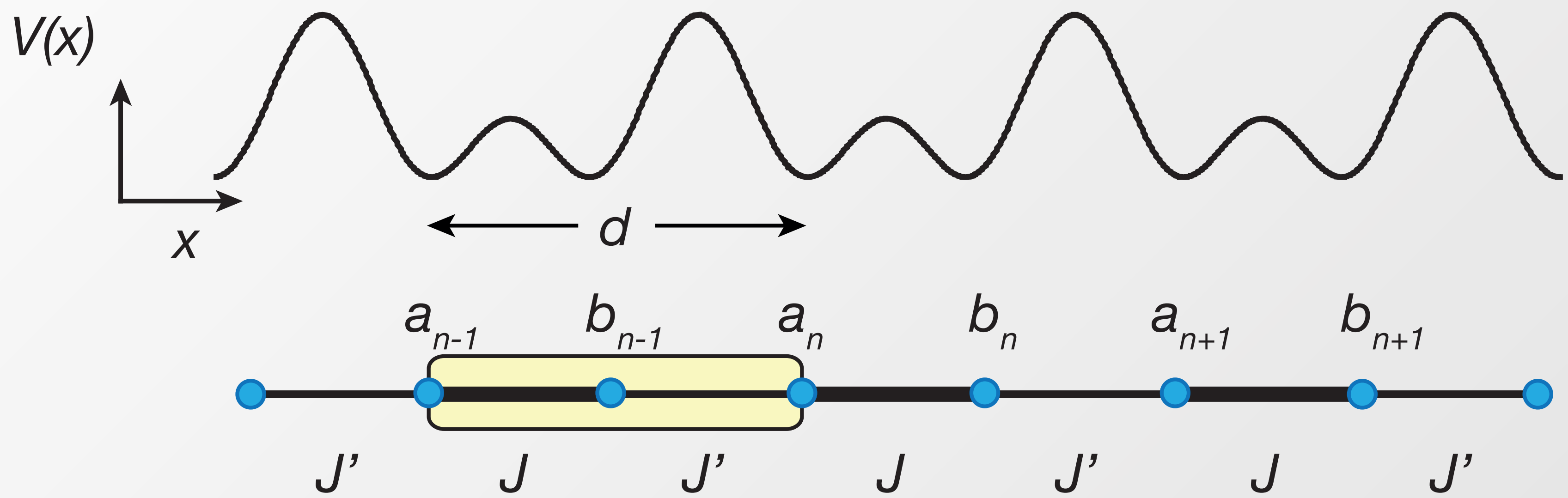


...ABABA... Lattice Structure....

$$\sum_x \Psi_x = \sum_x e^{ikx} \times \begin{cases} \alpha_k \\ \beta_k \; e^{ikd/2} \end{cases}$$

# SSH Energy Bands - Eigenstates

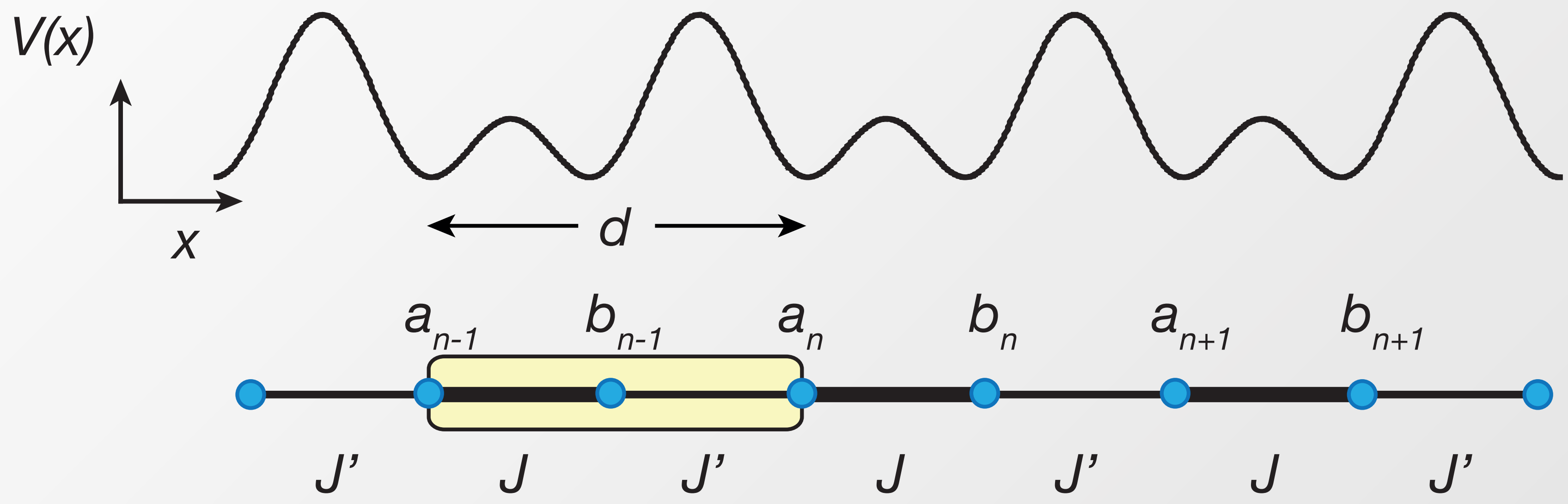


...ABABA... Lattice Structure....

$$\sum_x \Psi_x = \sum_x e^{ikx} \times \begin{cases} \alpha_k \\ \beta_k \; e^{ikd/2} \end{cases}$$

2x2 Hamiltonian:

$$\boxed{\begin{bmatrix} 0 & -\rho_k \\ -\rho_k^* & 0 \end{bmatrix} \begin{pmatrix} \alpha_k \\ \beta_k \end{pmatrix} = \tilde{\epsilon}_k \begin{pmatrix} \alpha_k \\ \beta_k \end{pmatrix}}$$

with $\quad \rho_k = J e^{ikd/2} + J' e^{-ikd/2} = |\epsilon_k| e^{i\theta_k}$

# SSH Energy Bands - Eigenstates

...ABABA... Lattice Structure....

$$\sum_x \Psi_x = \sum_x e^{ikx} \times \begin{cases} \alpha_k \\ \beta_k \; e^{ikd/2} \end{cases}$$

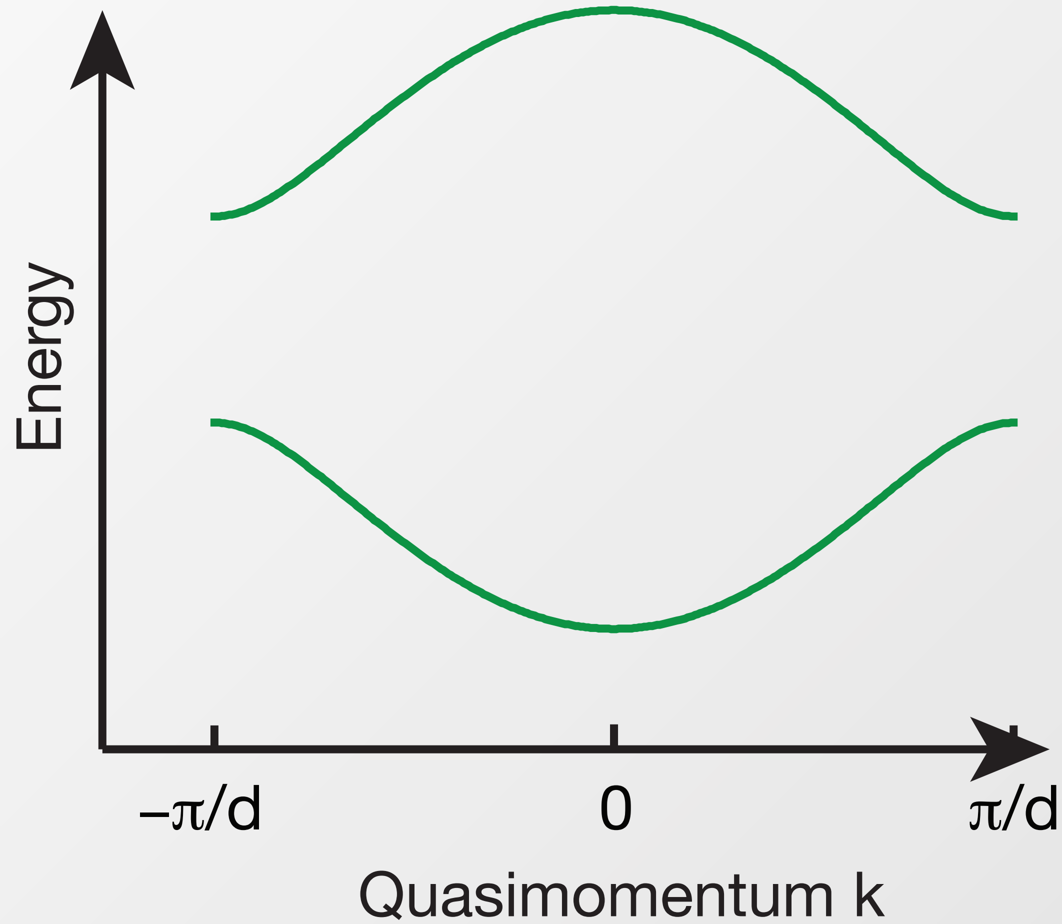


**Eigenstates**

$$\begin{pmatrix} \alpha_{k,\mp} \\ \beta_{k,\mp} \end{pmatrix} = \frac{1}{\sqrt{2}} \begin{pmatrix} \pm 1 \\ e^{-i\theta_k} \end{pmatrix}$$

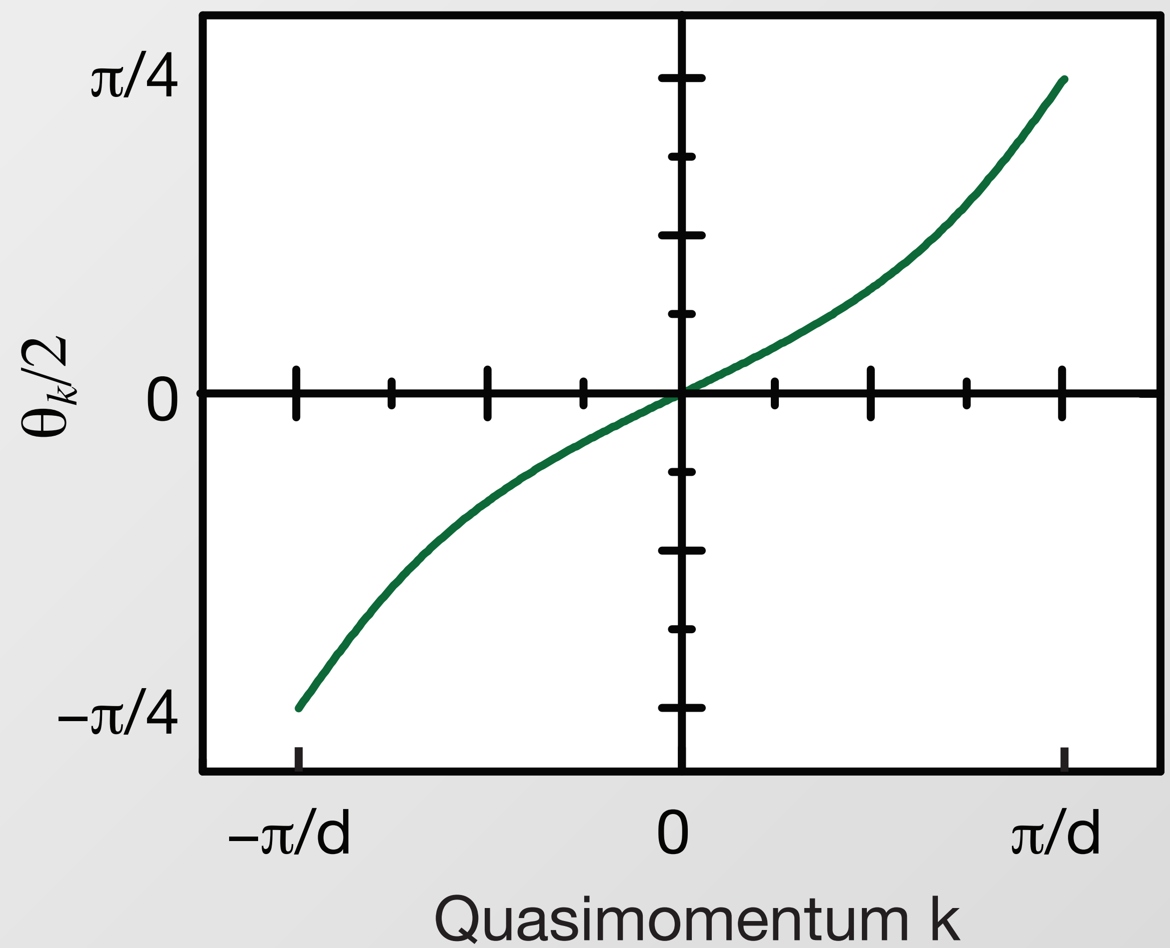

# SSH Energy Bands - Eigenstates

...ABABA... Lattice Structure....

$$\sum_x \Psi_x = \sum_x e^{ikx} \times \begin{cases} \alpha_k \\ \beta_k \; e^{ikd/2} \end{cases}$$

**Eigenstates**

$$\begin{pmatrix} \alpha_{k,\mp} \\ \beta_{k,\mp} \end{pmatrix} = \frac{1}{\sqrt{2}} \begin{pmatrix} \pm 1 \\ e^{-i\theta_k} \end{pmatrix}$$

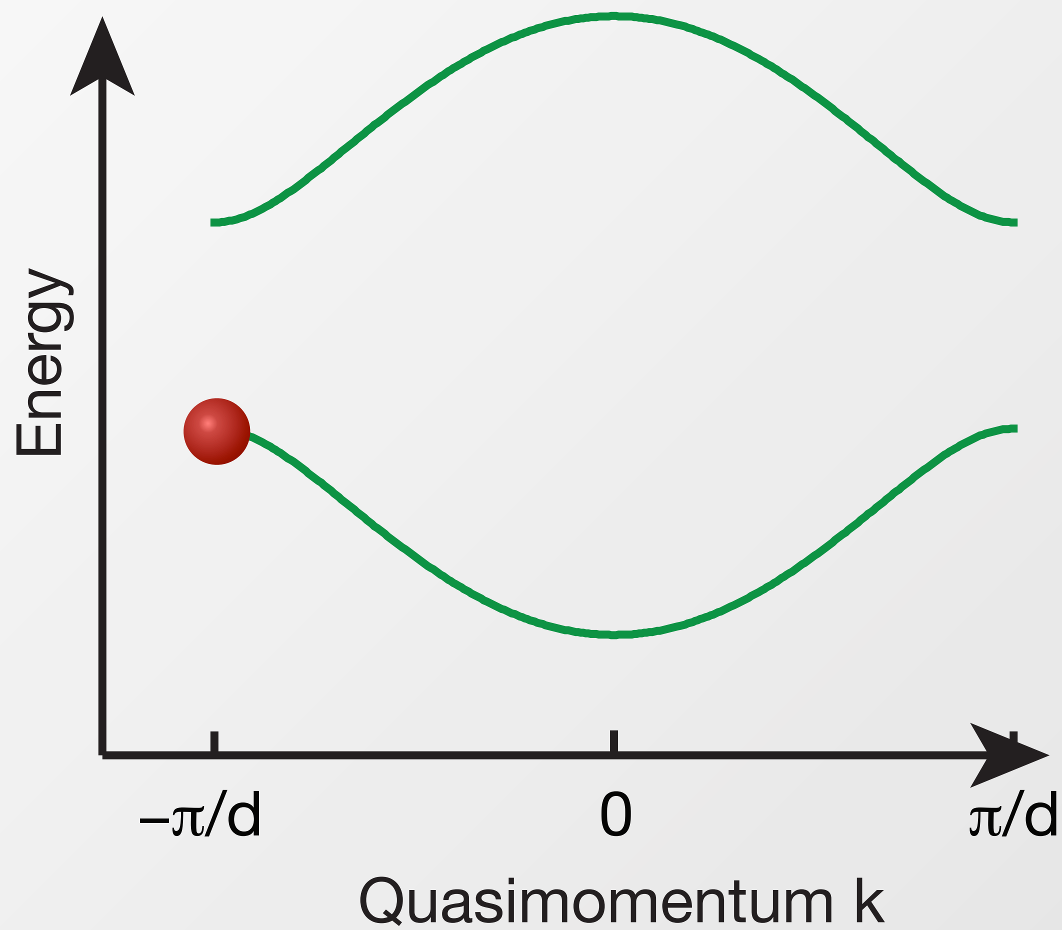


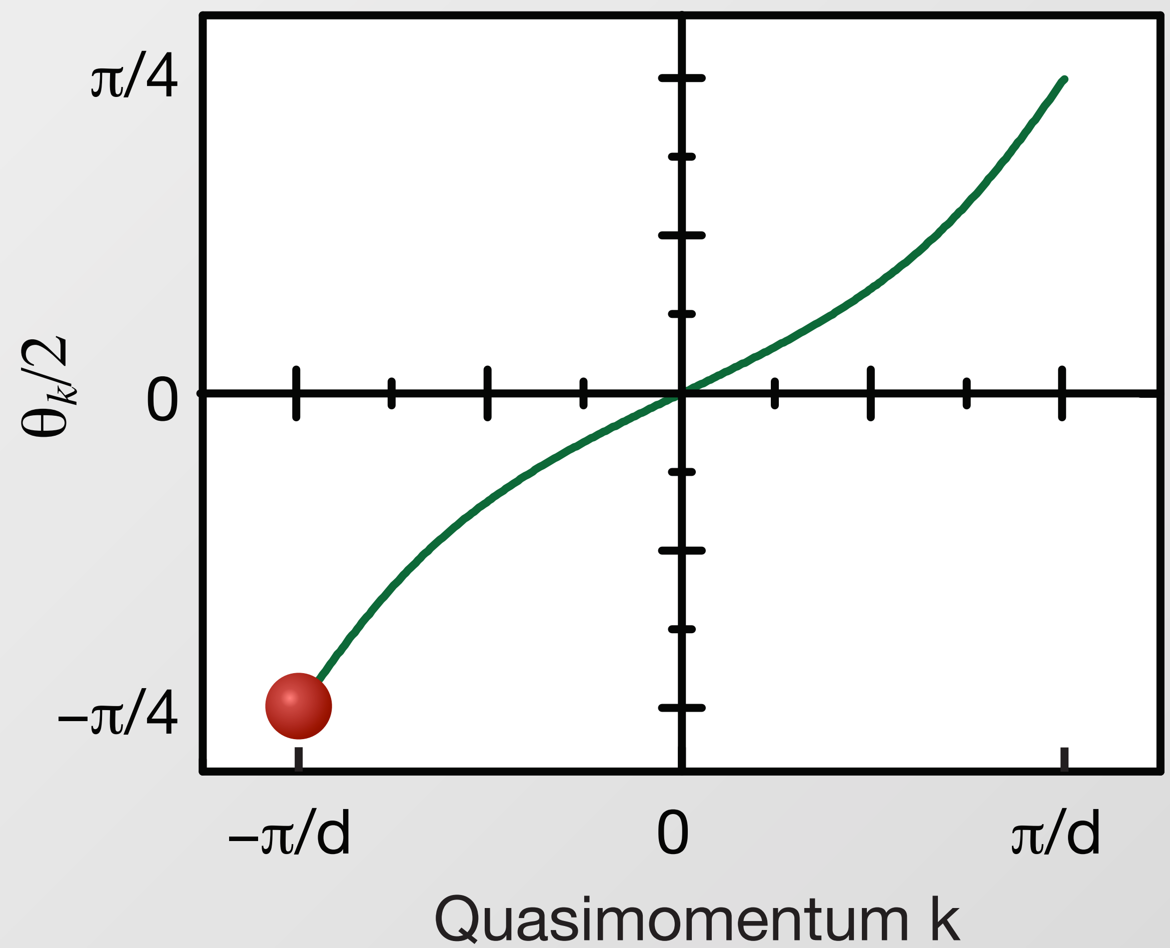


Adiabatic evolution in momentum space

# SSH Energy Bands - Eigenstates

...ABABA... Lattice Structure....

$$\sum_x \Psi_x = \sum_x e^{ikx} \times \begin{cases} \alpha_k \\ \beta_k \; e^{ikd/2} \end{cases}$$

**Eigenstates**

$$\begin{pmatrix} \alpha_{k,\mp} \\ \beta_{k,\mp} \end{pmatrix} = \frac{1}{\sqrt{2}} \begin{pmatrix} \pm 1 \\ e^{-i\theta_k} \end{pmatrix}$$

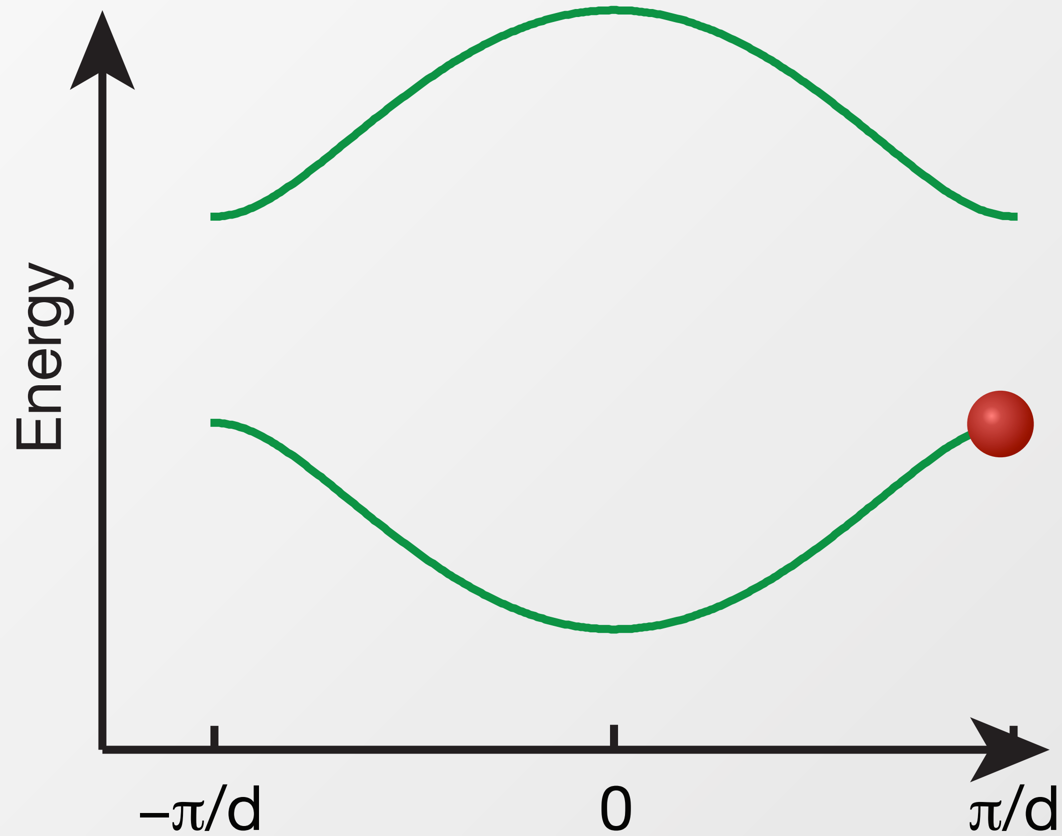


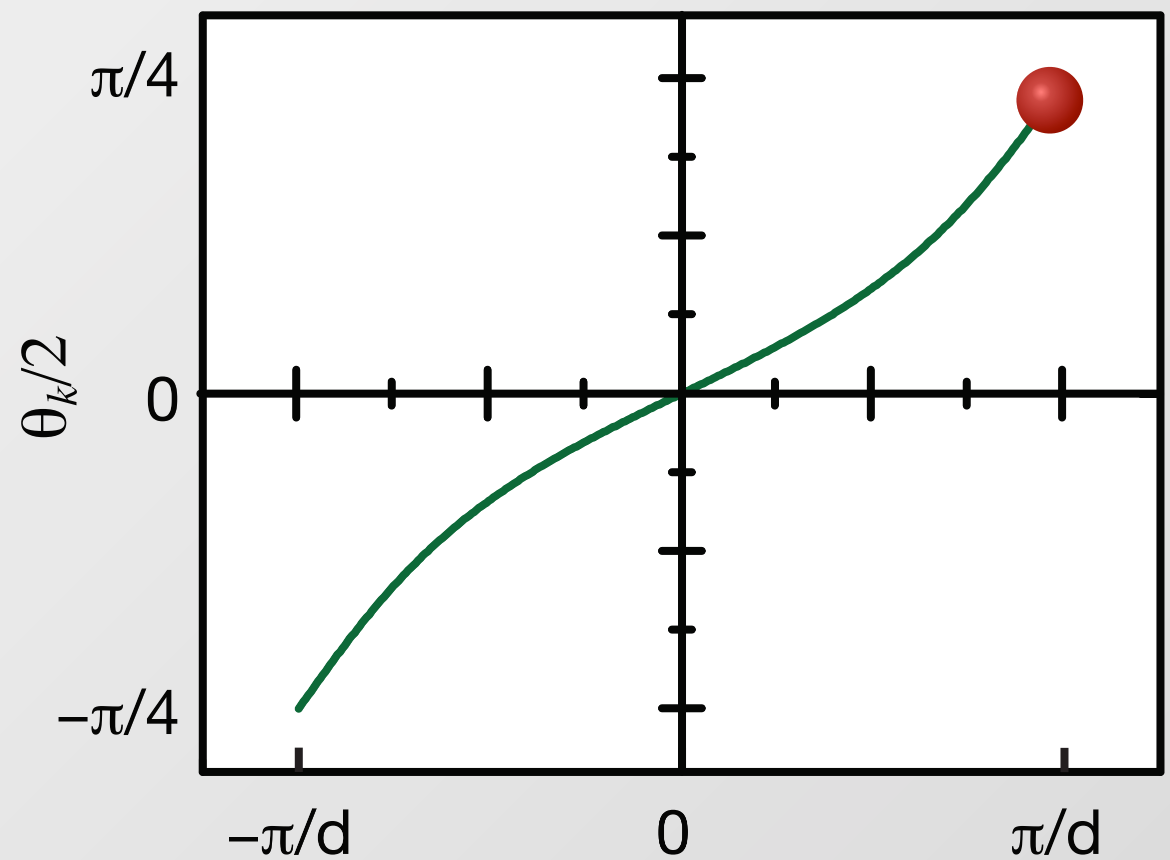


Adiabatic evolution in momentum space

# SSH Energy Bands - Eigenstates

...ABABA... Lattice Structure....

$$\sum_x \Psi_x = \sum_x e^{ikx} \times \begin{cases} \alpha_k \\ \beta_k \ e^{ikd/2} \end{cases}$$

**Eigenstates**

$$\begin{pmatrix} \alpha_{k,\mp} \\ \beta_{k,\mp} \end{pmatrix} = \frac{1}{\sqrt{2}} \begin{pmatrix} \pm 1 \\ e^{-i\theta_k} \end{pmatrix}$$

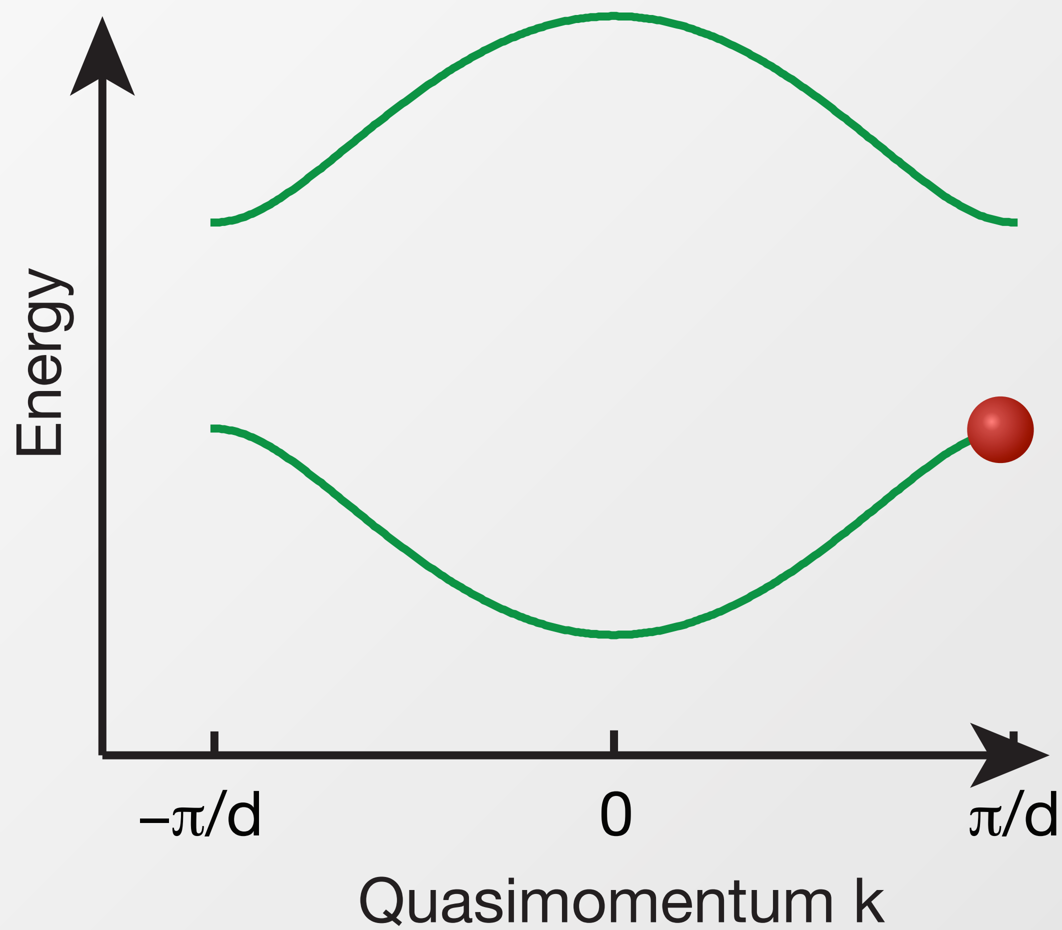


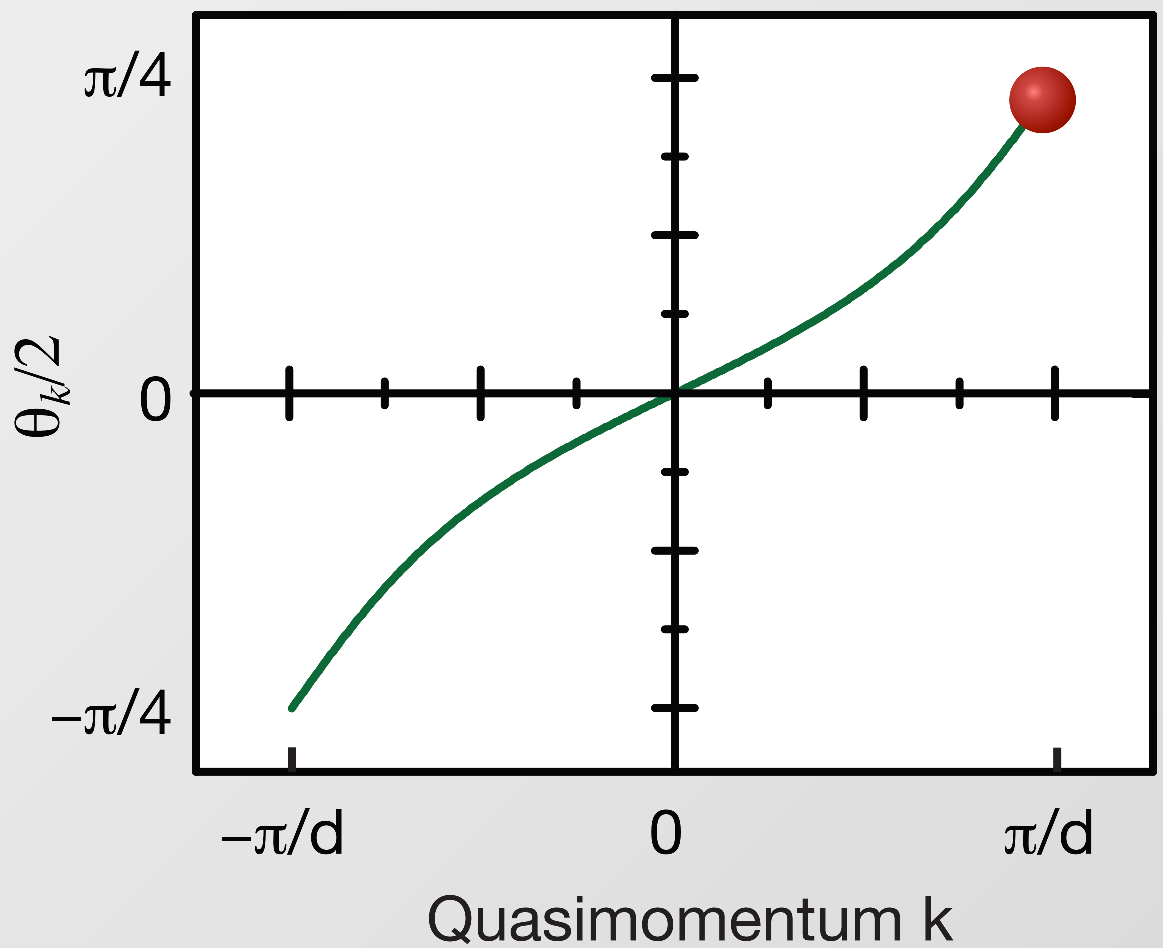


$$\boxed{\varphi_{Zak} = i \int_{k_0}^{k_0+G} \left( \alpha_k^* \partial_k \alpha_k + \beta_k^* \partial_k \beta_k \right) \ dk}$$

Zak Phase
SSH Model

# SSH Energy Bands - Eigenstates

...ABABA... Lattice Structure....

$$\sum_x \Psi_x = \sum_x e^{ikx} \times \begin{cases} \alpha_k \\ \beta_k \; e^{ikd/2} \end{cases}$$

**Eigenstates**

$$\begin{pmatrix} \alpha_{k,\mp} \\ \beta_{k,\mp} \end{pmatrix} = \frac{1}{\sqrt{2}} \begin{pmatrix} \pm 1 \\ e^{-i\theta_k} \end{pmatrix}$$

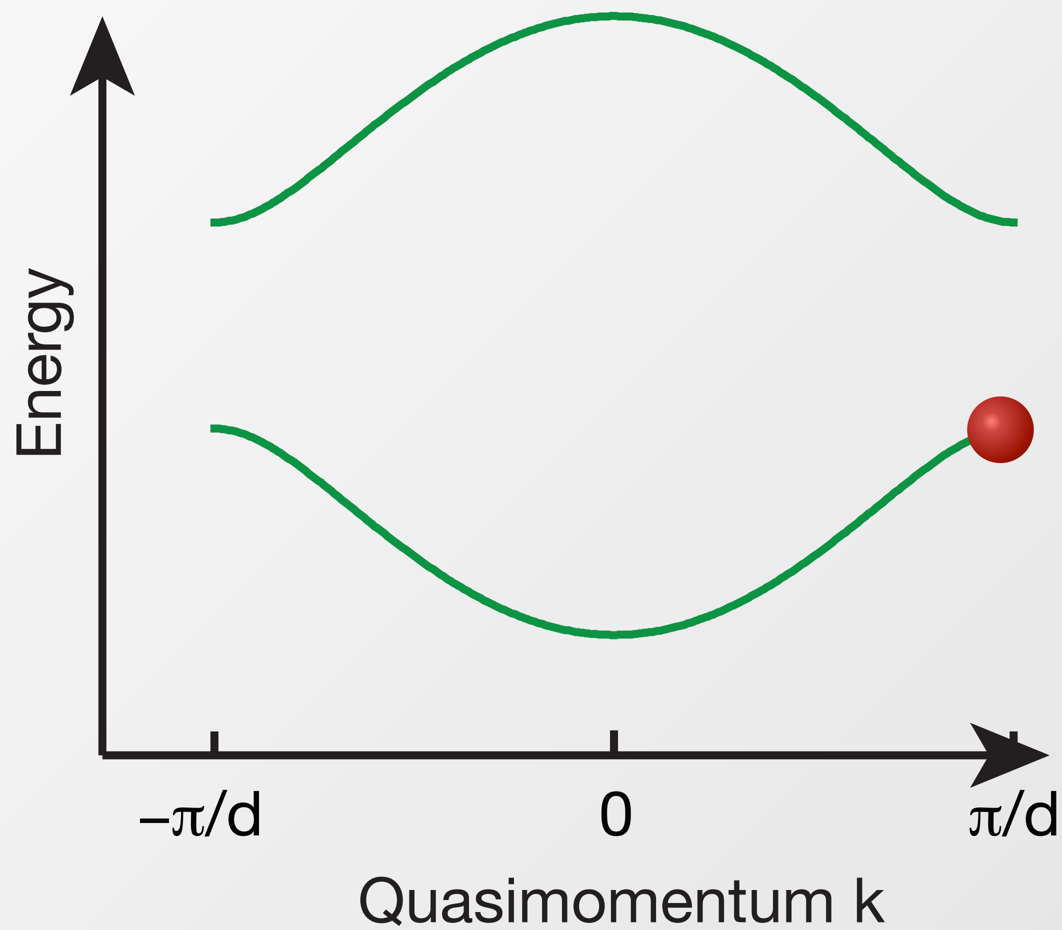


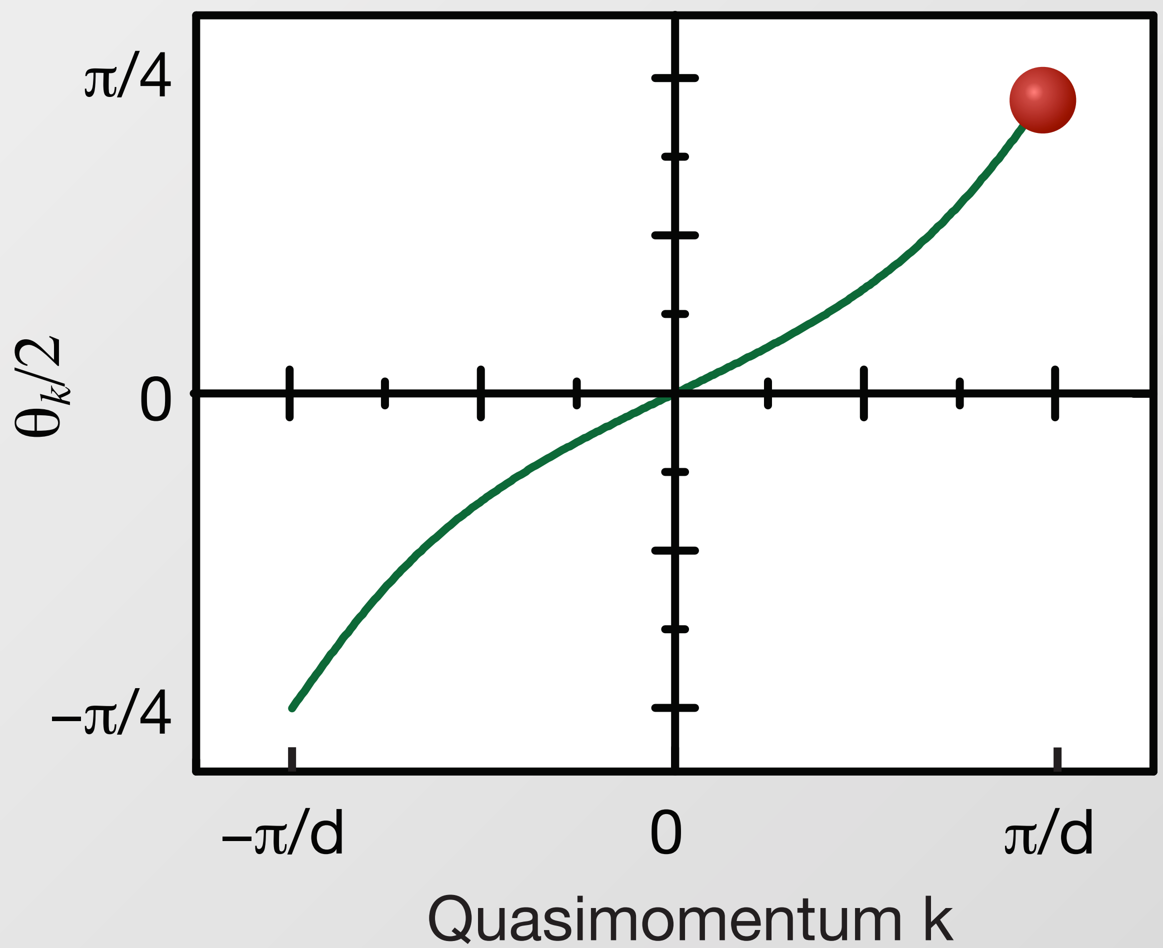


$$\boxed{\varphi_{Zak} = \frac{1}{2} \int_{k_0}^{G+k_0} \partial_k \theta_k \; dk}$$

# SSH Energy Bands - Eigenstates

...ABABA... Lattice Structure....

$$\sum_x \Psi_x = \sum_x e^{ikx} \times \begin{cases} \alpha_k \\ \beta_k \ e^{ikd/2} \end{cases}$$

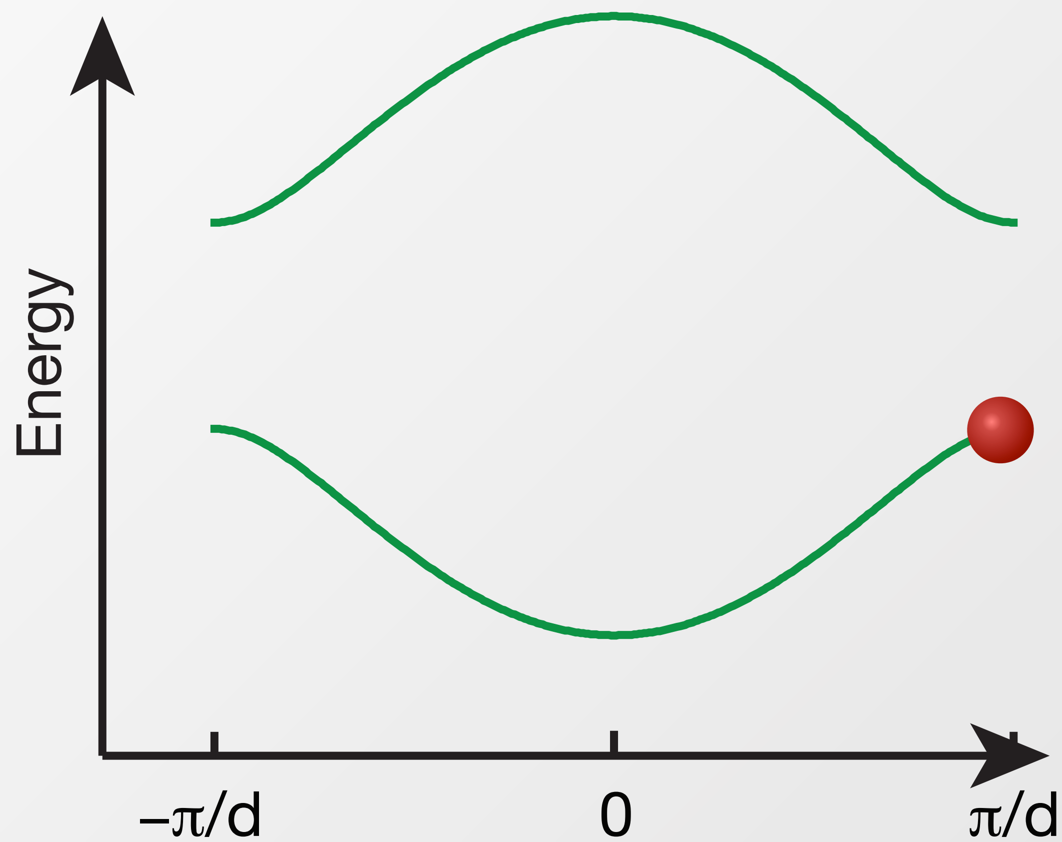


**DI:** $J > J'$

$$\boxed{\varphi^{D1}_{Zak} = \frac{\pi}{2}}$$

**Eigenstates**

$$\begin{pmatrix} \alpha_{k,\mp} \\ \beta_{k,\mp} \end{pmatrix} = \frac{1}{\sqrt{2}} \begin{pmatrix} \pm 1 \\ e^{-i\theta_k} \end{pmatrix}$$

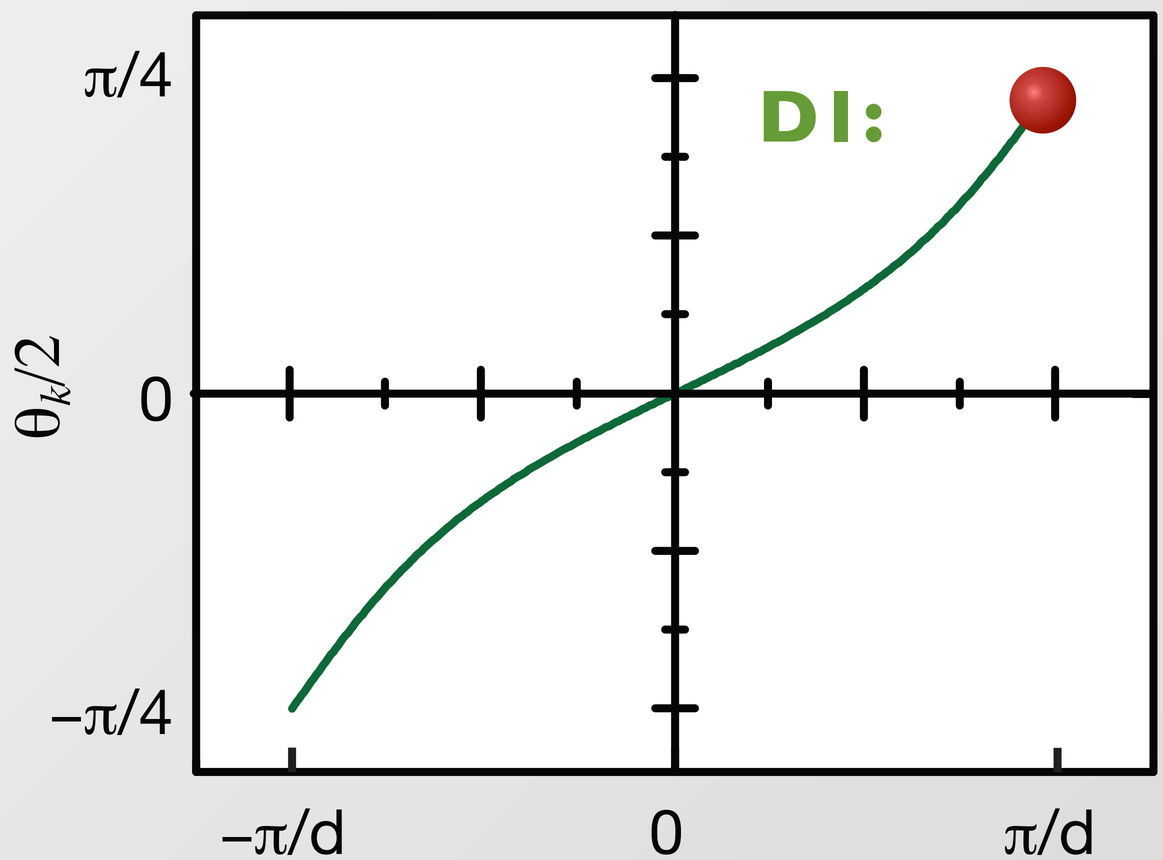

# SSH Energy Bands - Eigenstates

...ABABA... Lattice Structure....

$$\sum_x \Psi_x = \sum_x e^{ikx} \times \begin{cases} \alpha_k \\ \beta_k \; e^{ikd/2} \end{cases}$$

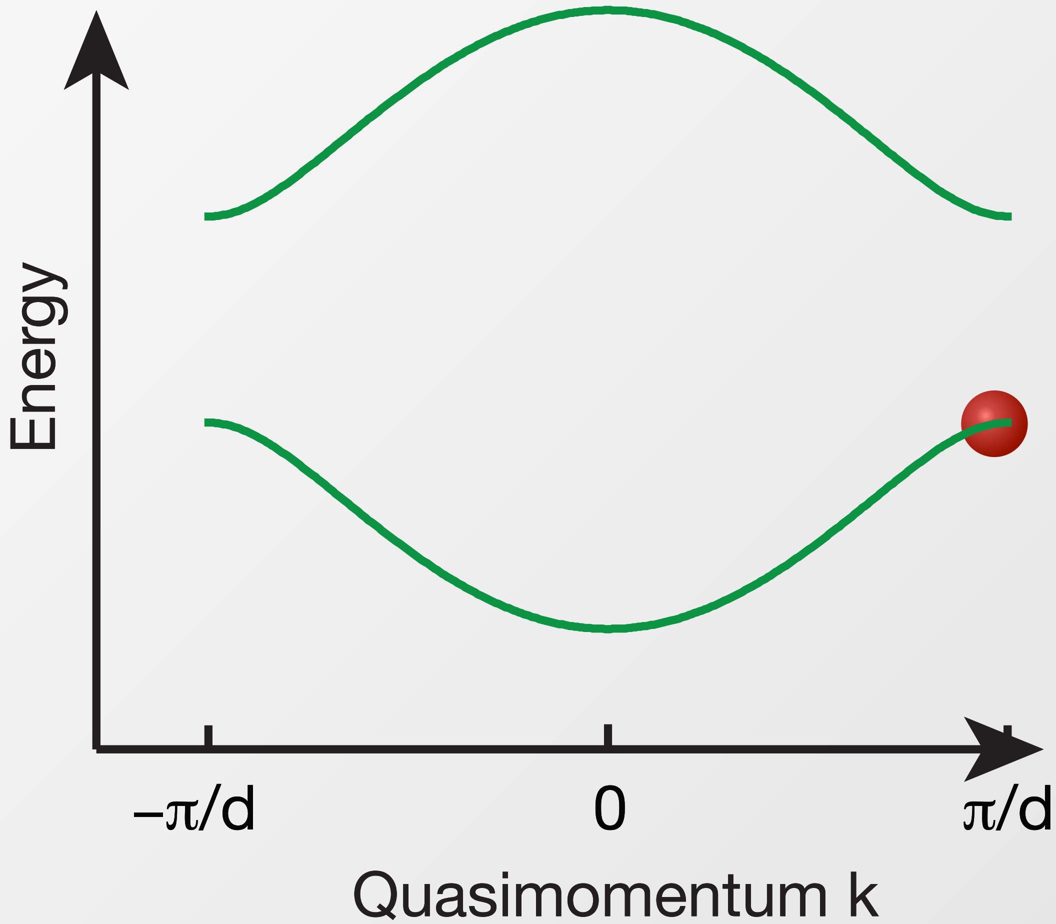


**Eigenstates**

$$\begin{pmatrix} \alpha_{k,\mp} \\ \beta_{k,\mp} \end{pmatrix} = \frac{1}{\sqrt{2}} \begin{pmatrix} \pm 1 \\ e^{-i\theta_k} \end{pmatrix}$$

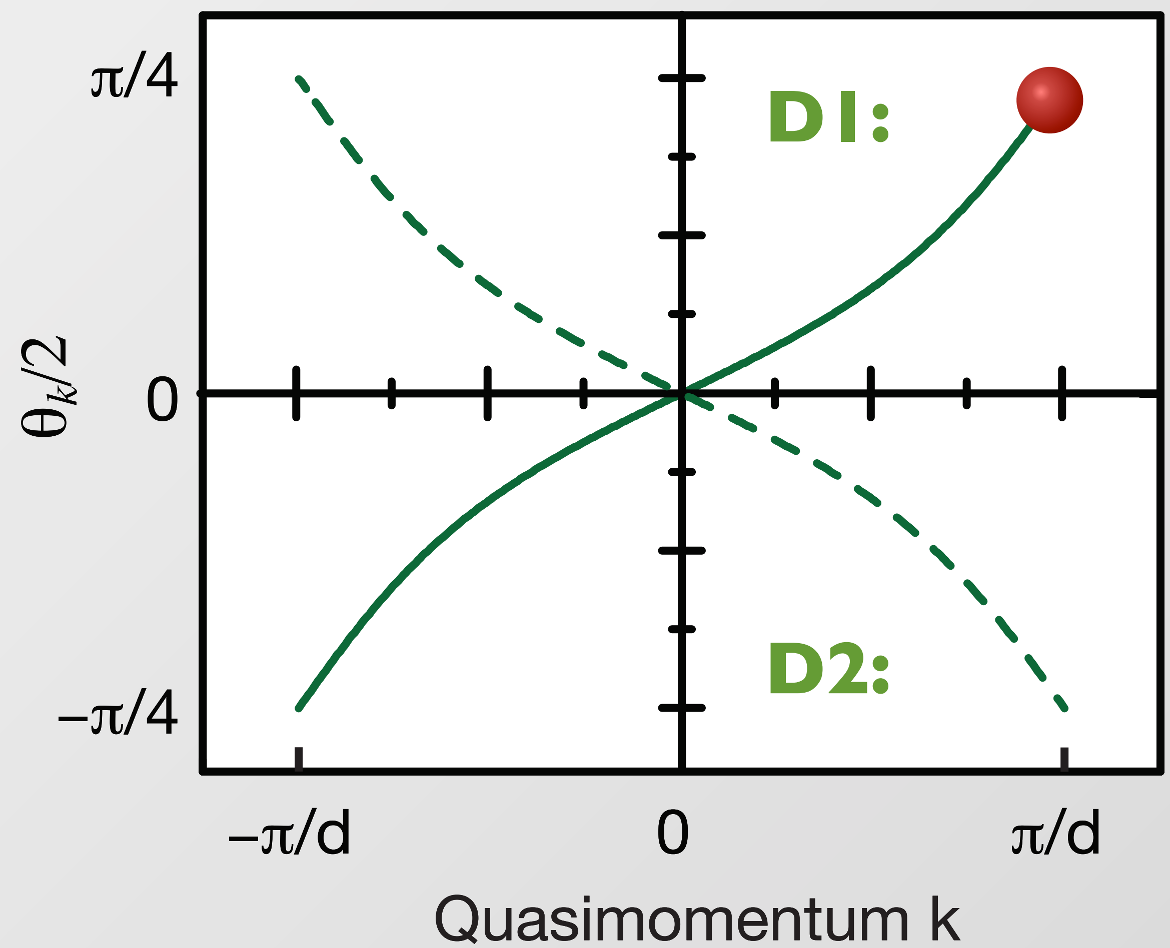


**D1:** $J > J'$ $\boxed{\varphi^{D1}_{Zak} = \frac{\pi}{2}}$

**D2:** $J' > J$ $\boxed{\varphi^{D2}_{Zak} = -\frac{\pi}{2}}$

# Realization with ultracold atoms

$$H_{\mathrm{SSH}} = -\sum_n \{J a_n^\dagger b_n + J' a_n^\dagger b_{n-1} + \mathrm{h.c.}\}$$

767 nm
1534 nm

**D1:** $J > J'$

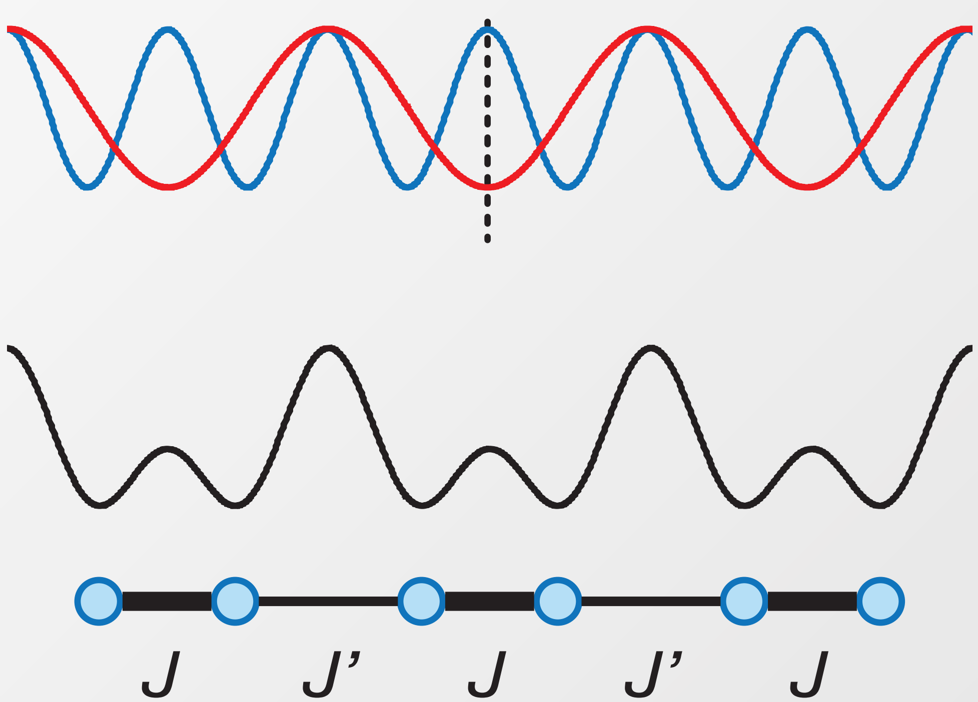


**D2:** $J' > J$

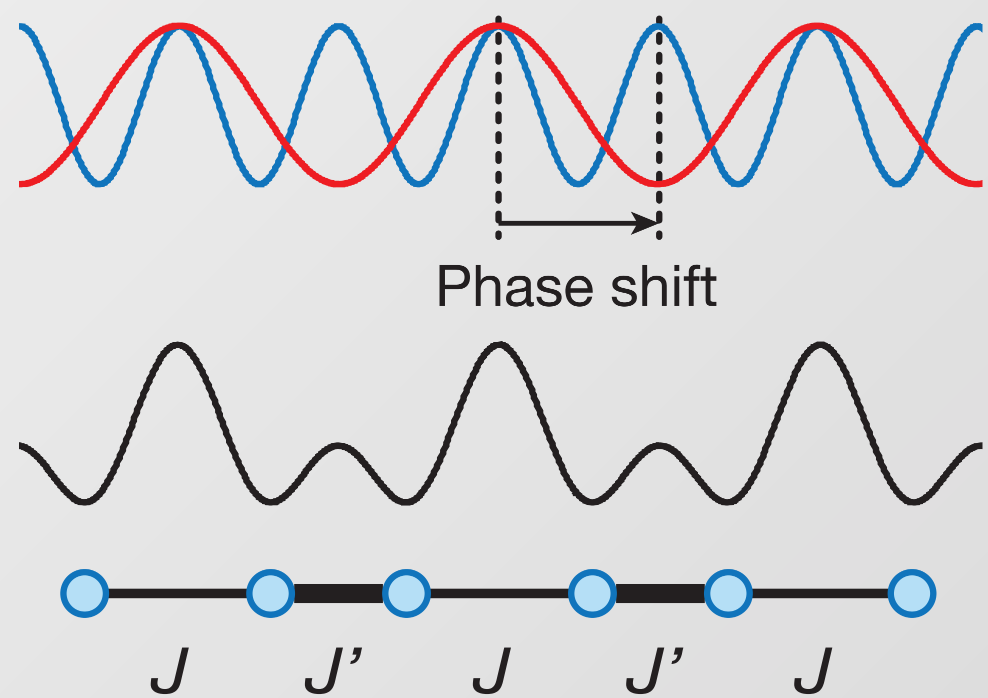


$$\delta\varphi_{Zak} = \varphi_{Zak}^{D1} - \varphi_{Zak}^{D2} = \pi$$

# Measuring the Berry-Zak Phase (SSH Model)

**DI:** $J > J'$ Spin-dependent Bloch oscillations + Ramsey interferometry

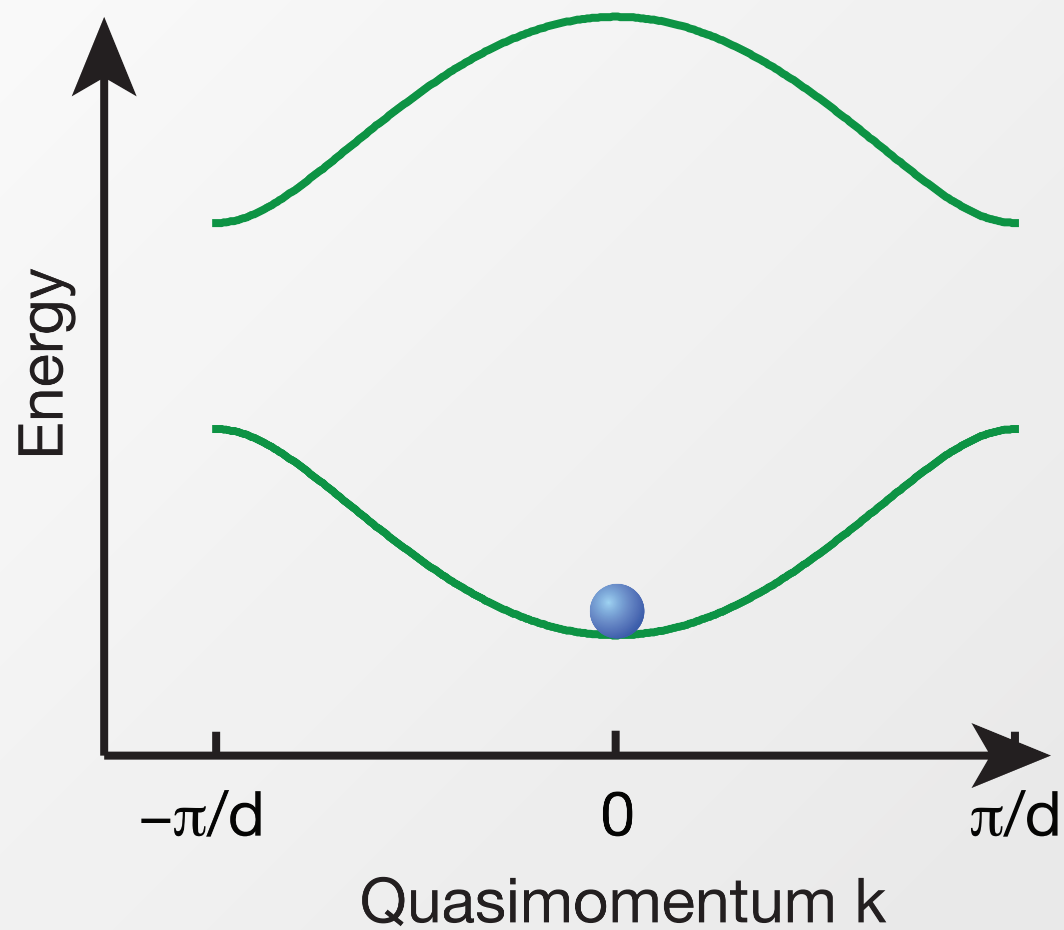


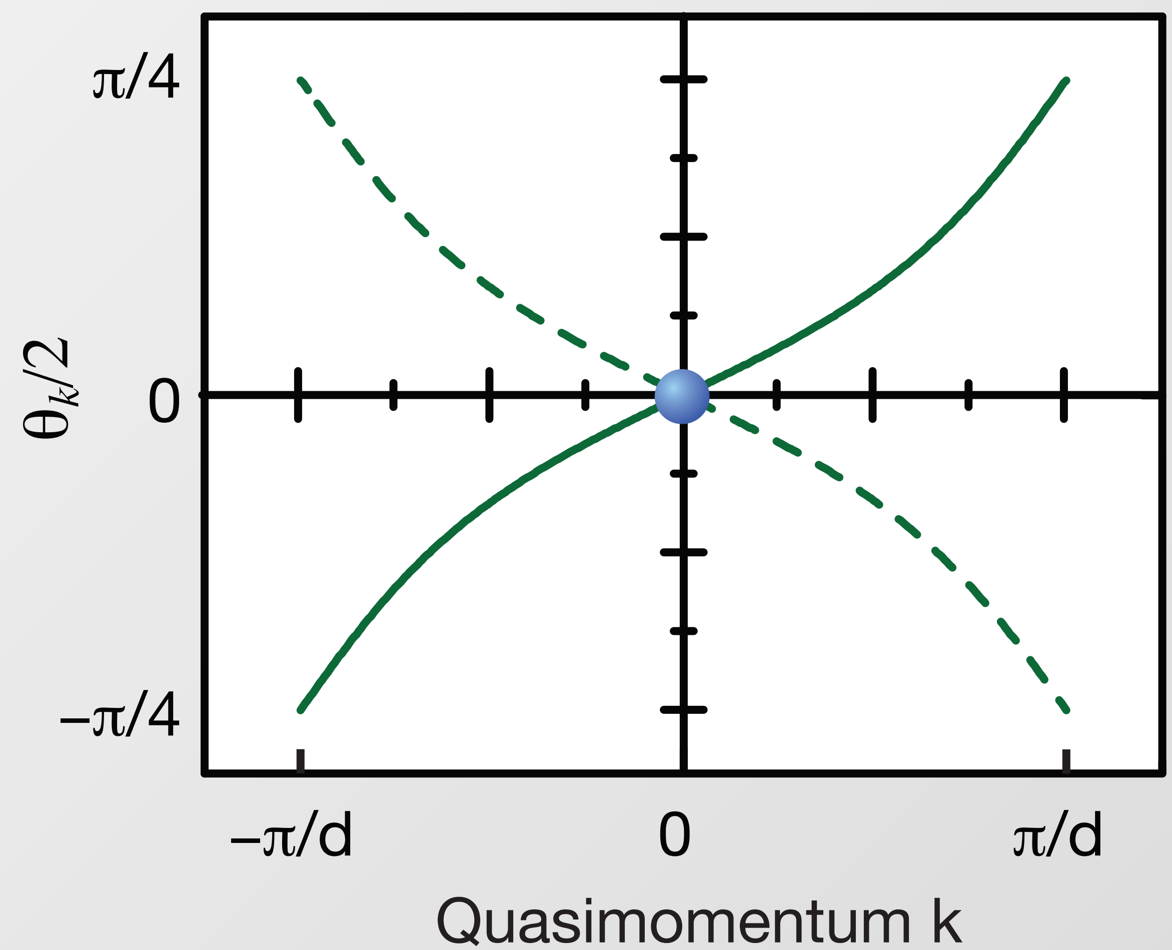


Prepare BEC in state $|\sigma, k\rangle = |\downarrow, 0\rangle\,, \quad \text{with } \sigma = \uparrow, \downarrow$

# Measuring the Berry-Zak Phase (SSH Model)

**DI:** $J > J'$

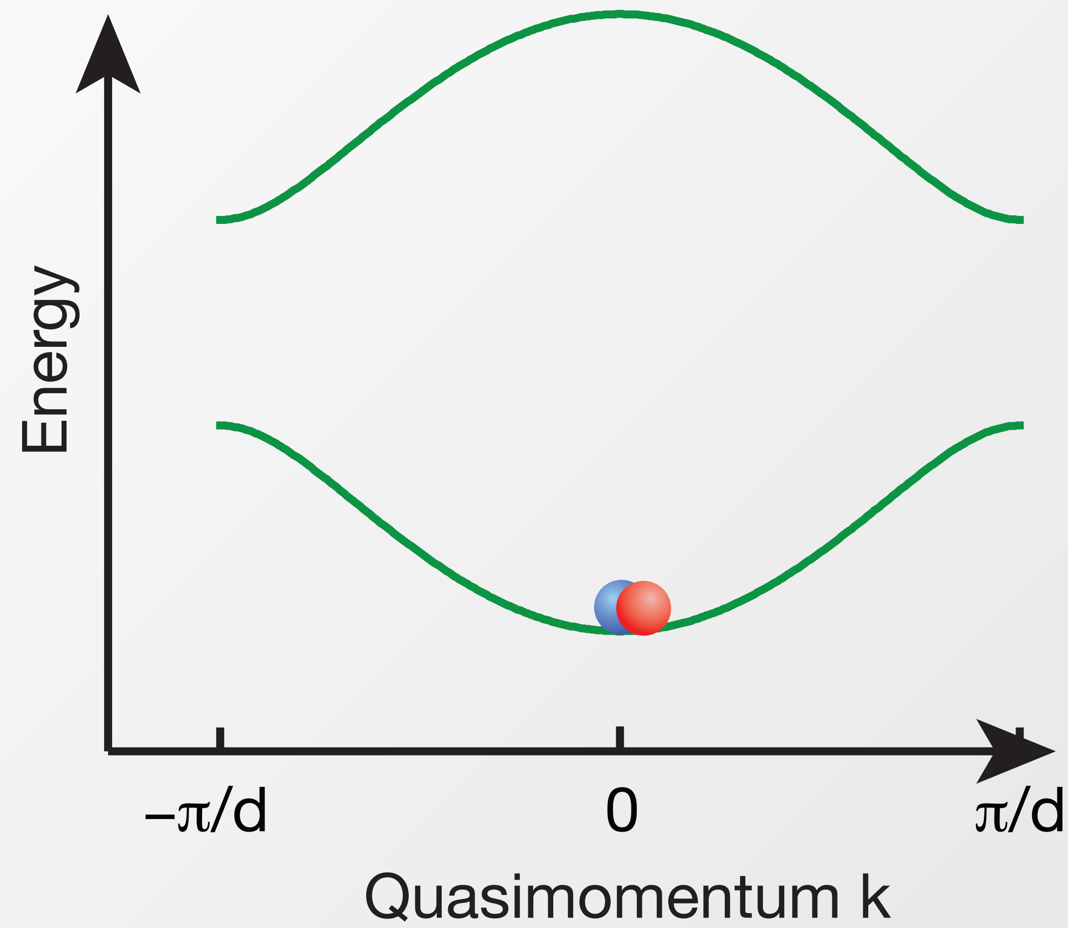


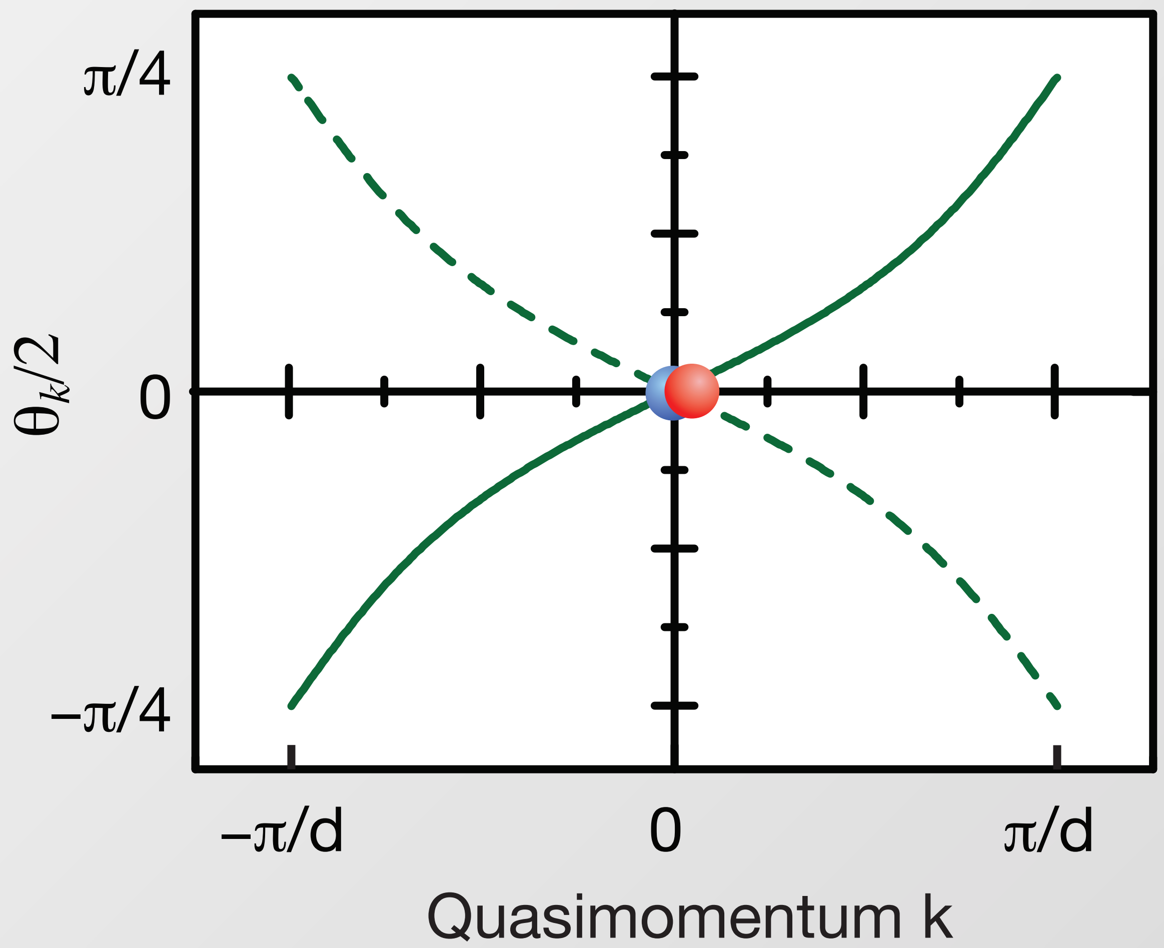


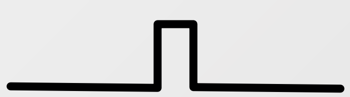


Create coherent superposition $\frac{1}{\sqrt{2}}\left(|\uparrow,0\rangle + |\downarrow,0\rangle\right)$

# Measuring the Berry-Zak Phase (SSH Model)

**DI:** $J > J'$

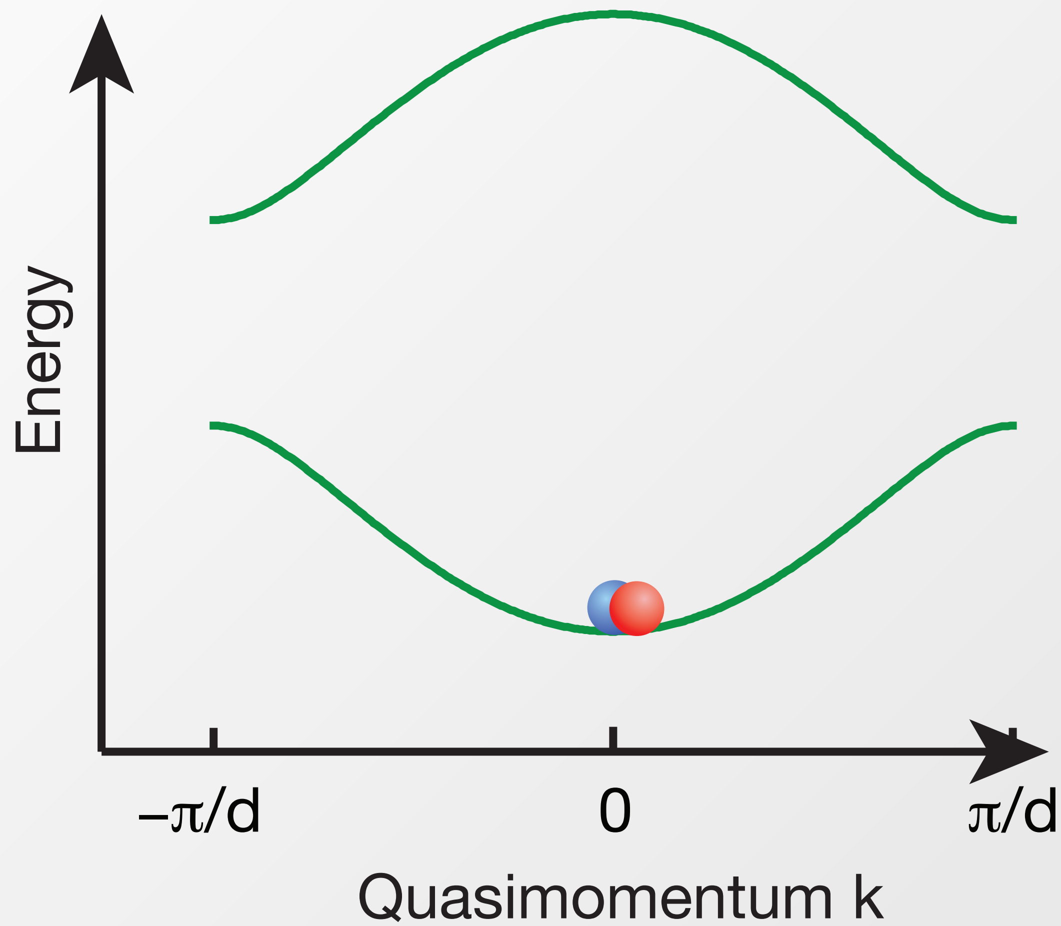


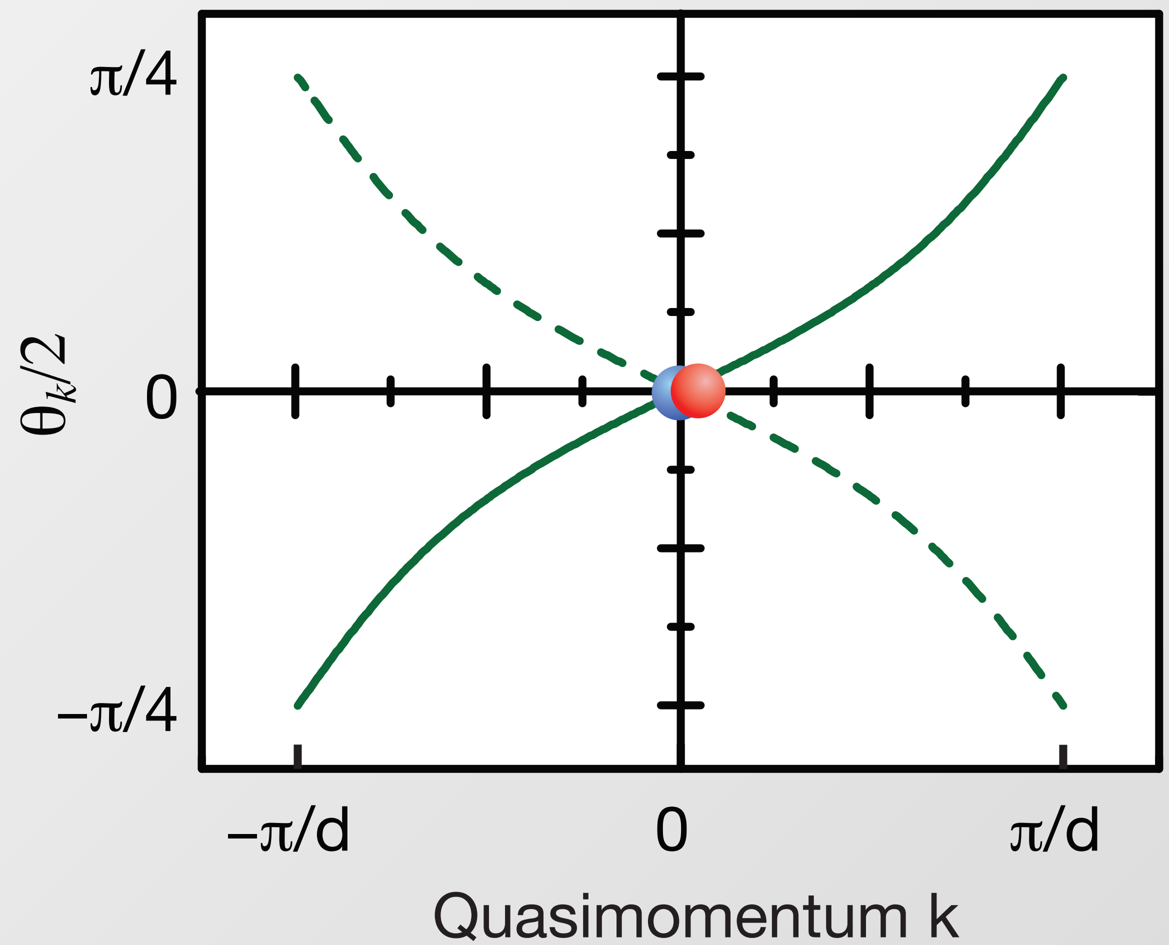


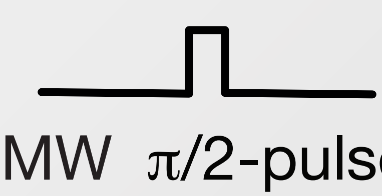


Spin components with opposite magnetic moments!

Create coherent superposition $\frac{1}{\sqrt{2}}\left(|\uparrow, 0\rangle + |\downarrow, 0\rangle\right)$

# Measuring the Berry-Zak Phase (SSH Model)

**DI:** $J > J'$

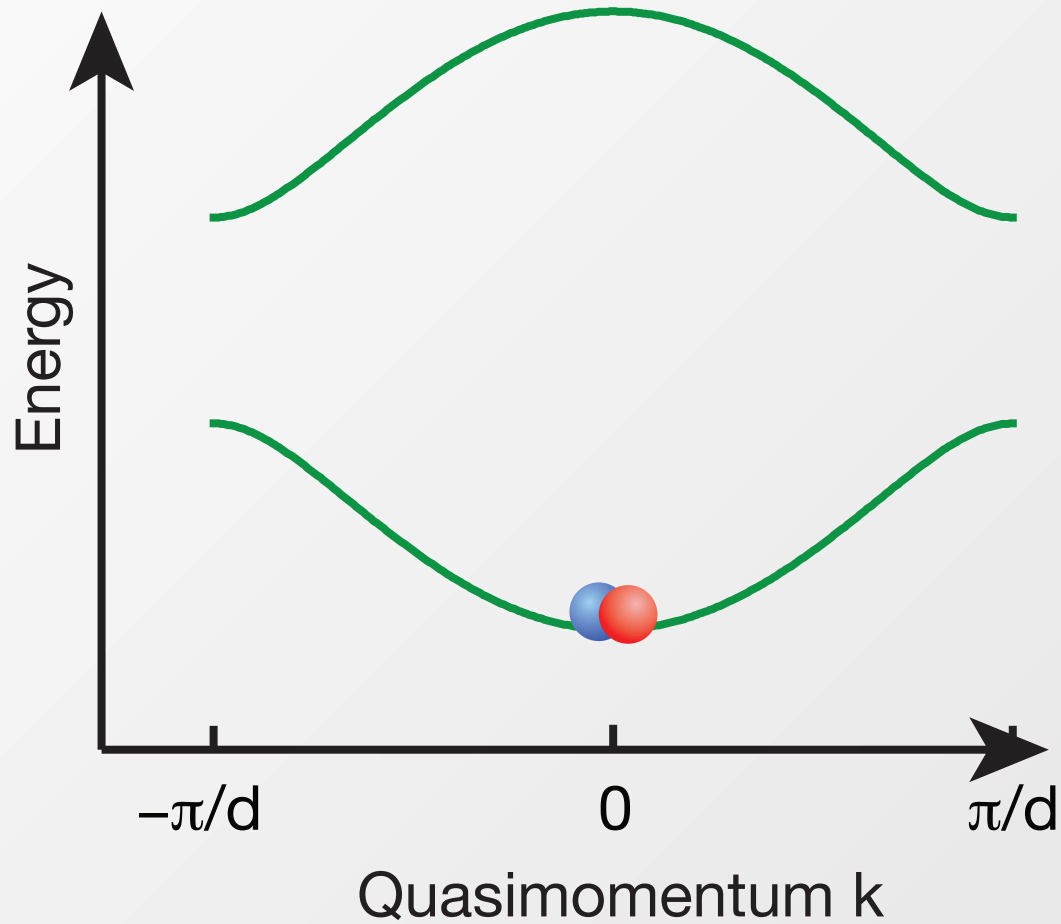


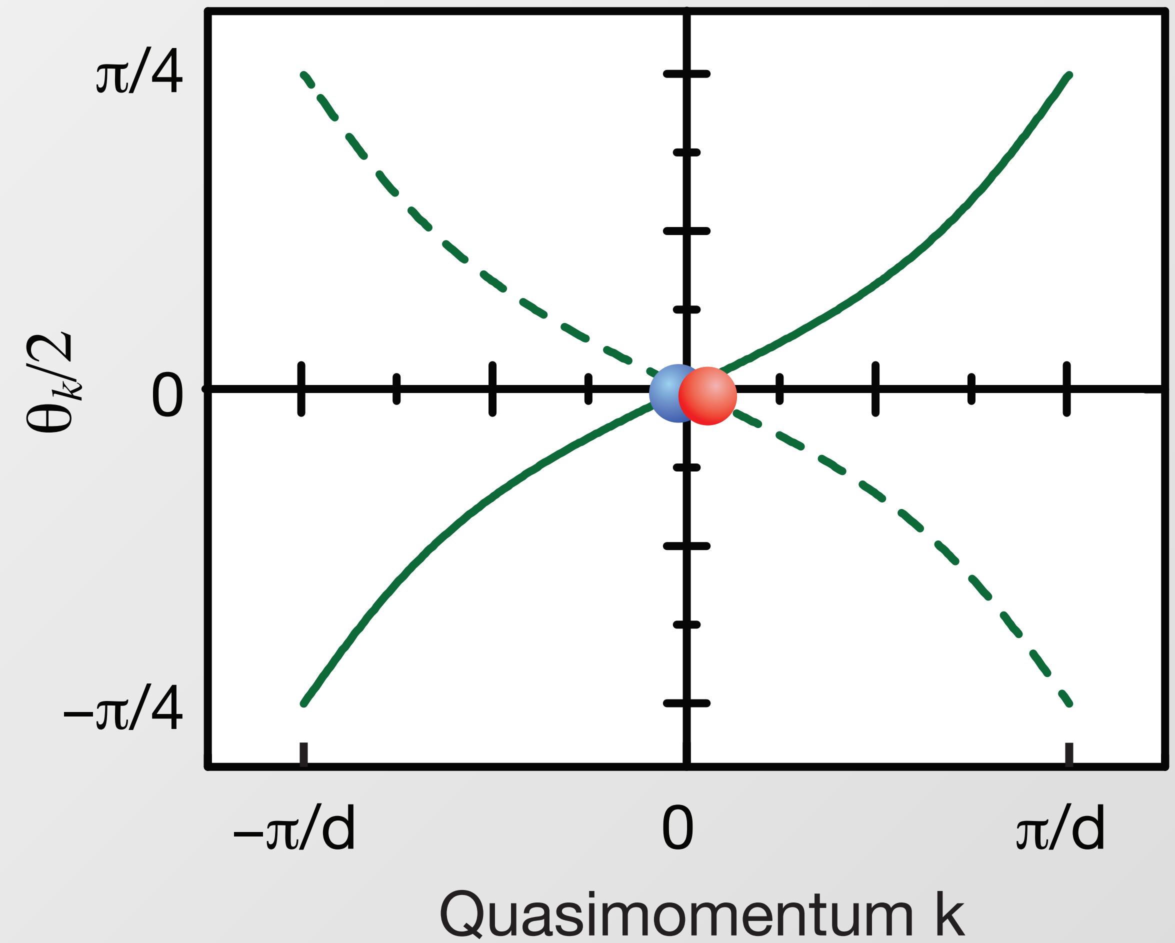


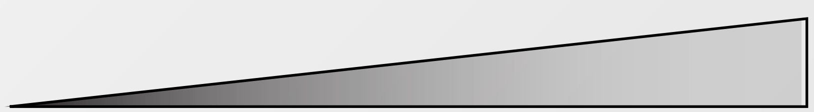

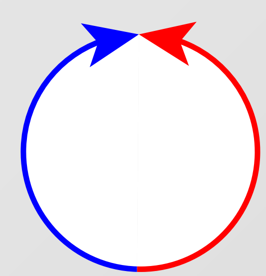

Closed Loop in *k*-Space

Apply magnetic field gradient $\longrightarrow$ adiabatic evolution in momentum space

# Measuring the Berry-Zak Phase (SSH Model)

**DI:** $J > J'$

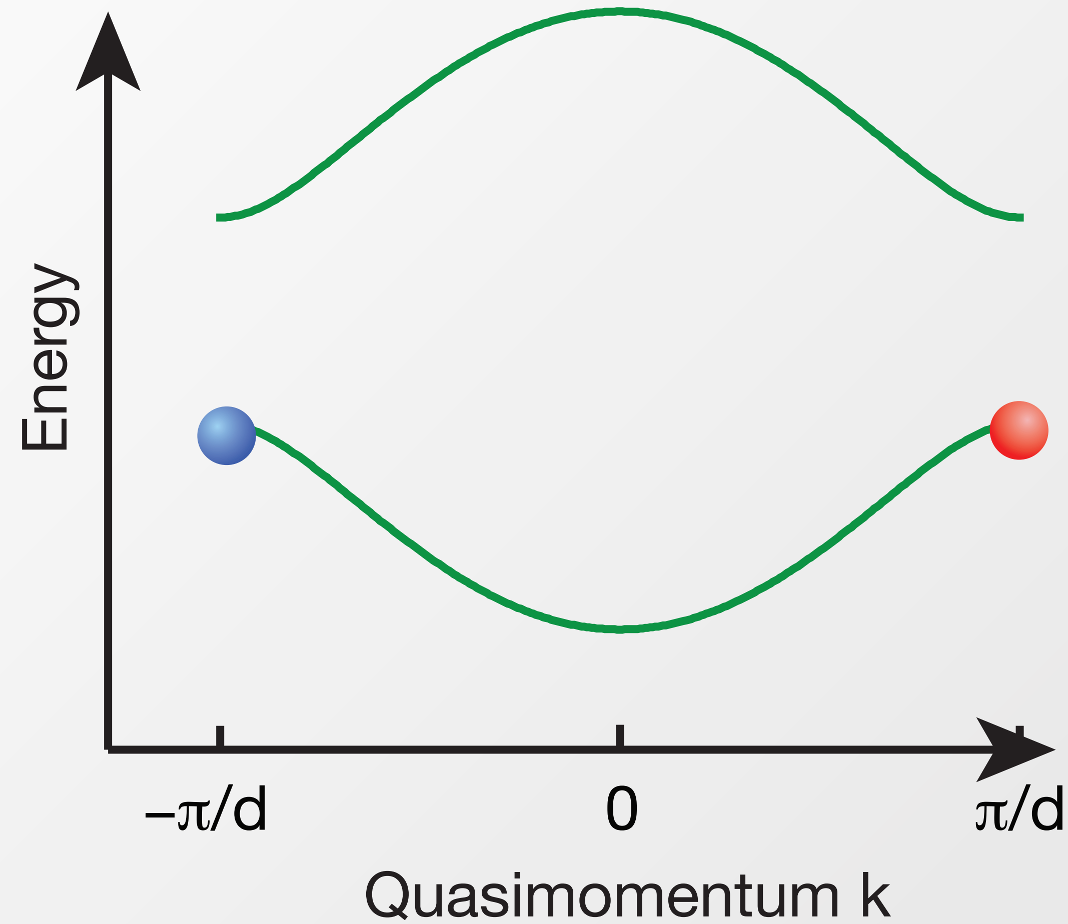


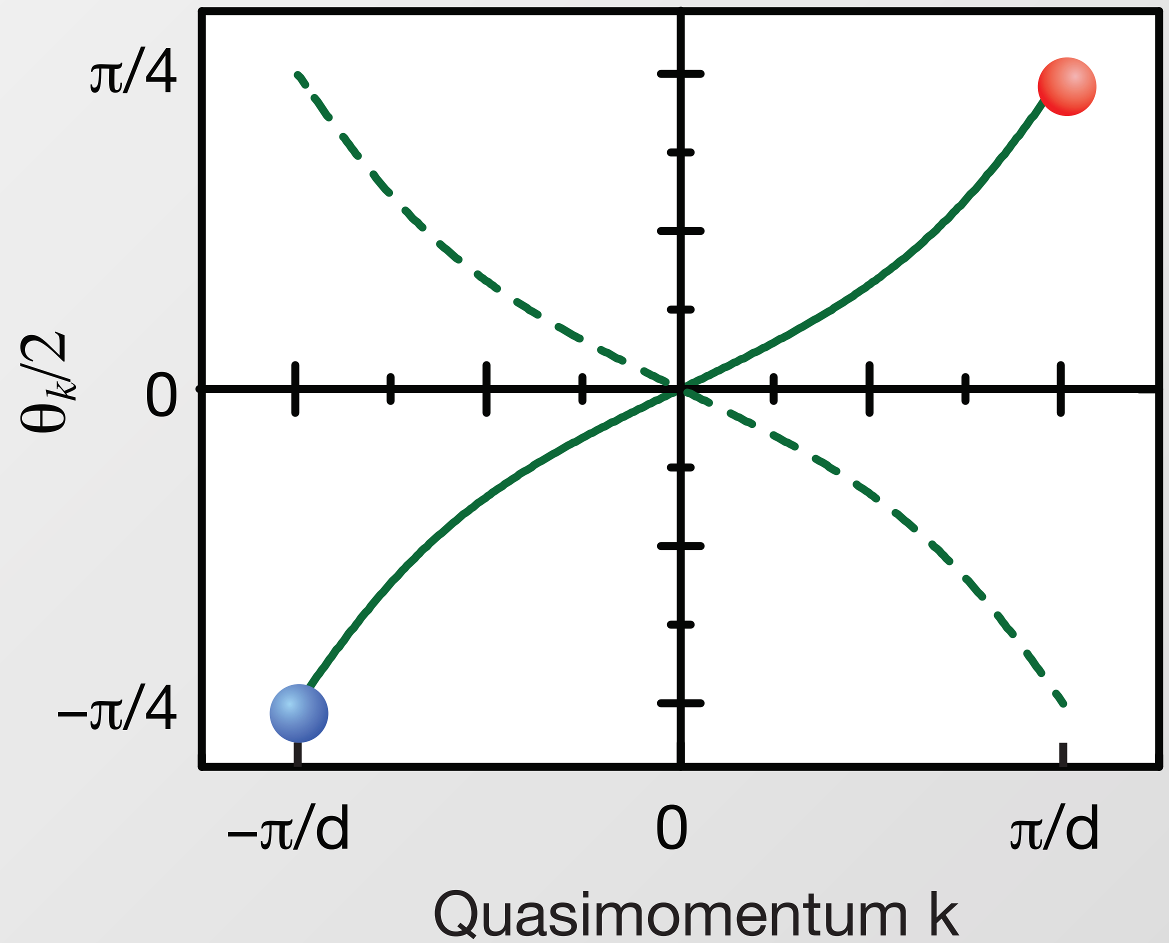


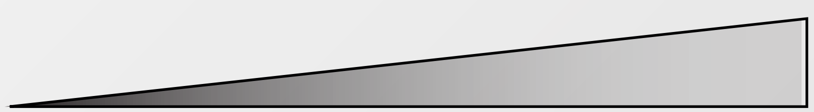

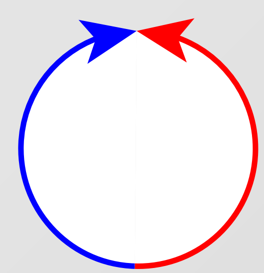

Closed Loop in *k*-Space

Apply magnetic field gradient $\longrightarrow$ adiabatic evolution in momentum space

# Measuring the Berry-Zak Phase (SSH Model)

**DI:** $J > J'$

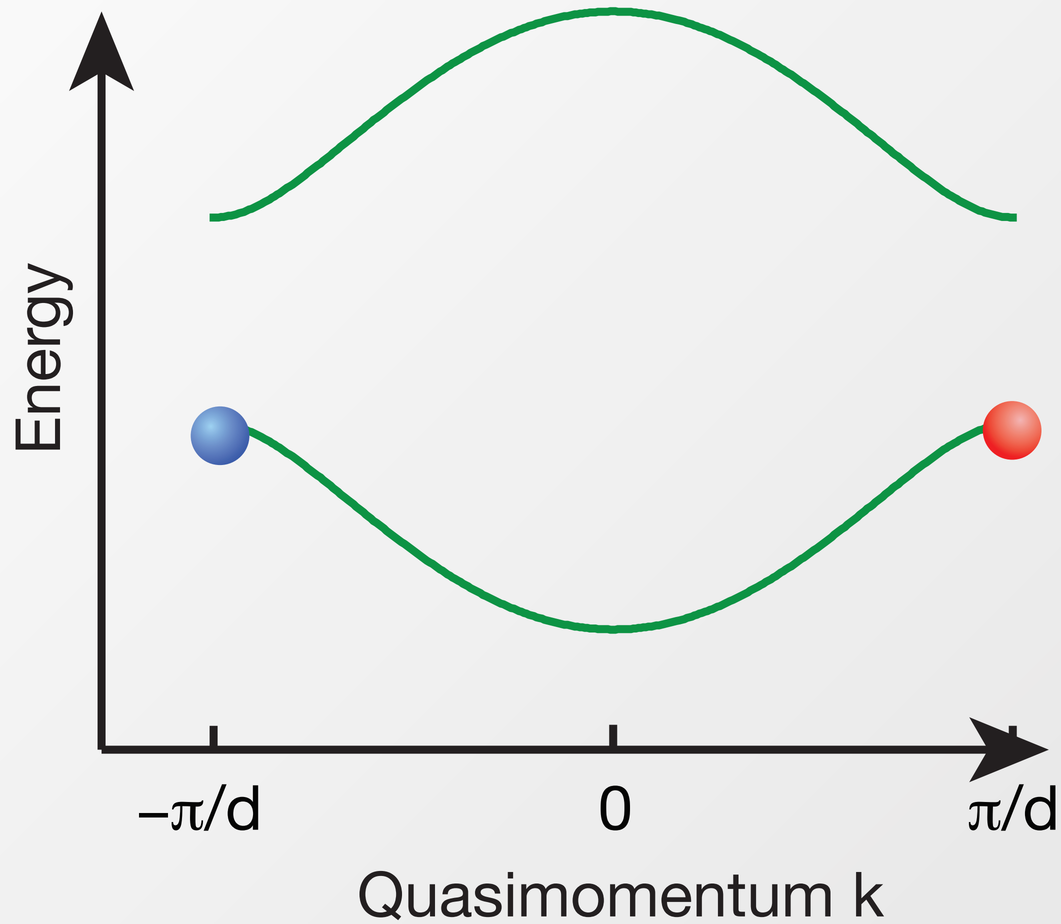


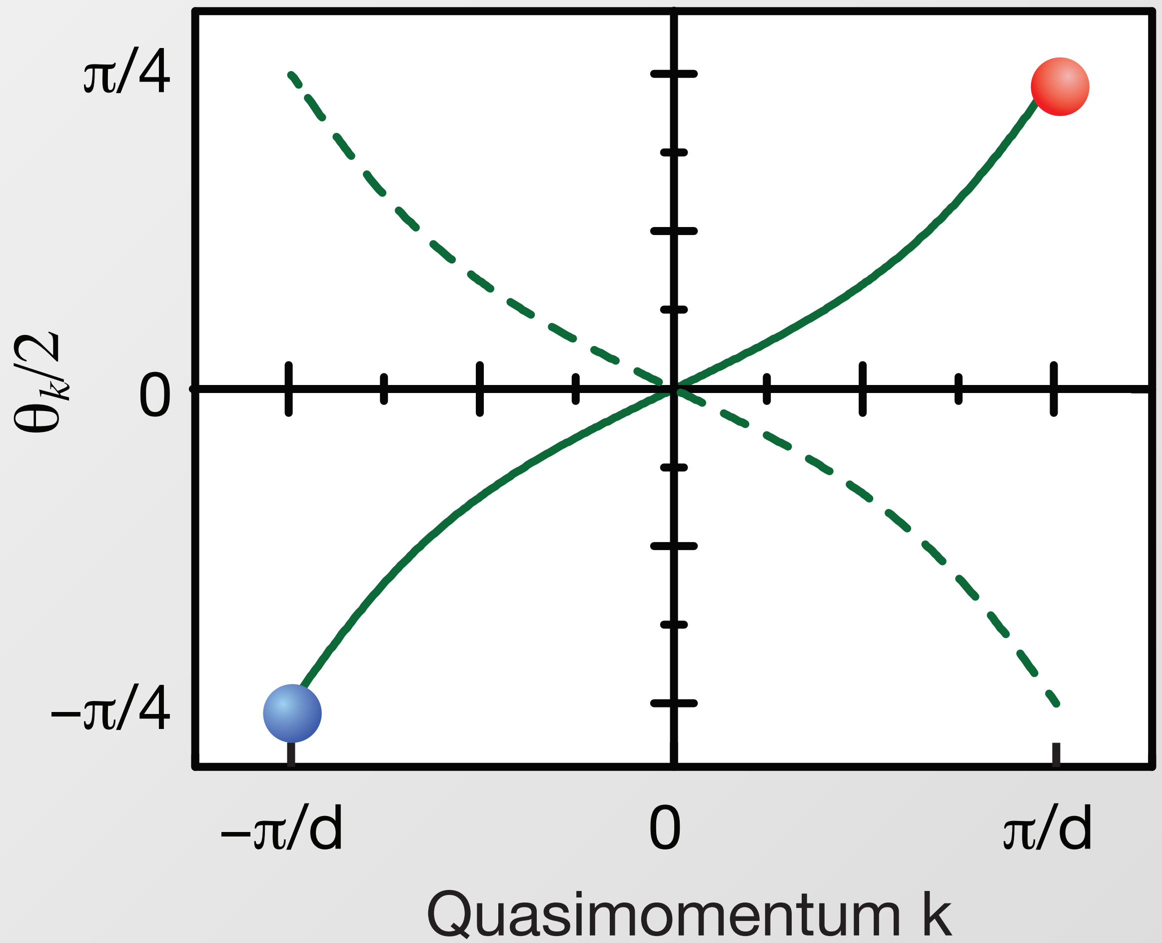


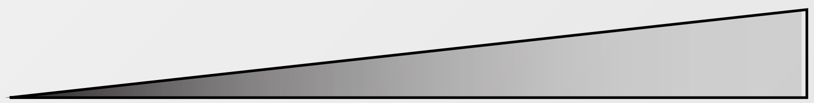

$$\delta\varphi_{Zak} = \varphi_{Zak}^{D1} + \varphi_{dyn} + \varphi_{Zeeman}$$

# Measuring the Berry-Zak Phase (SSH Model)

**DI:** $J > J'$

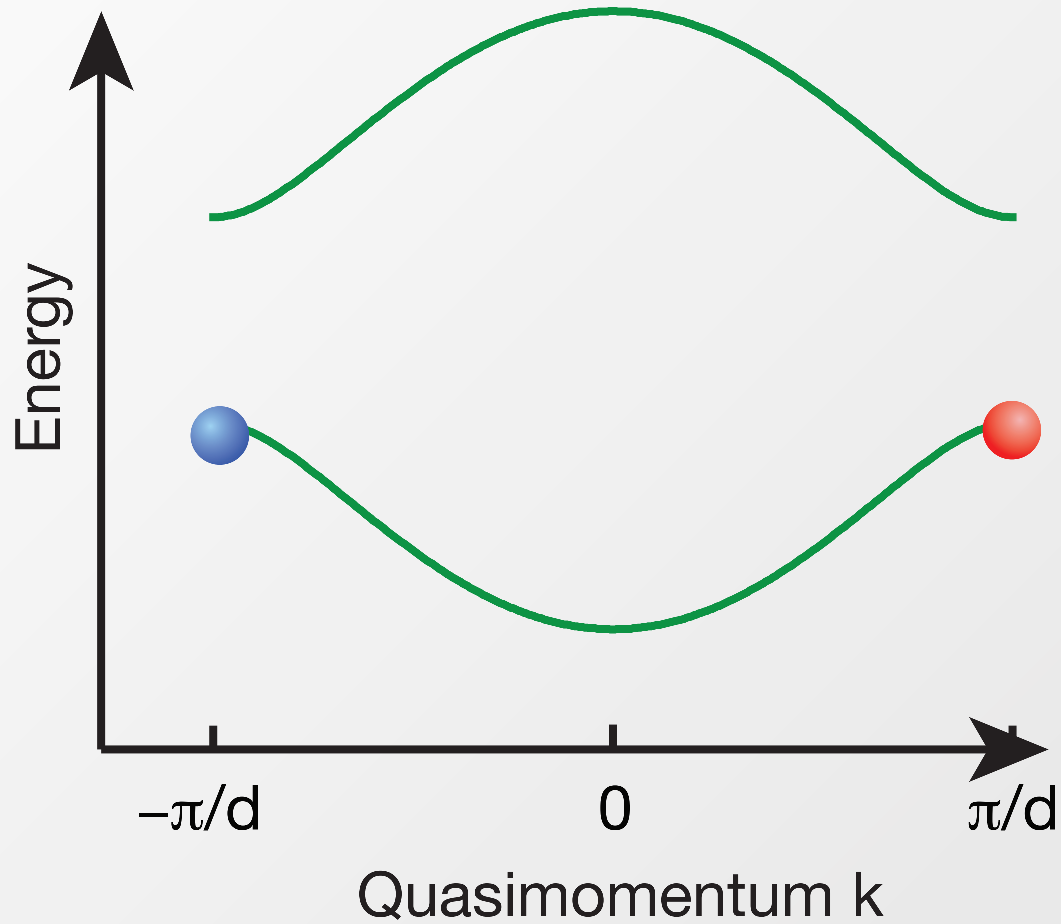


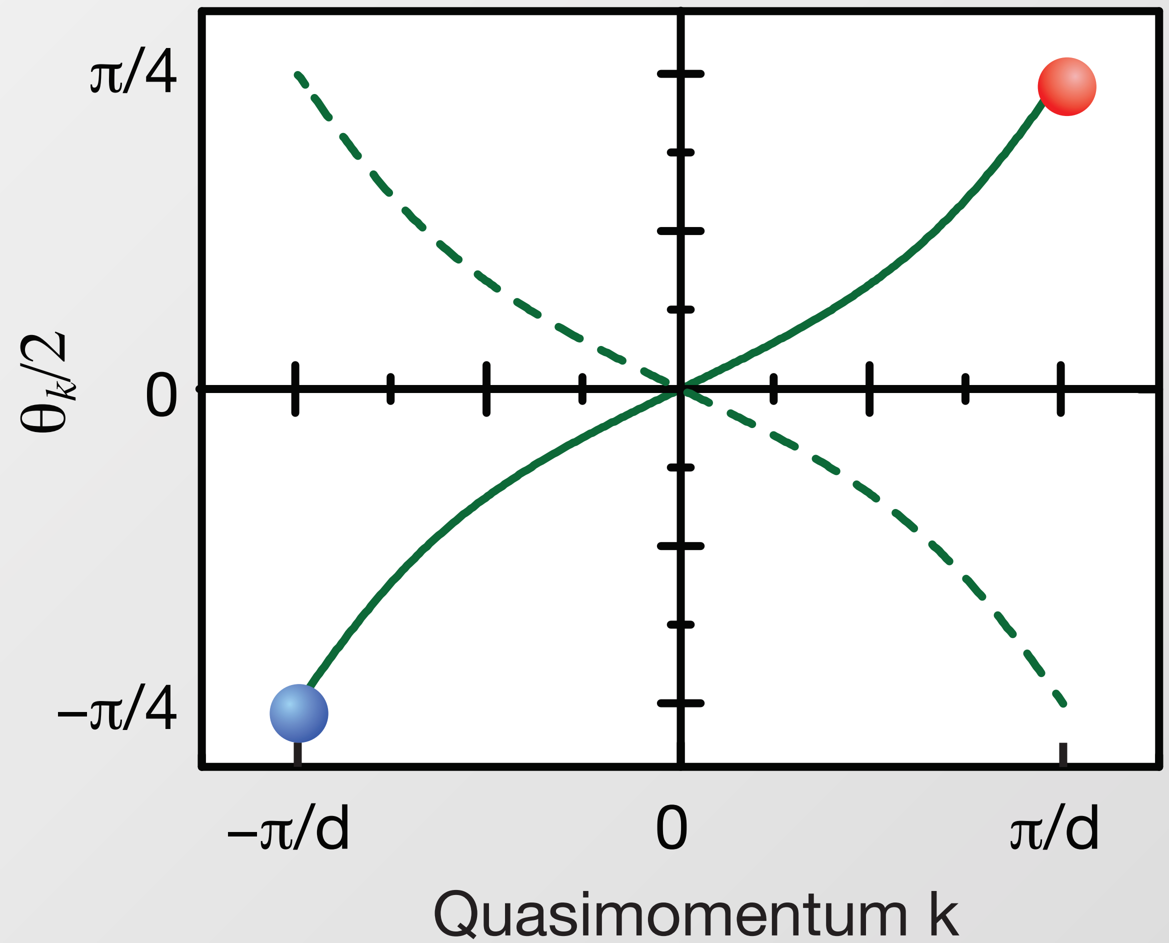


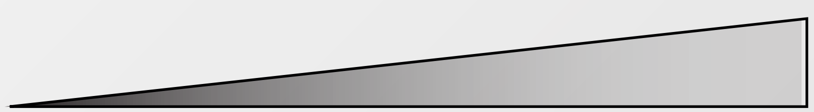

$$\varphi_{dyn} = \int E(t)/\hbar \, \mathrm{dt}$$

$$E(k) = E(-k)$$

$$\boxed{\delta\varphi_{Zak} = \varphi_{Zak}^{D1} + \cancel{\varphi_{dyn}} + \varphi_{Zeeman}}$$

# Reference measurement

**Phase of reference fringe:**

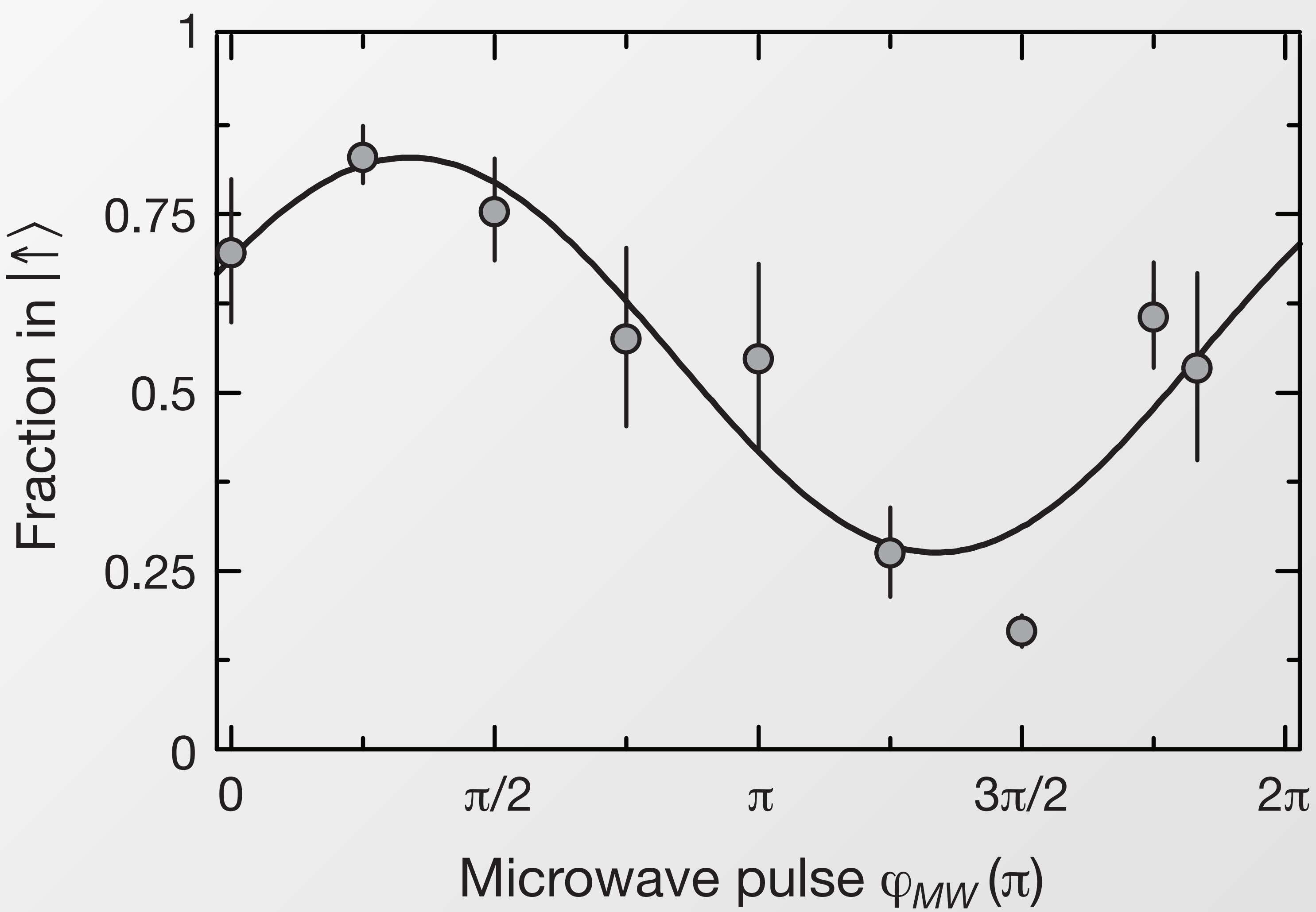


$\delta\varphi \neq 0$

Average of five individual measurements

Exp. imperfections: - Small detuning of the MW-pulse
- Magnetic field drifts

# Measuring the Zak Phase (SSH Model)

**Measured Topological invariant:**
**Zak phase difference**

$$\varphi^{D1}_{Zak} - \varphi^{D2}_{Zak} = \pi$$

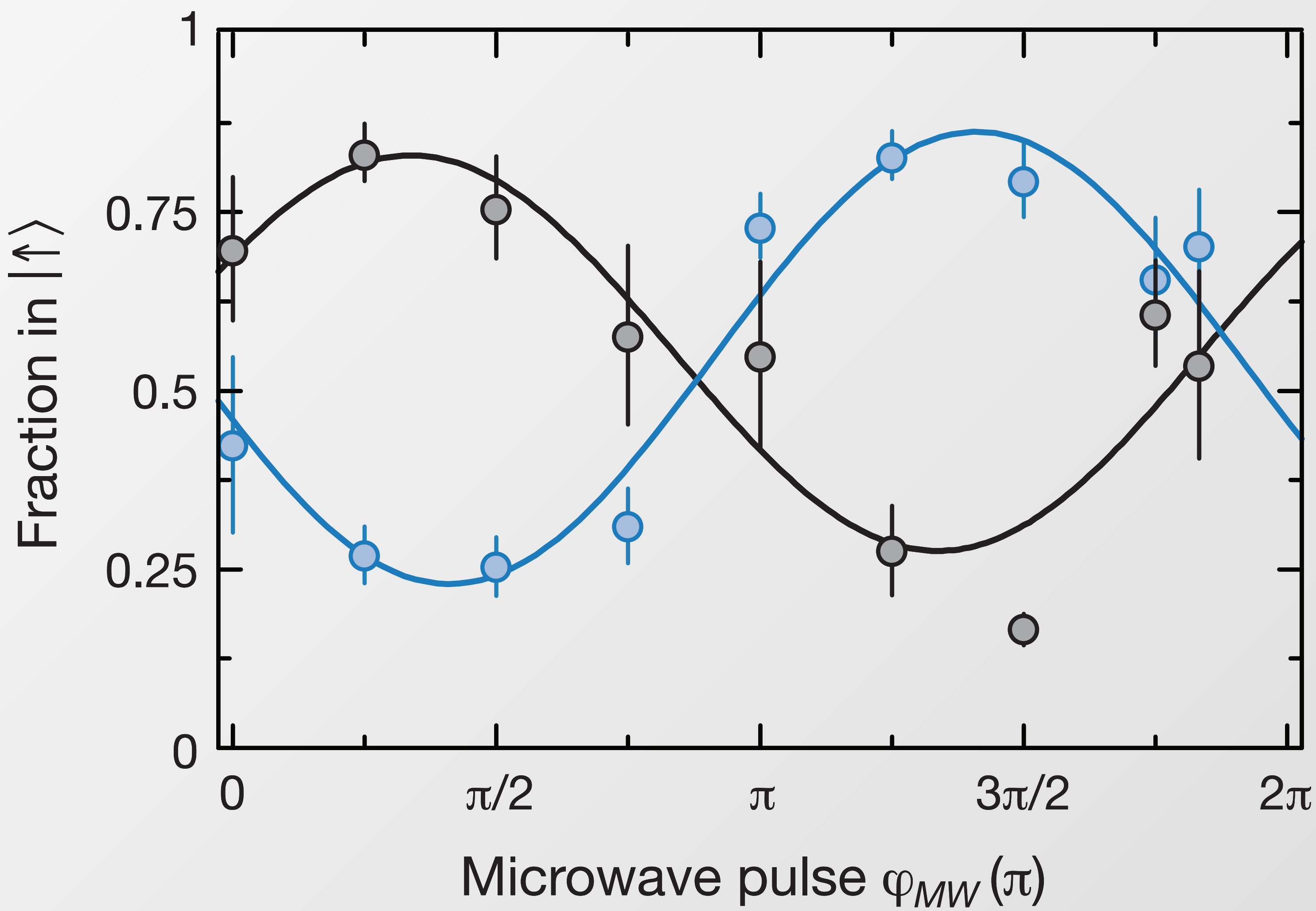


$$\delta\varphi_{Zak} = 0.97(2)\pi$$

obtained from 14 independent measurements

# Measuring the Zak Phase (SSH Model)

**Measured Topological invariant:**
**Zak phase difference**

$$\varphi_{Zak}^{D1} - \varphi_{Zak}^{D2} = \pi$$

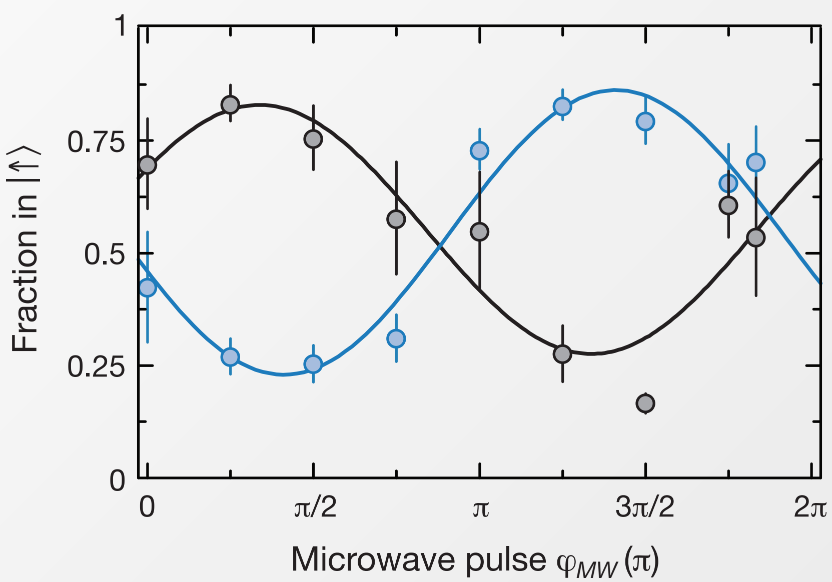


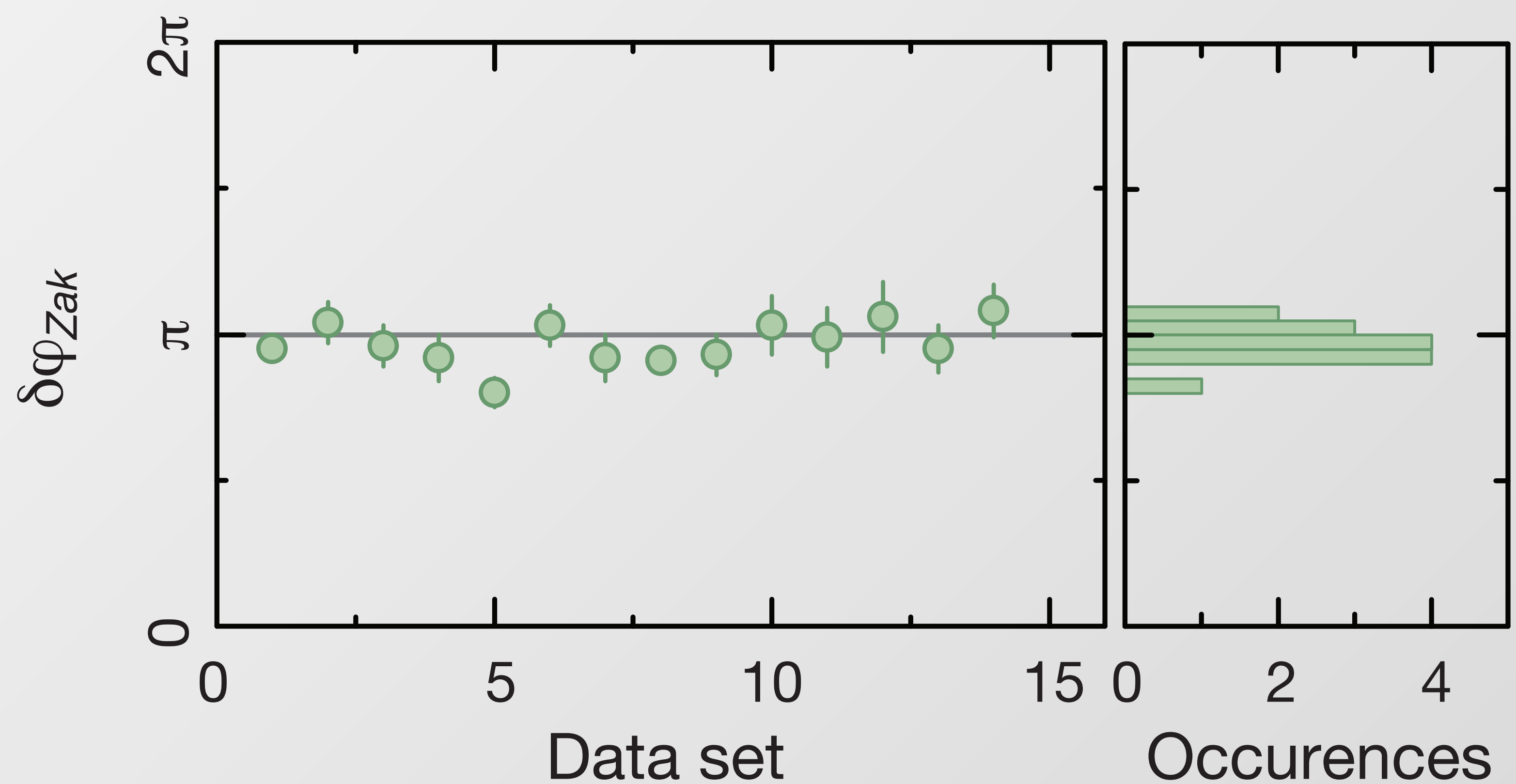


$$\delta\varphi_{Zak} = 0.97(2)\pi$$

obtained from 14 independent measurements

# Fractional Zak Phase

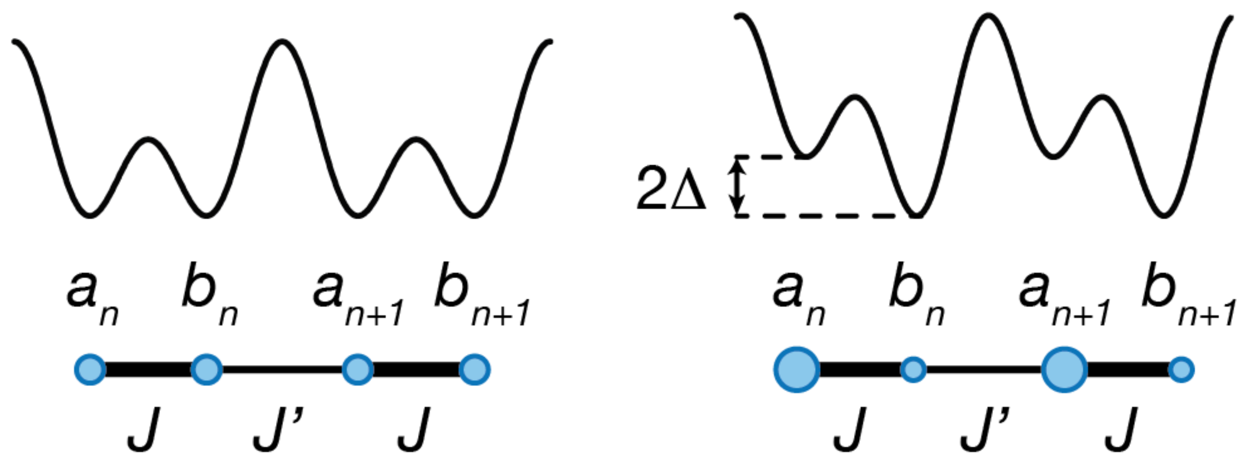


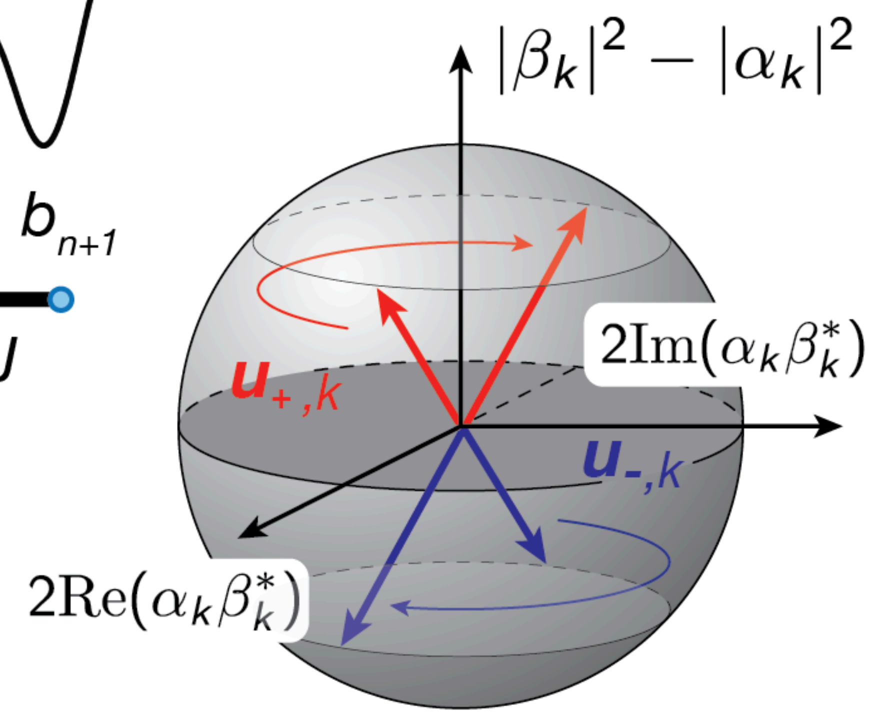


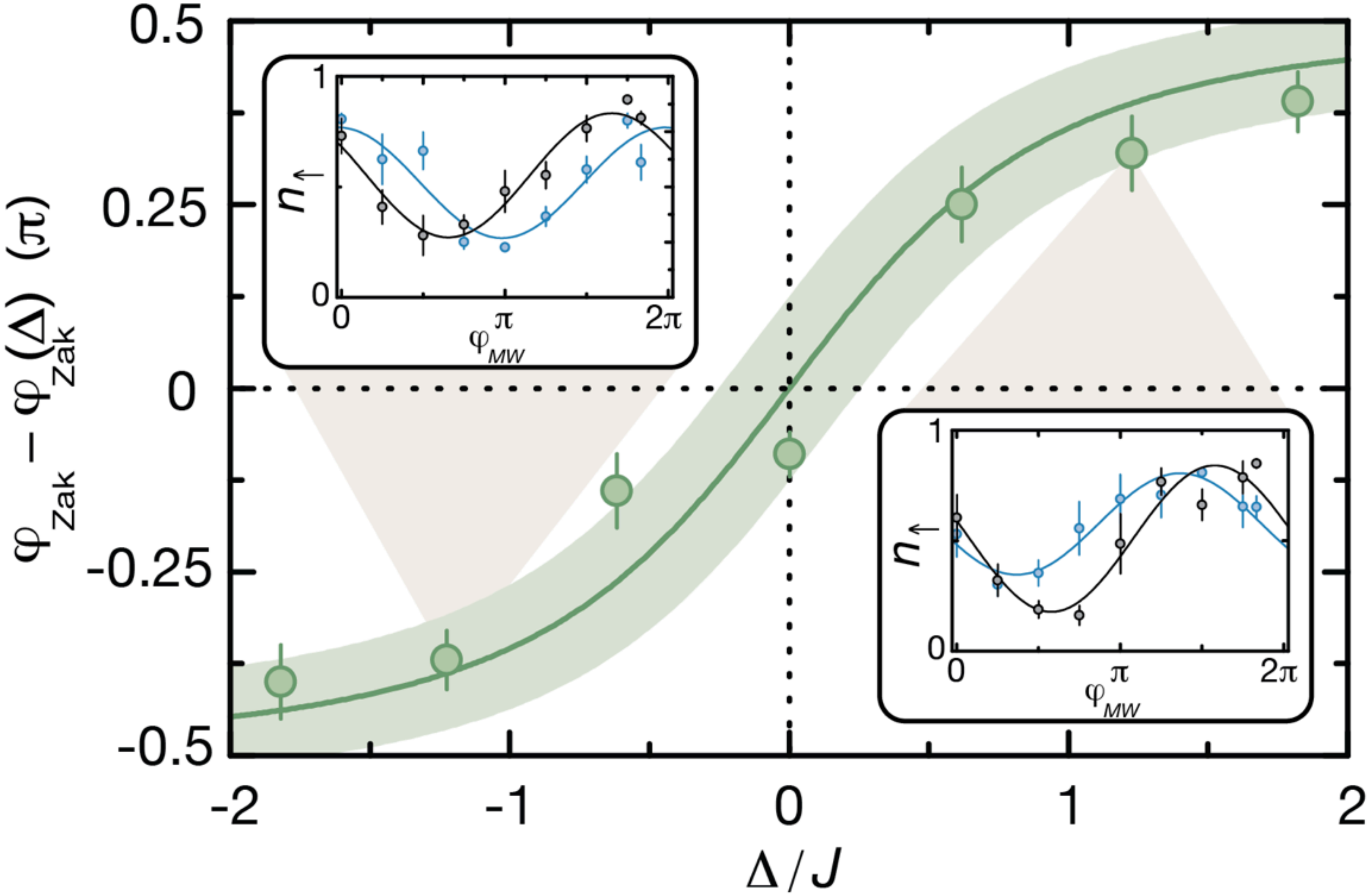


Zak Phase becomes **fractional** for heteropolar dimerization!

# Measuring Fractional Charge

## Probability Density of Eigenstates

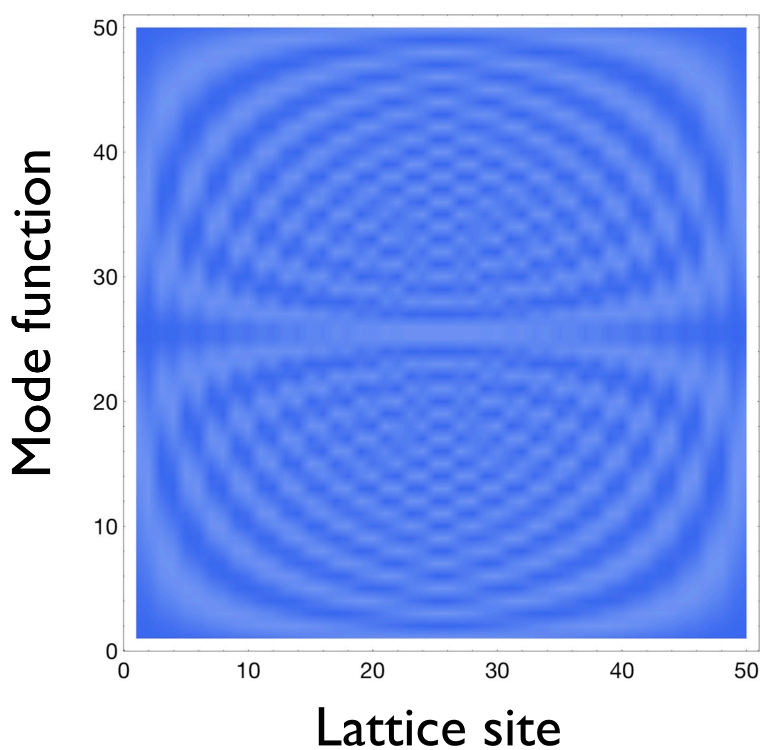


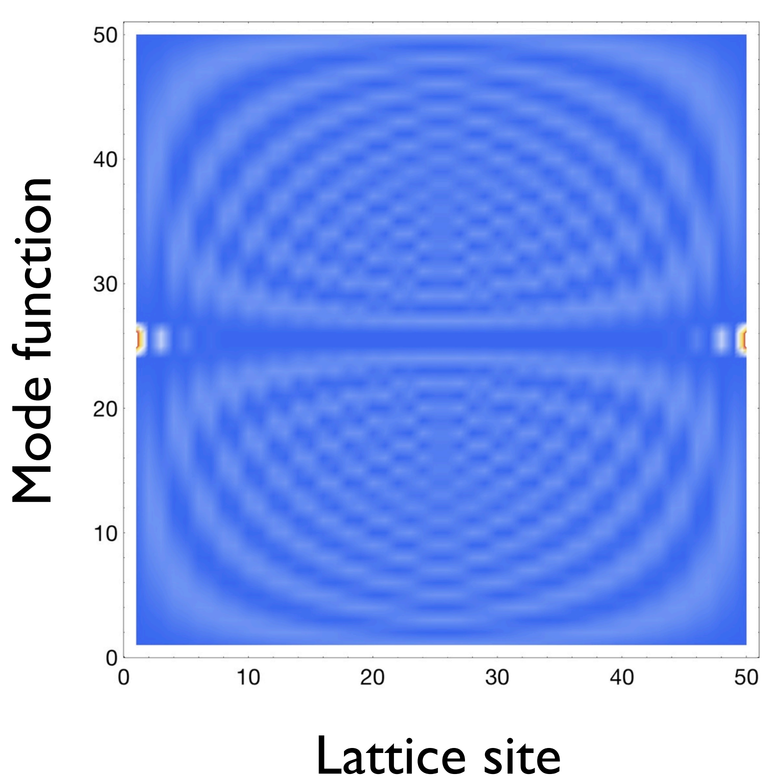


## Lattice Topology

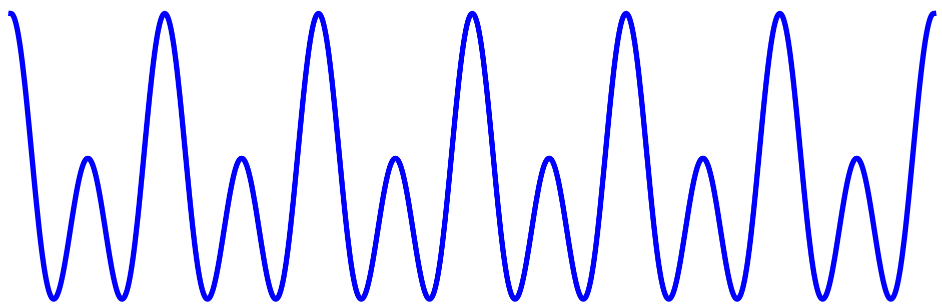

Topologically Trivial

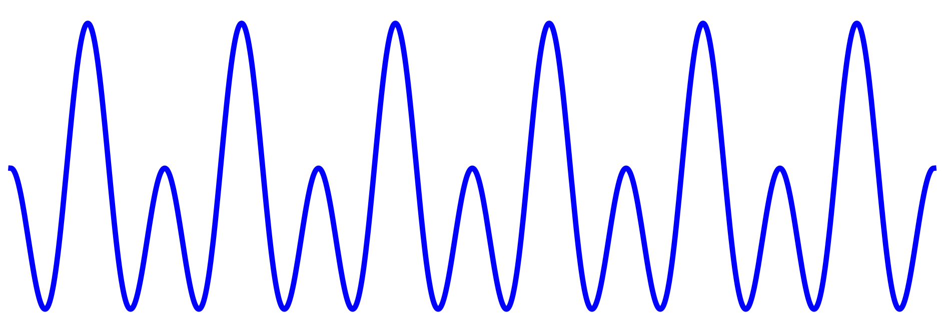

Topologically Non-Trivial

# Fractional Charge

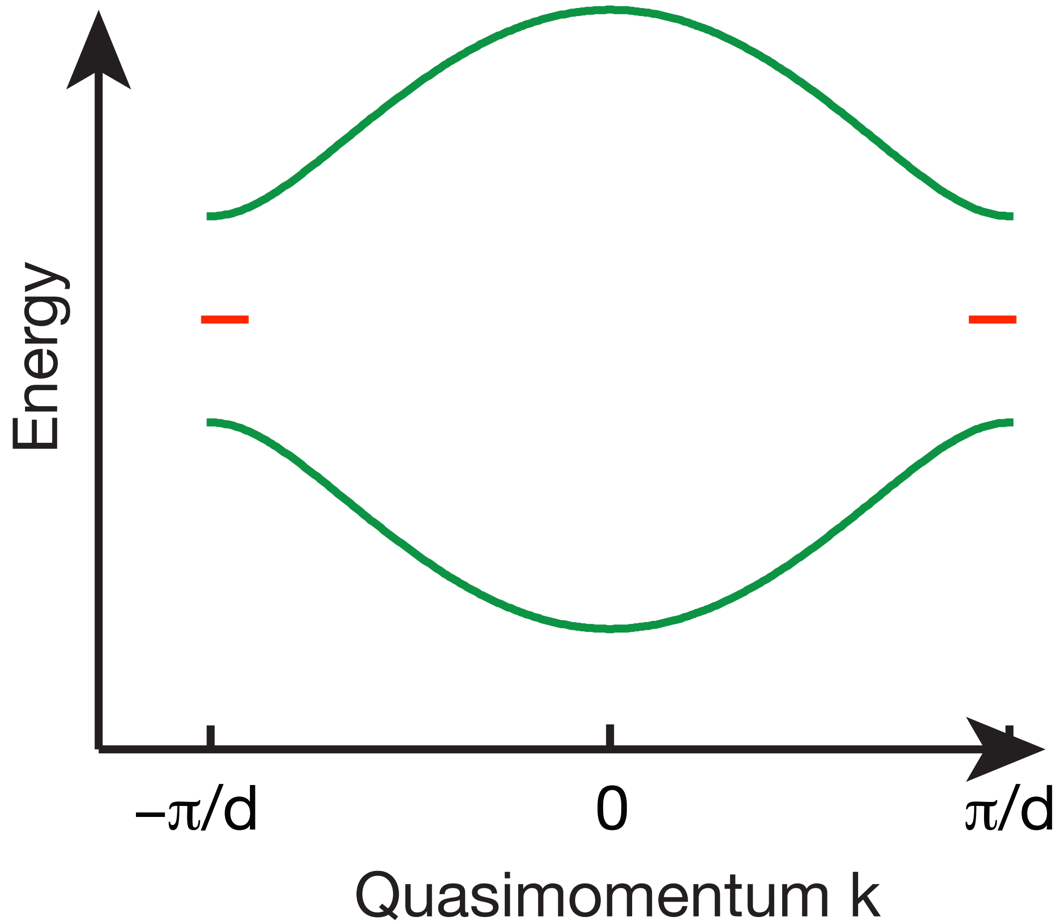


R. Rajaraman & J. Bell, Phys. Lett B 1982, Nucl. Phys. B 1983

# Fractional Charge

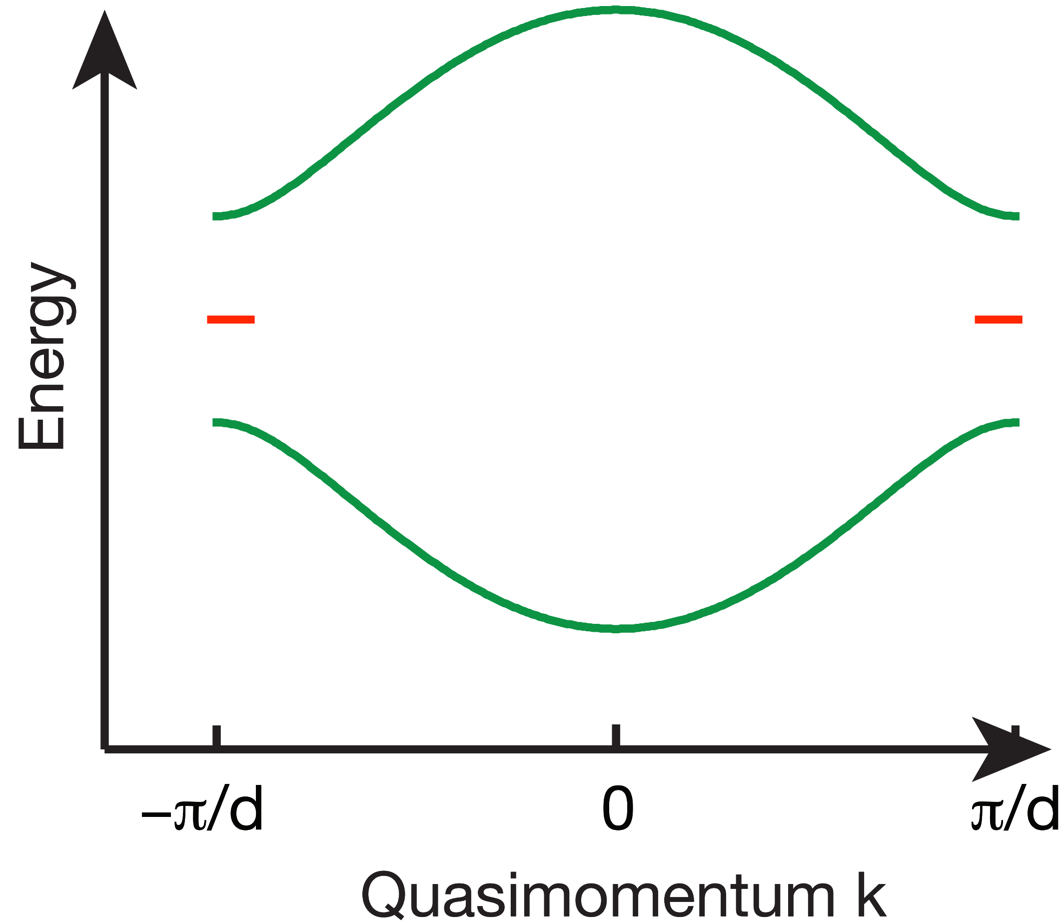


R. Rajaraman & J. Bell, Phys. Lett B 1982, Nucl. Phys. B 1983

# Fractional Charge

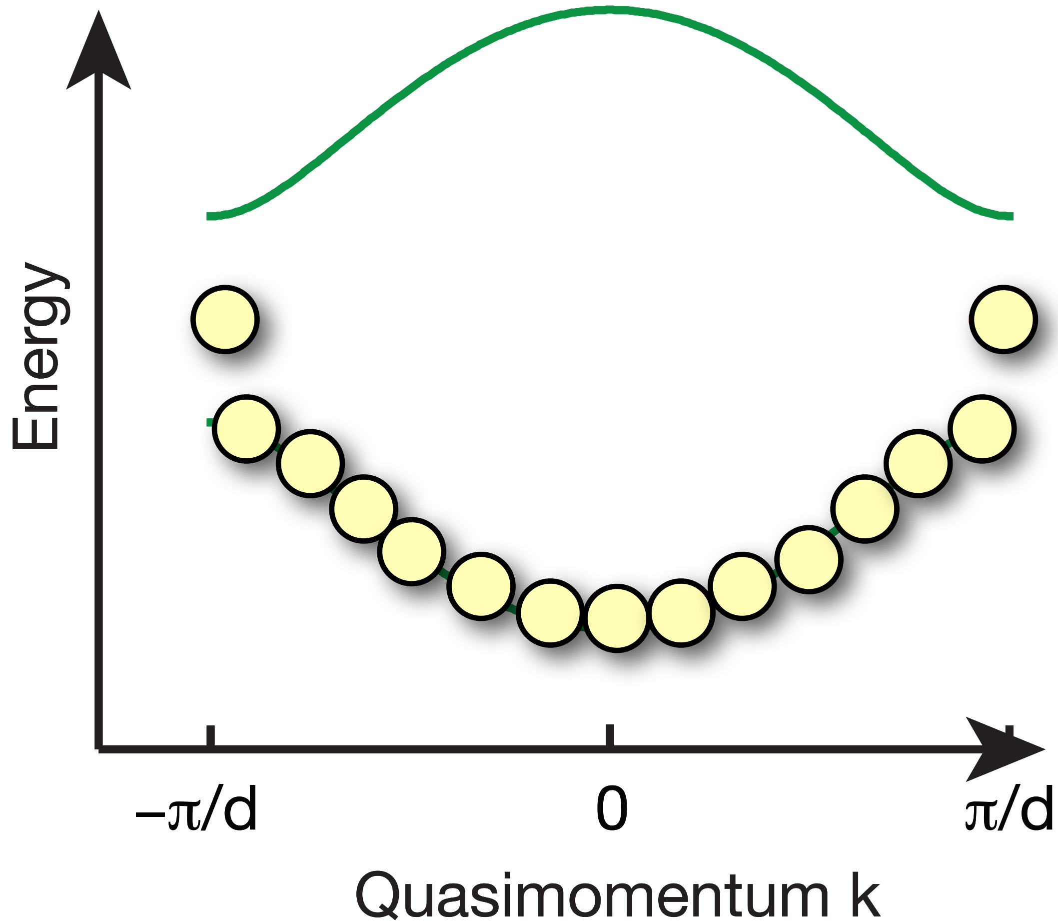


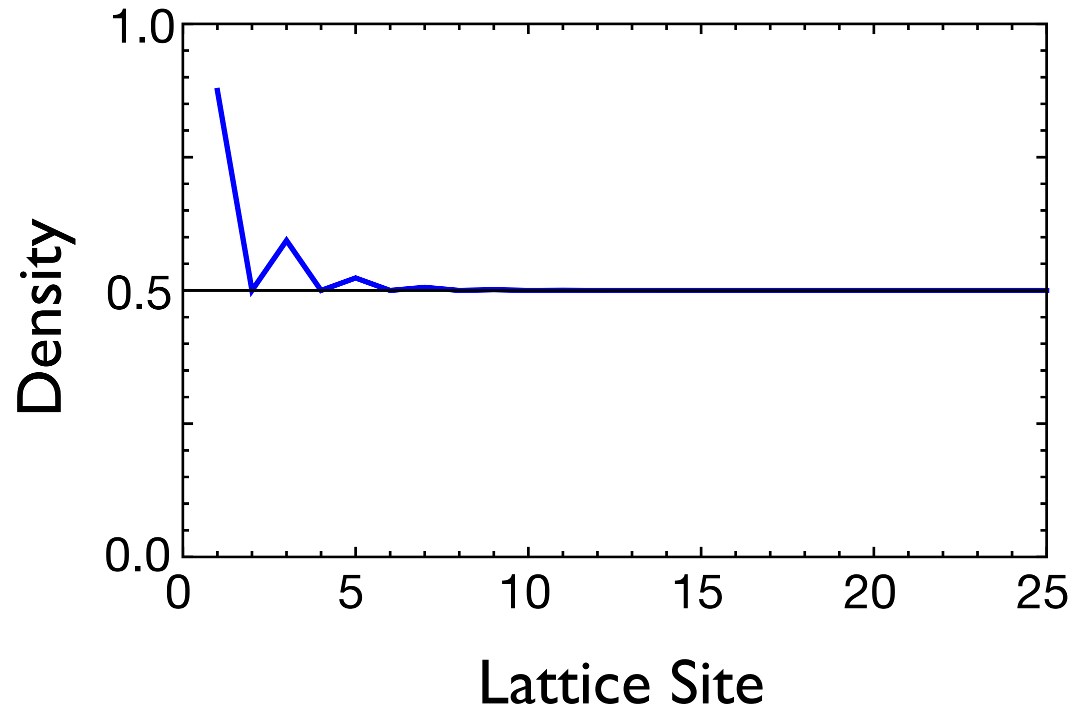


R. Rajaraman & J. Bell, Phys. Lett B 1982, Nucl. Phys. B 1983

# Fractional Charge

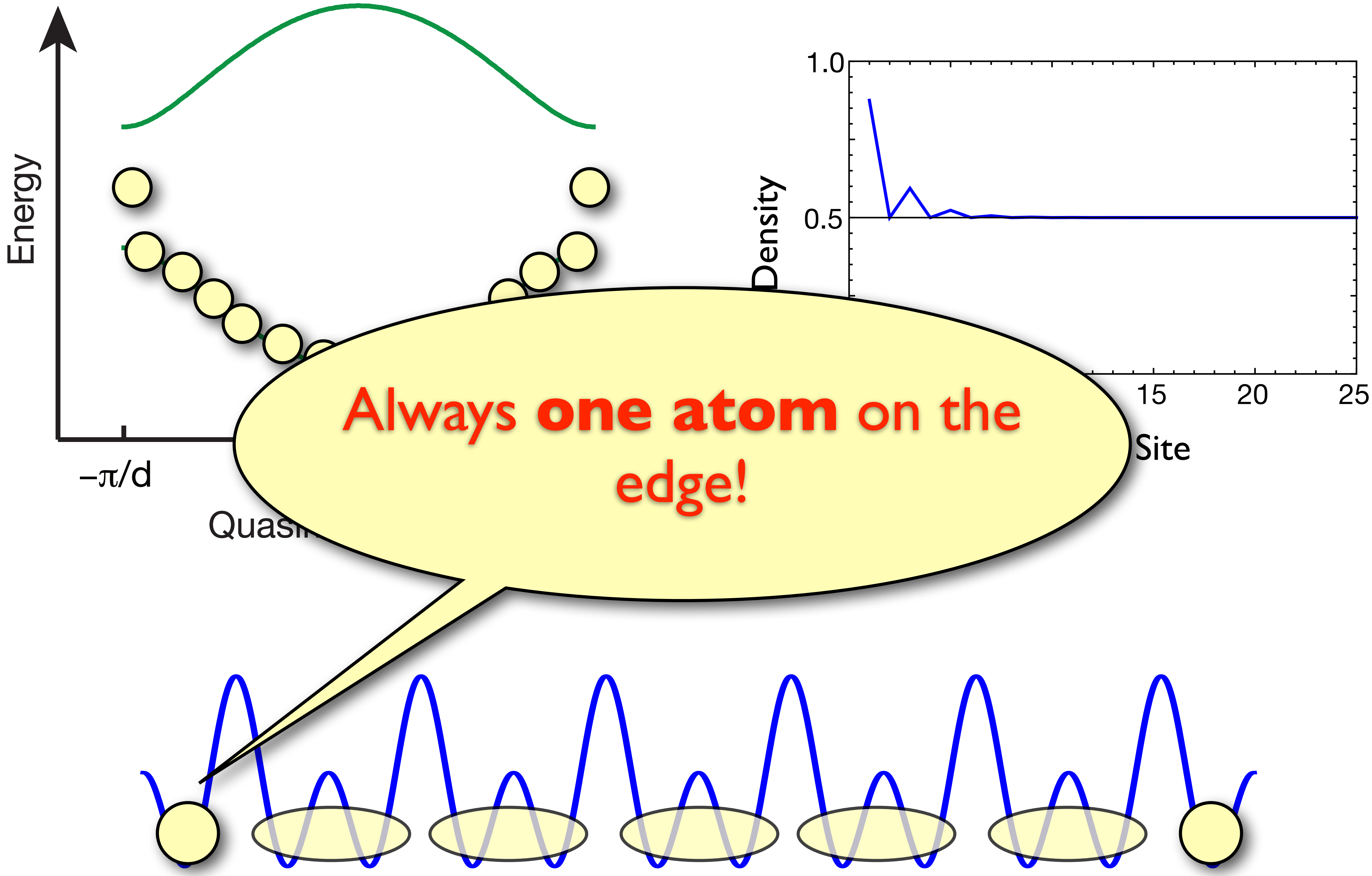


R. Rajaraman & J. Bell, Phys. Lett B 1982, Nucl. Phys. B 1983

# An Aharonov Bohm Interferomer for Determining Bloch Band Topology

$\pi$-Magnetic Flux

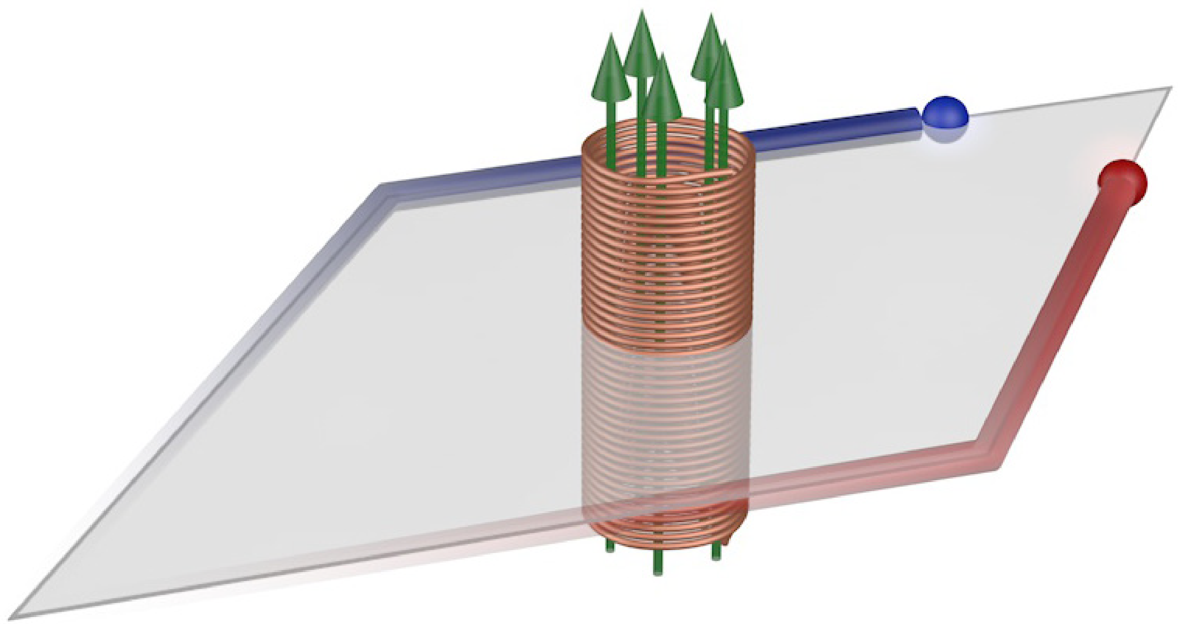

Real space

$\pi$-Berry Flux

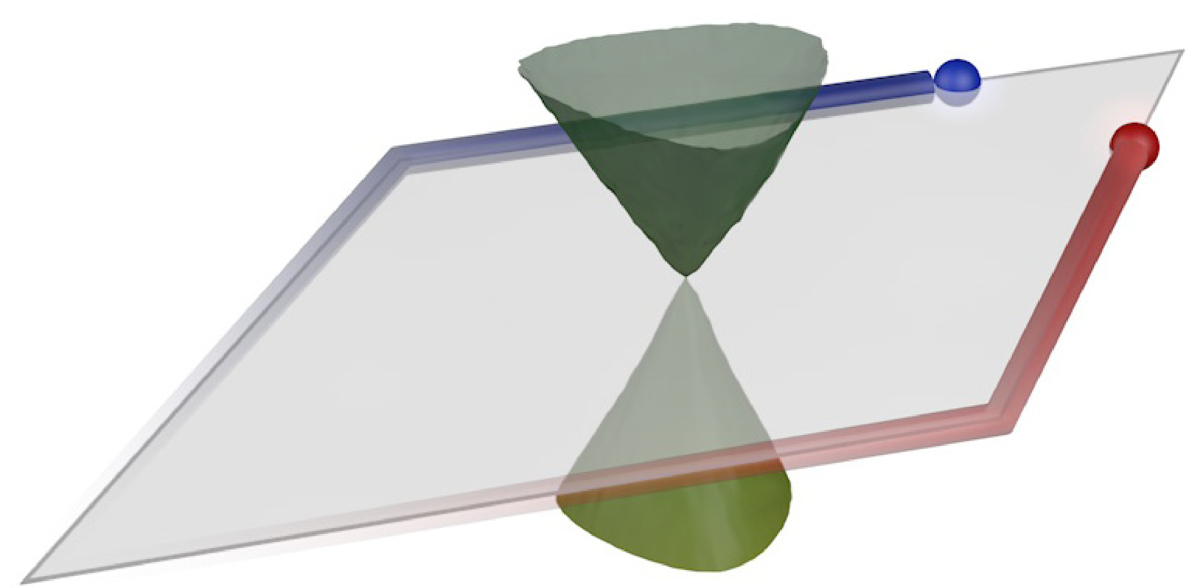

Crystal momentum space

D. Abanin E. Demler

D. Abanin et al. PRL **110**, 165304 (2013)

# Aharonov-Bohm Effect

**Real Space**

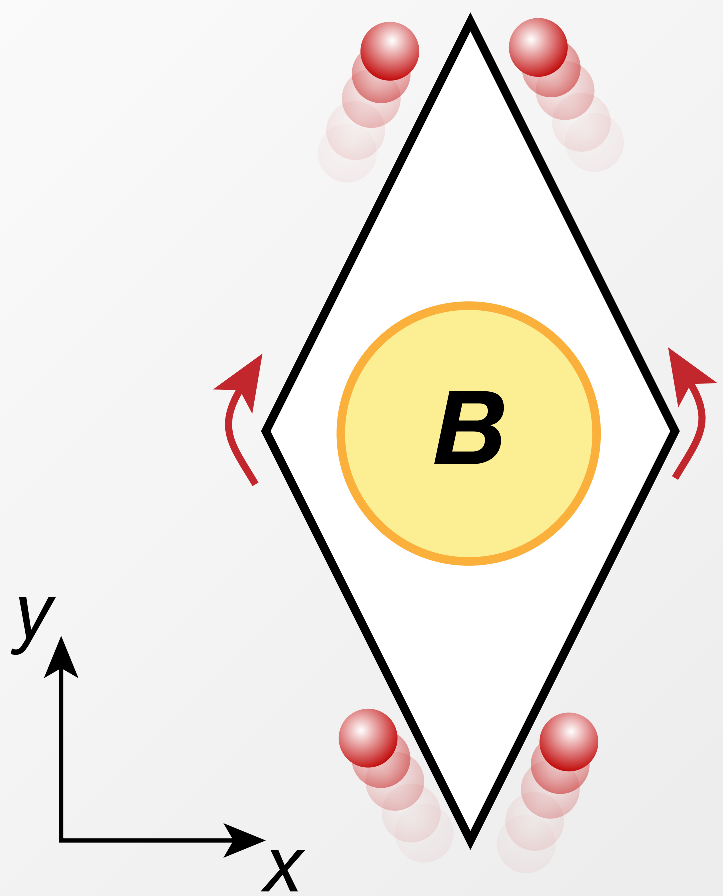


$$\varphi_{AB} = \frac{q}{\hbar}\oint_C \mathbf{A}(\mathbf{r})\,d\mathbf{r} = \frac{q}{\hbar}\int_S \nabla\times\mathbf{A}(\mathbf{r})\;d^2r$$

$$\boxed{\varphi_{AB} = \frac{q}{\hbar}\int \mathbf{B}\,d\mathbf{S} = 2\pi\Phi/\Phi_0}$$

*Aharonov-Bohm Phase*

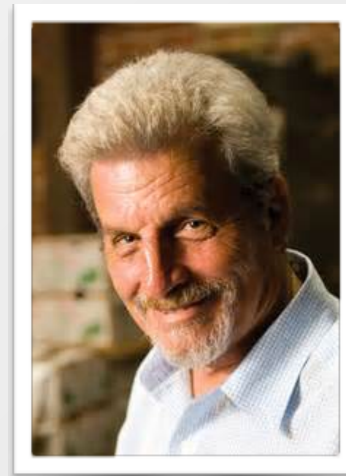

Y. Aharonov

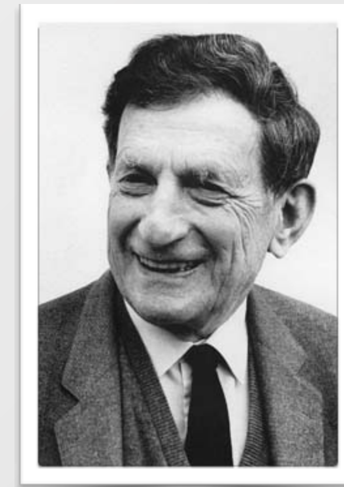

D. Bohm

..., contrary to the conclusions of classical mechanics, **there exist effects of potentials on charged particles, even in the region where all the fields (and therefore the forces on the particles) vanish.**

Y. Aharonov & D. Bohm Phys. Rev.(1959)
W. Ehrenberg & R. Siday Proc. Phys. Soc B (1949)
**Exp:** A. Tonomura, et al. Phys. Rev. Lett. (1986)

# Hexagonal Lattices

**Lattice:** A and B degenerate sublattices

$$H = H_0 - J \sum_{\mathbf{R}} \sum_{i=1}^{3} \left( \hat{a}_{\mathbf{R}} \hat{b}^{\dagger}_{\mathbf{R}+\mathbf{d}_i} + \text{h.c.} \right)$$

Real Space

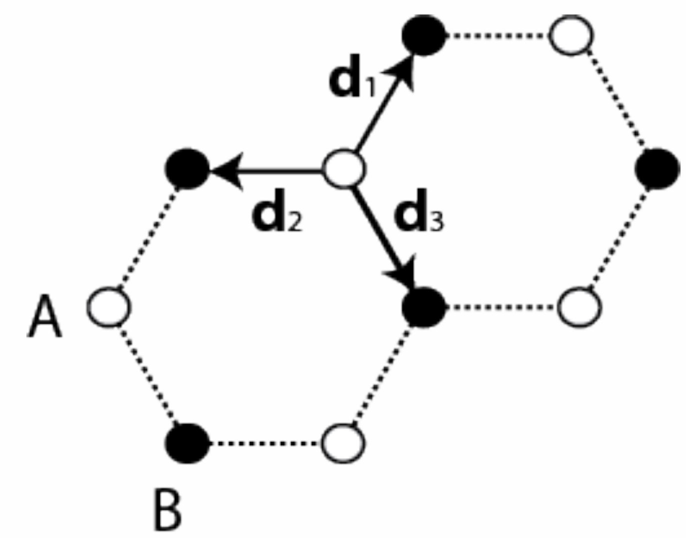


**Lowest energy bands:**

**Dirac points** at the corners of the first BZ

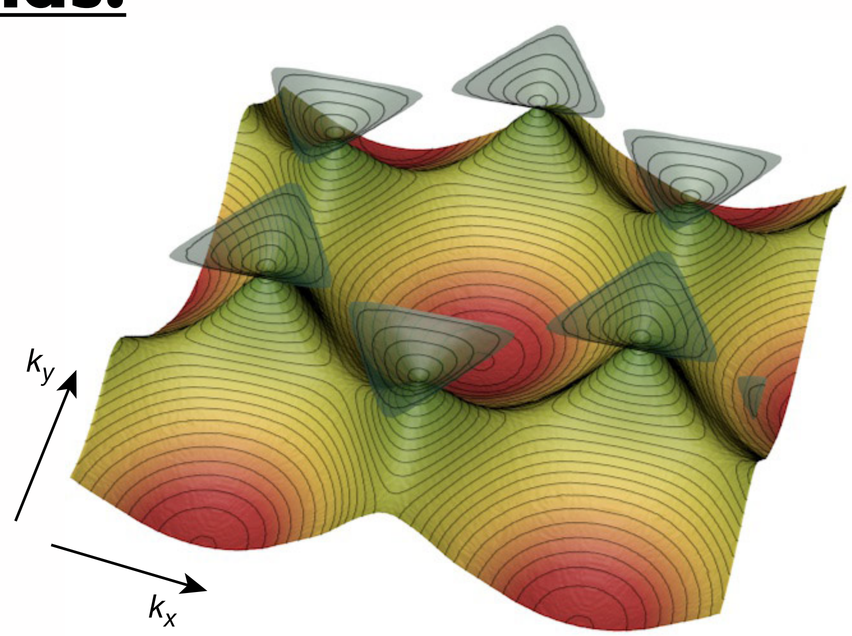


Reciprocal Space

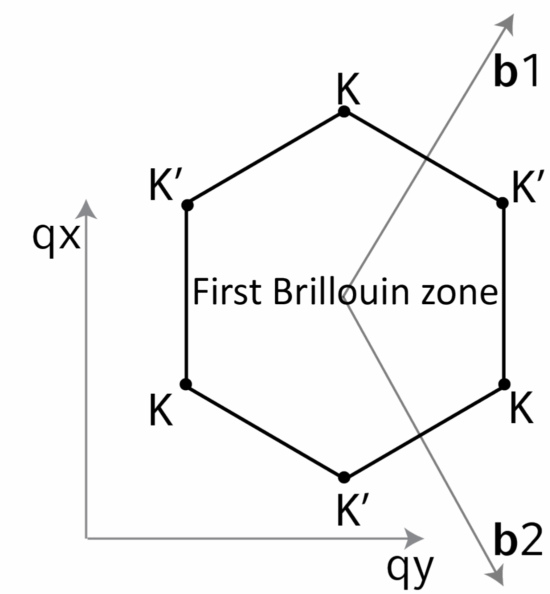


A. Castro Neto et al., Rev. Mod. Phys. **81**, 109 (2009)

**cold atoms:** hexagonal - K. Sengtsock (Hamburg), brick wall - T. Esslinger (Zürich)

# Scalar & Geometric Features

Band structure characterized by **scalar** & **geometric** features!

Eigenstates: Bloch waves $\boxed{\psi_{\mathbf{q},n}(\mathbf{r}) = e^{i\mathbf{q}\mathbf{r}} u_{\mathbf{q},n}(\mathbf{r})}$

## Scalar Features

Dispersion relation

$$E_{\mathbf{q},n}$$

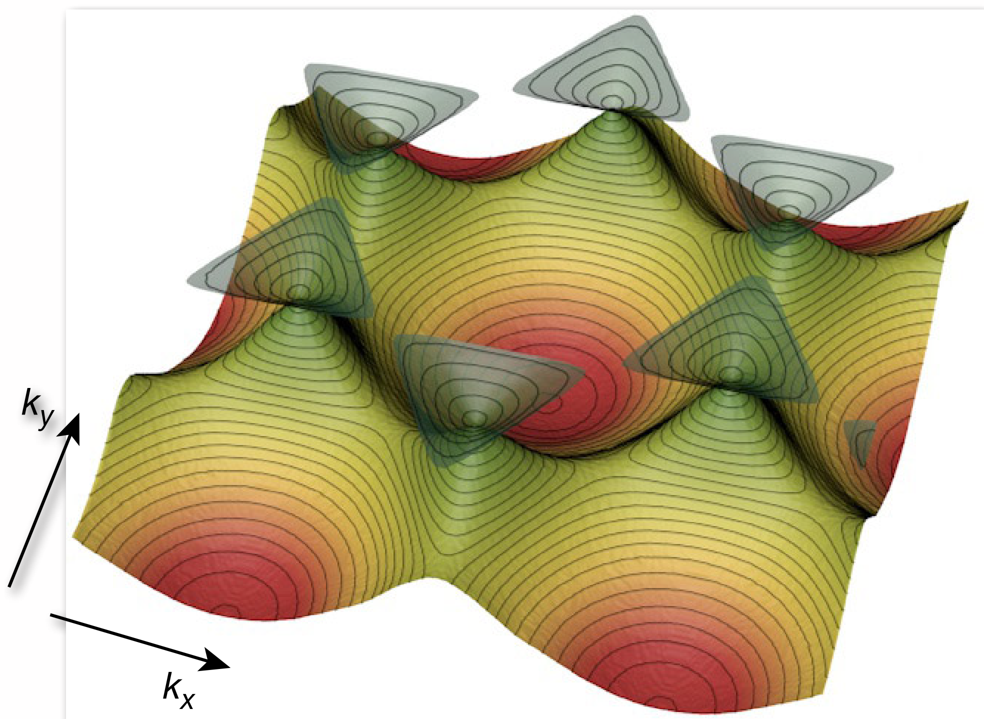


## Geometric Features

Berry connection

$$\mathbf{A}_n(\mathbf{q}) = i\langle u_{\mathbf{q},n}|\nabla_{\mathbf{q}}|u_{\mathbf{q},n}\rangle$$

Berry curvature

$$\Omega_n(\mathbf{q}) = \nabla_{\mathbf{q}} \times \mathbf{A}_{\mathbf{n}}(\mathbf{q}) \cdot \mathbf{e}_z$$

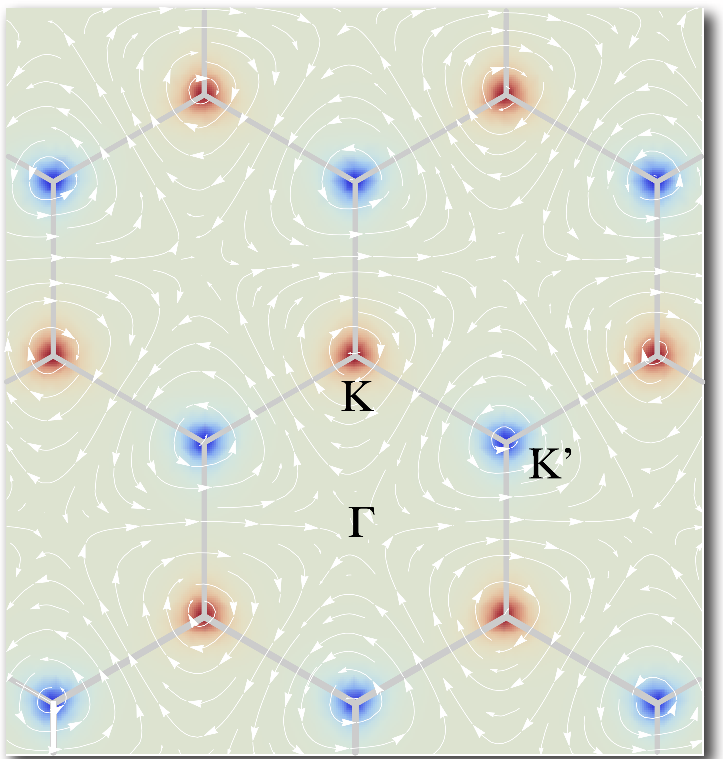

# Mapping the dispersion relation

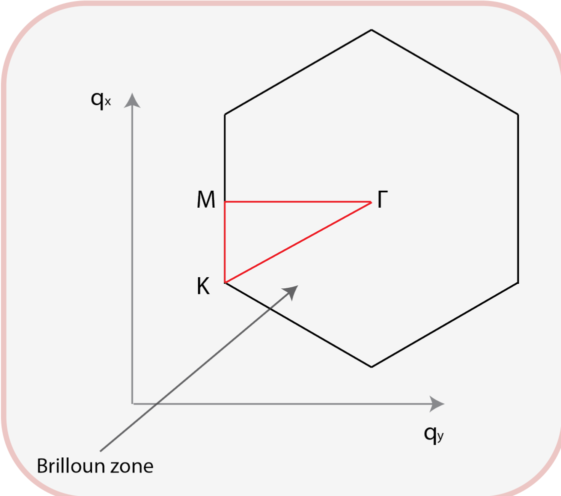


Mapped path

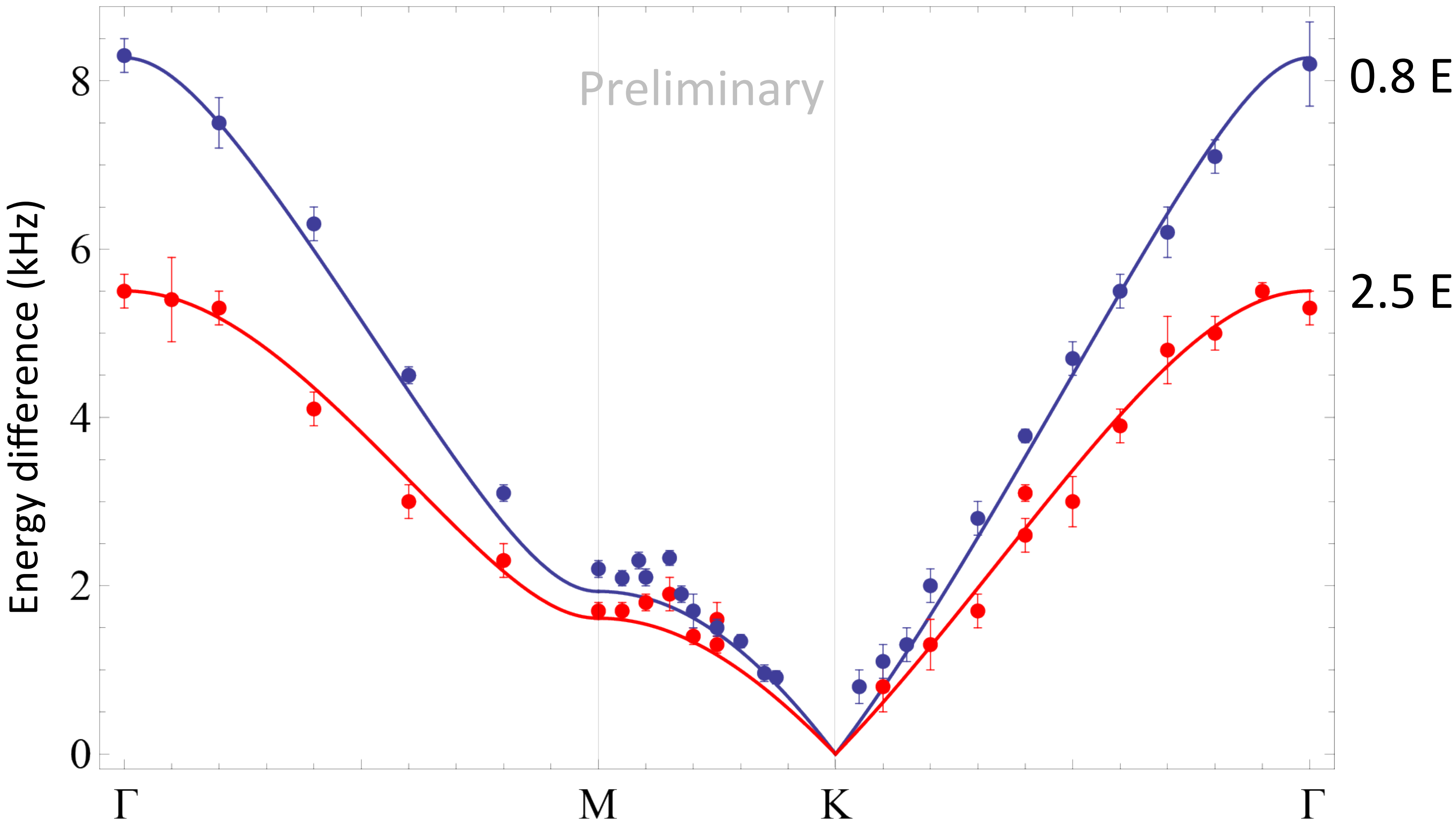


- Energy difference at the K point <10% of lattice bandwidth!

# ‘Aharonov Bohm’ Interferometer in Momentum Space

## Real Space

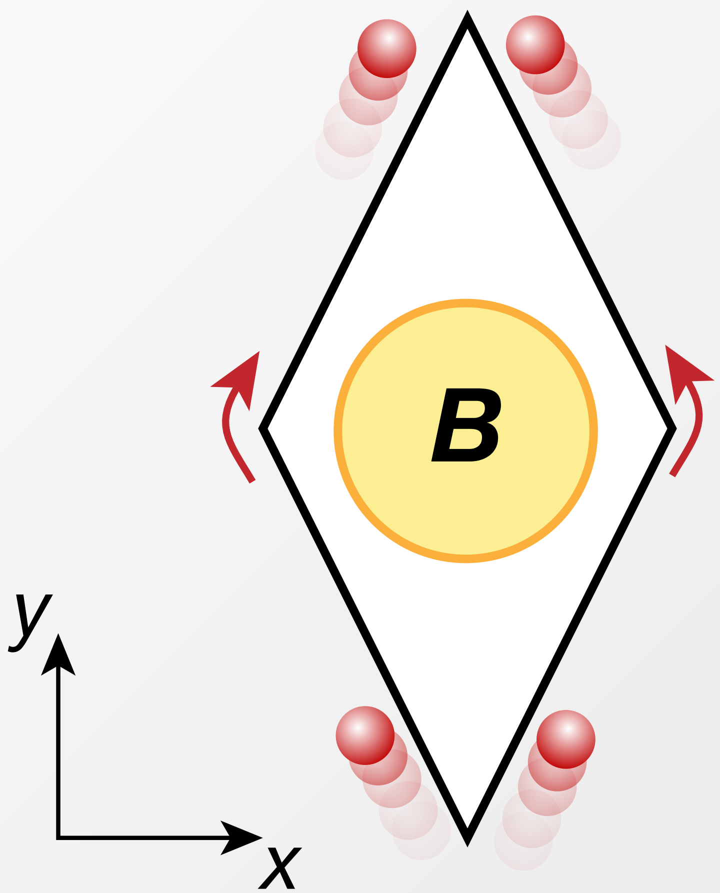


$$\varphi_{AB} = \frac{q}{\hbar}\oint_C \mathbf{A}(\mathbf{r})\, d\mathbf{r} = \frac{q}{\hbar}\int_S \nabla \times \mathbf{A}(\mathbf{r})\, d^2 r$$

$$\boxed{\varphi_{AB} = \frac{q}{\hbar}\int \mathbf{B}\, d\mathbf{S} = 2\pi\Phi/\Phi_0}$$

*Aharonov-Bohm Phase*

# 'Aharonov Bohm' Interferometer in Momentum Space

## Real Space

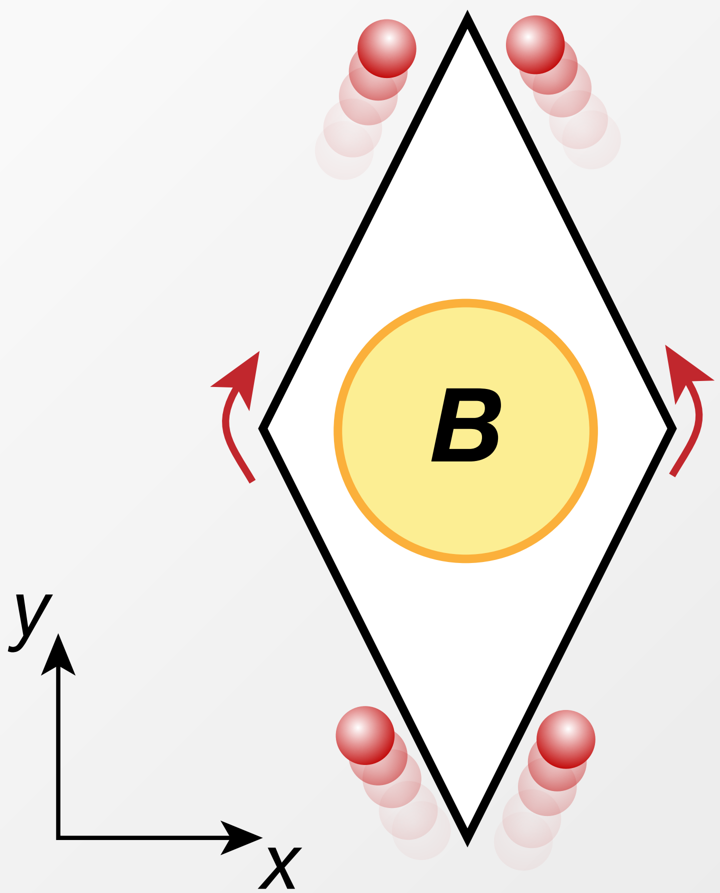


$$\varphi_{AB} = \frac{q}{\hbar}\oint_C \mathbf{A}(\mathbf{r})\, d\mathbf{r} = \frac{q}{\hbar}\int_S \nabla \times \mathbf{A}(\mathbf{r})\; d^2 r$$

$$\boxed{\varphi_{AB} = \frac{q}{\hbar}\int \mathbf{B}\, d\mathbf{S} = 2\pi\Phi/\Phi_0}$$

*Aharonov-Bohm Phase*

## Momentum Space

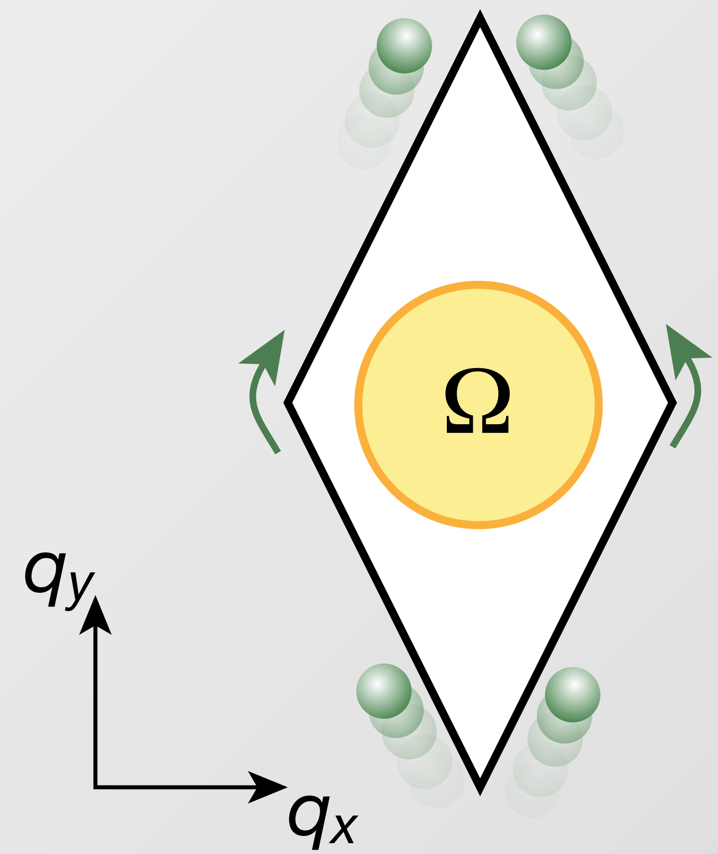


$$\varphi_{\text{Berry}} = \oint_C \mathbf{A}_n(\mathbf{q})\, d\mathbf{q} = \int_{S_q} \nabla \times \mathbf{A}_n(\mathbf{r})\; d\mathbf{S}_q$$

$$\boxed{\varphi_{\text{Berry}} = \int \Omega_n(\mathbf{q})\, d\mathbf{S}_q}$$

*Berry Phase*

# Berry Curvature in Hexagonal Lattices

Berry curvature **concentrated to Dirac cones, alternating in sign**!

Breaking time reversal or inversion symmetry gaps Dirac cones
and spreads Berry curvature out

Hexagonal Lattice Hamiltonian

$$H(\mathbf{q}) = \begin{pmatrix} \Delta & f(\mathbf{q}) \\ f(\mathbf{q}) & -\Delta \end{pmatrix}$$

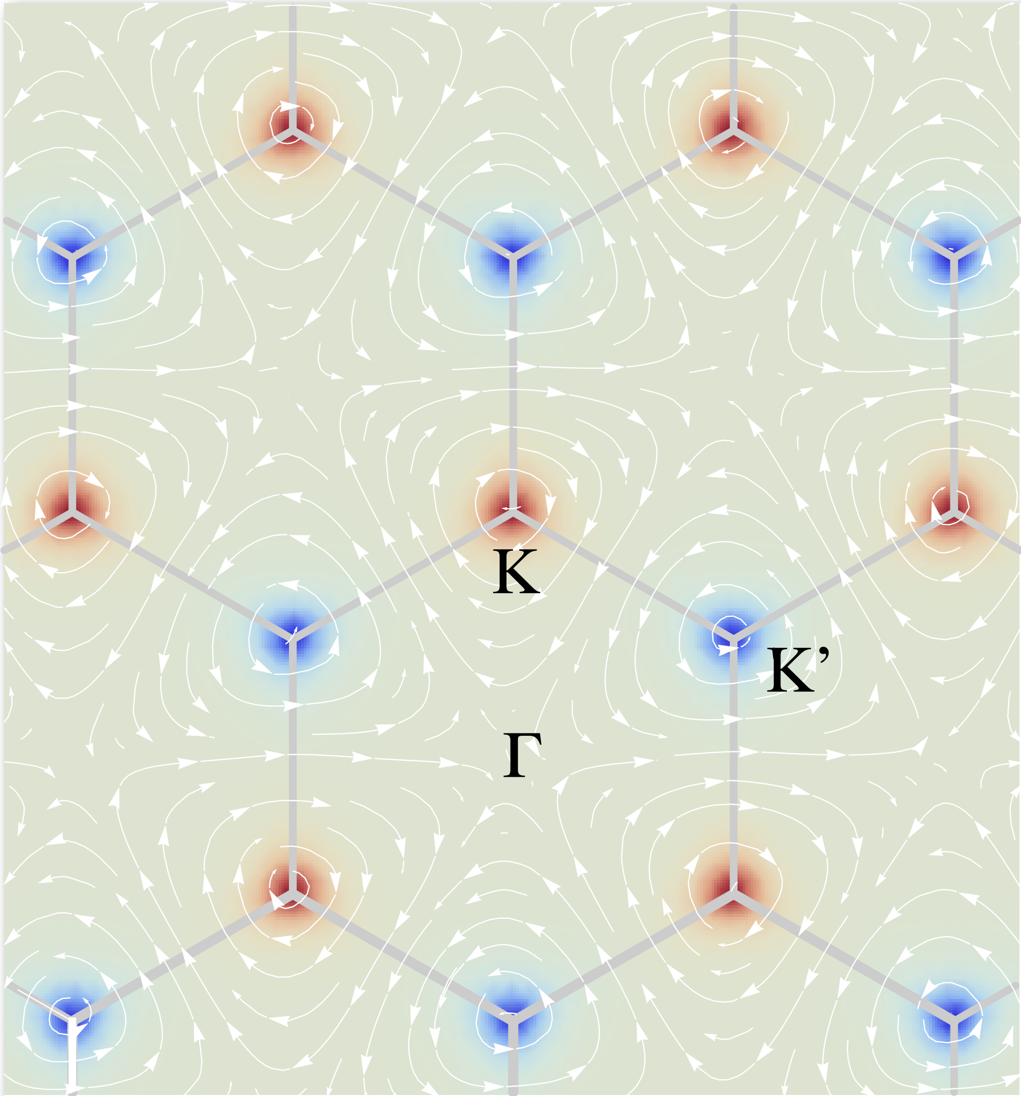


Expanding momenta close to K Dirac point

$$H(\tilde{\mathbf{q}}) = \begin{pmatrix} 0 & \tilde{q}_x + i\tilde{q}_y \\ \tilde{q}_x - i\tilde{q}_y & 0 \end{pmatrix}$$

Eigenstates

$$u^{\pm}_{\mathbf{K},\tilde{\mathbf{q}}} = \frac{1}{2}\left(e^{i\theta(\mathbf{q})/2} \pm e^{-i\theta(\mathbf{q})/2}\right)$$

# Berry Phases in Graphene

Berry Phase around K-Dirac cone

$$\varphi_{\text{Berry},\mathbf{K}} = \oint_C \mathbf{A}(\mathbf{q})\, d\mathbf{q} = \pi$$

Berry Phase around K'-Dirac cone

$$\varphi_{\text{Berry},\mathbf{K}'} = -\pi$$

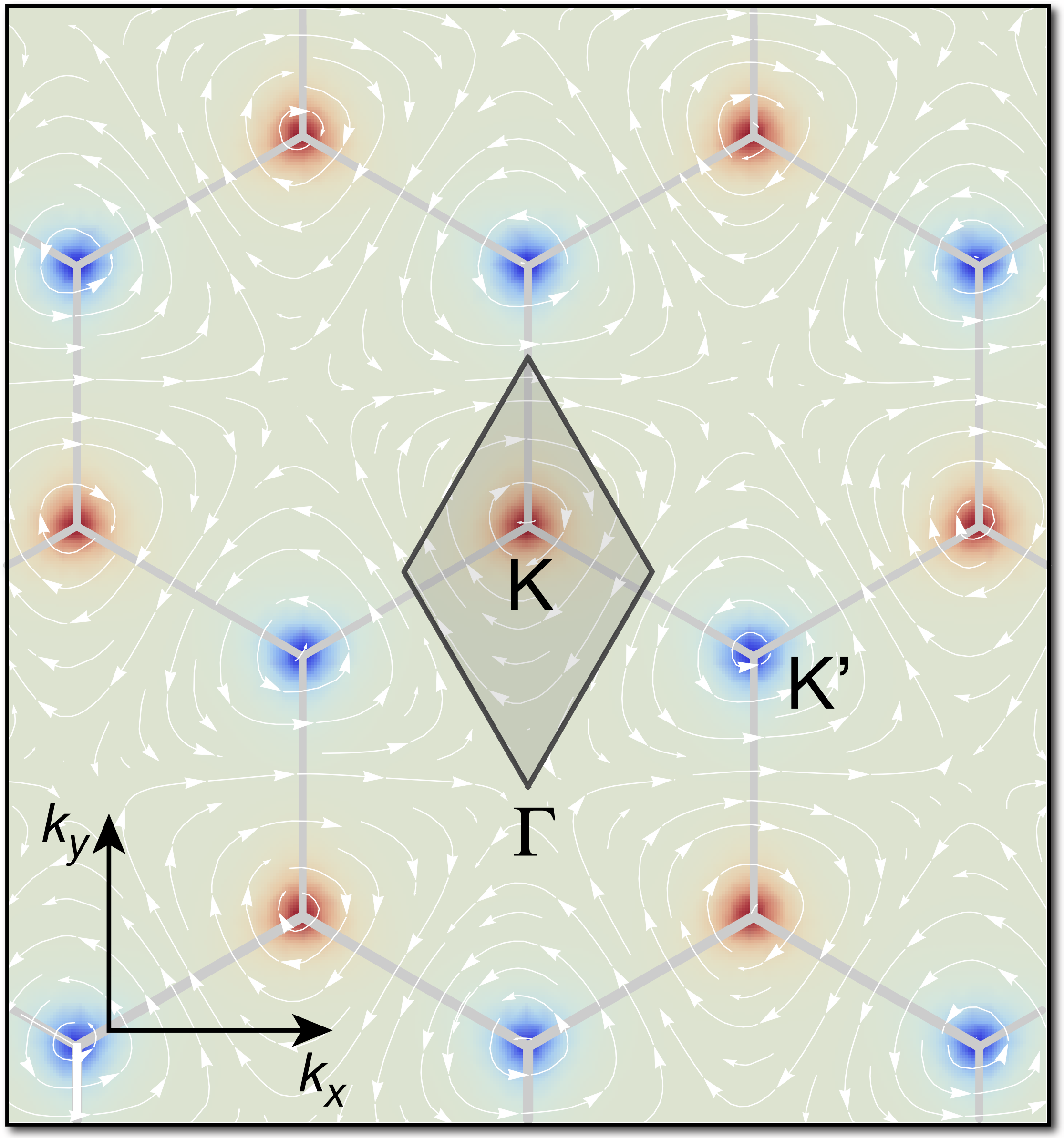

# Accelerating the Lattice

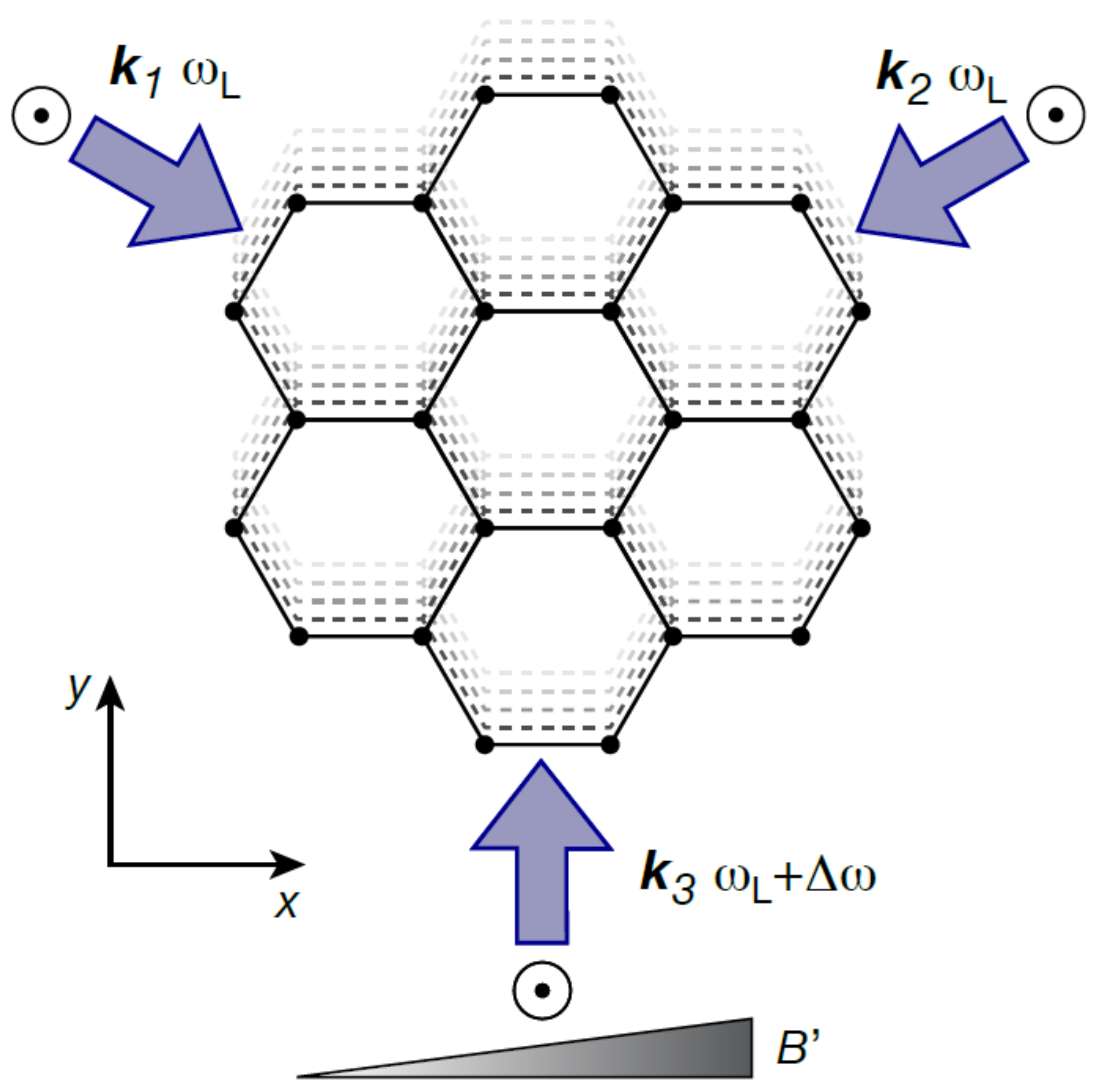


*Arbitrary accelerations in any direction can be applied!*

# The Interferometer

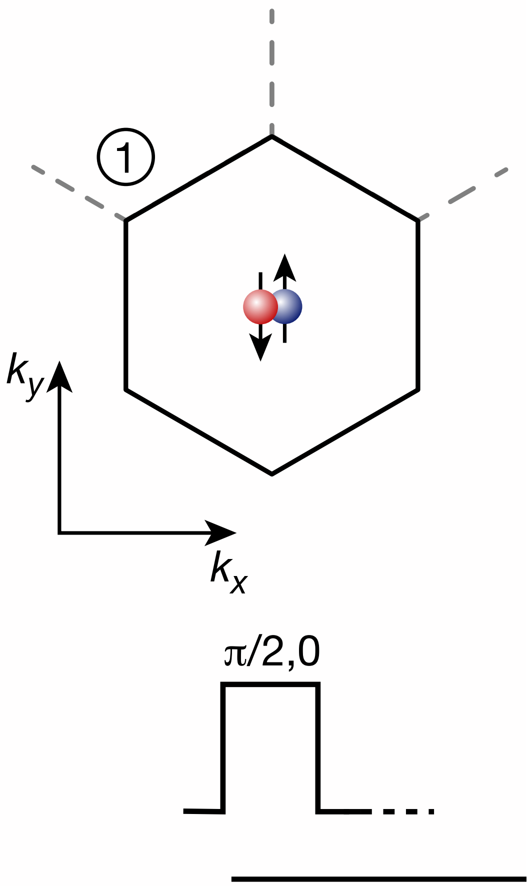


Forces applied by **lattice acceleration** and **magnetic gradients**!

# The Interferometer

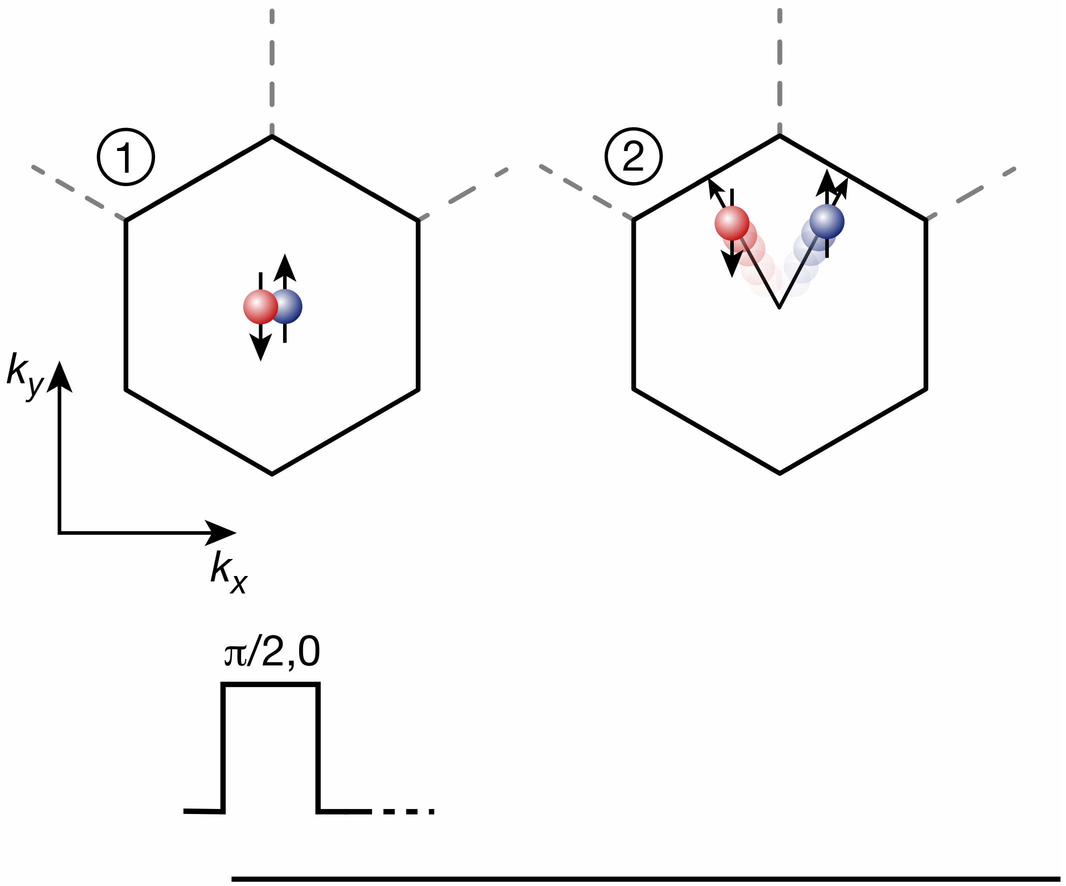


Forces applied by **lattice acceleration** and **magnetic gradients**!

# The Interferometer

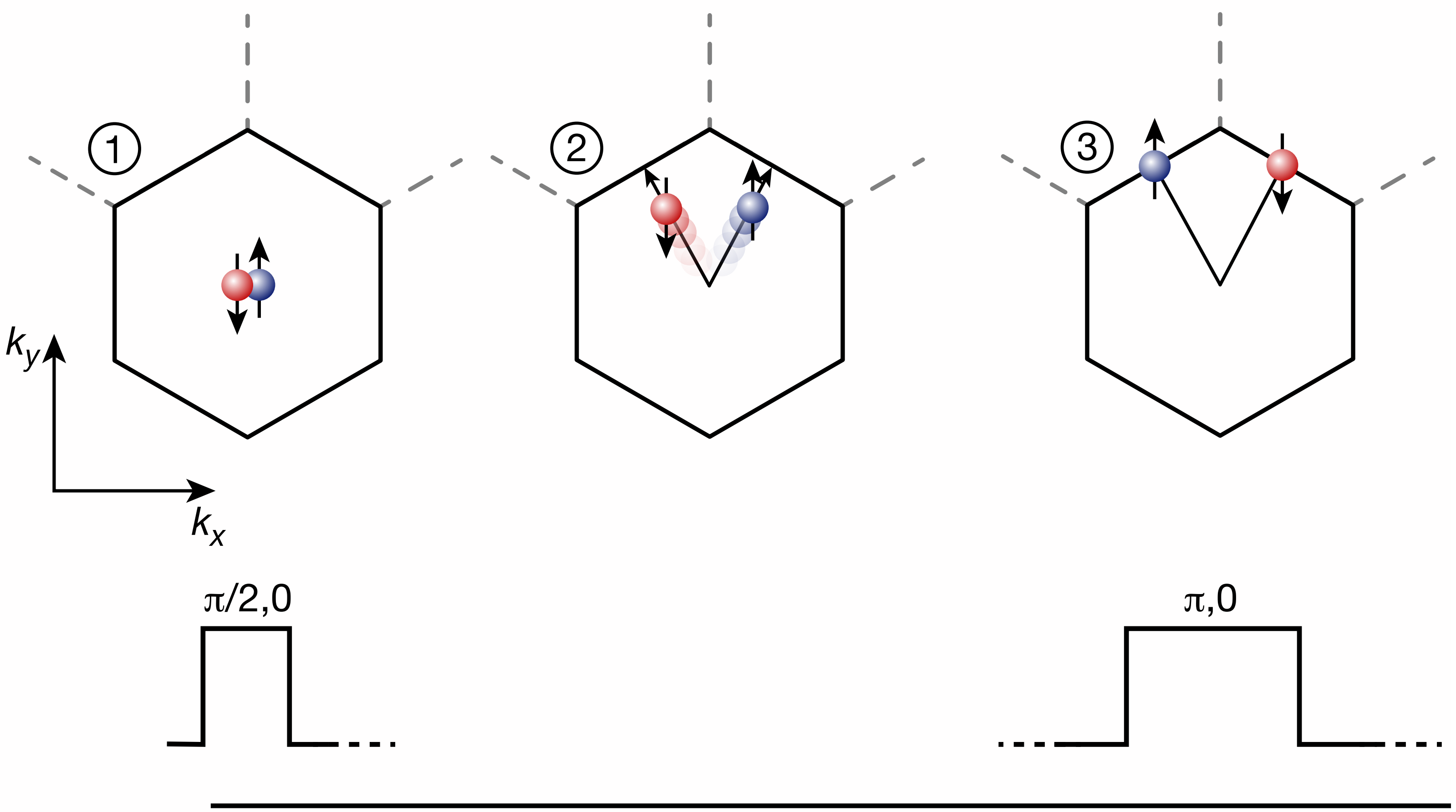


Forces applied by **lattice acceleration** and **magnetic gradients**!

# The Interferometer

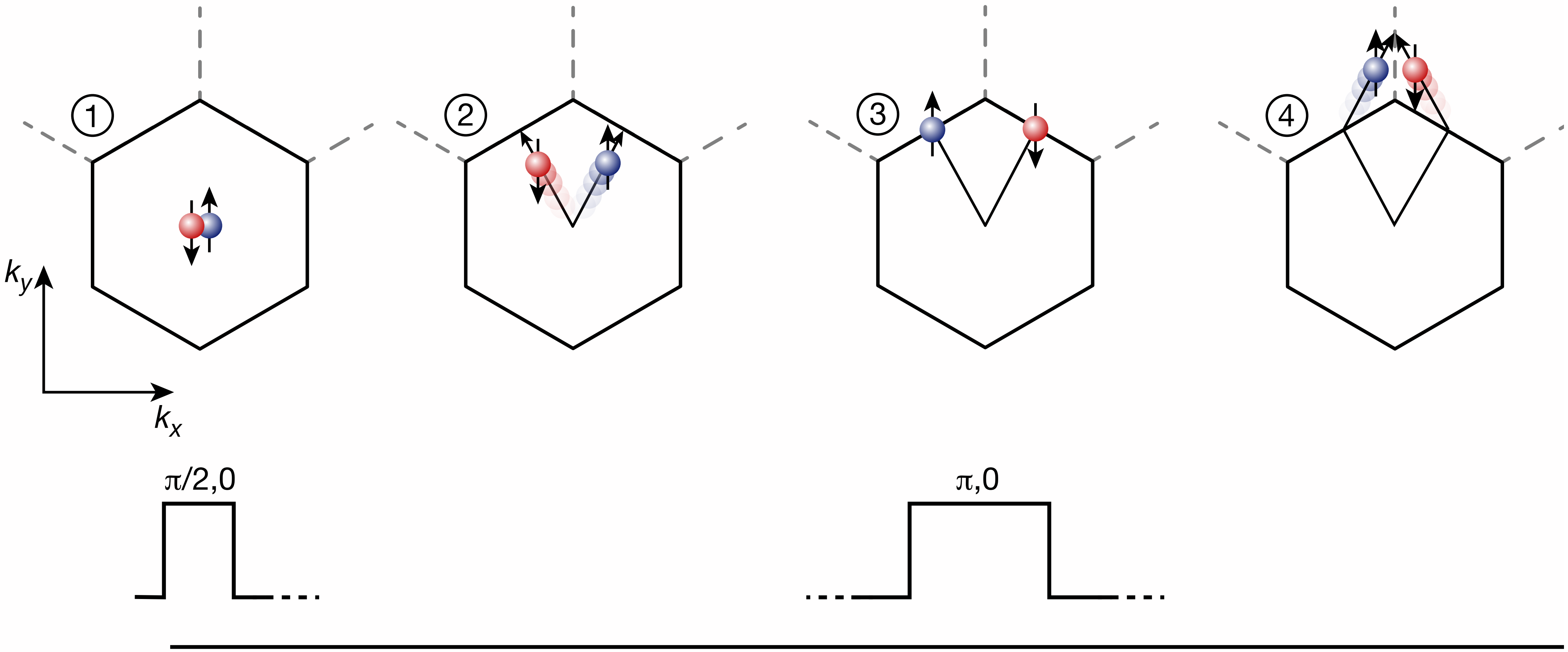


Forces applied by **lattice acceleration** and **magnetic gradients**!

# The Interferometer

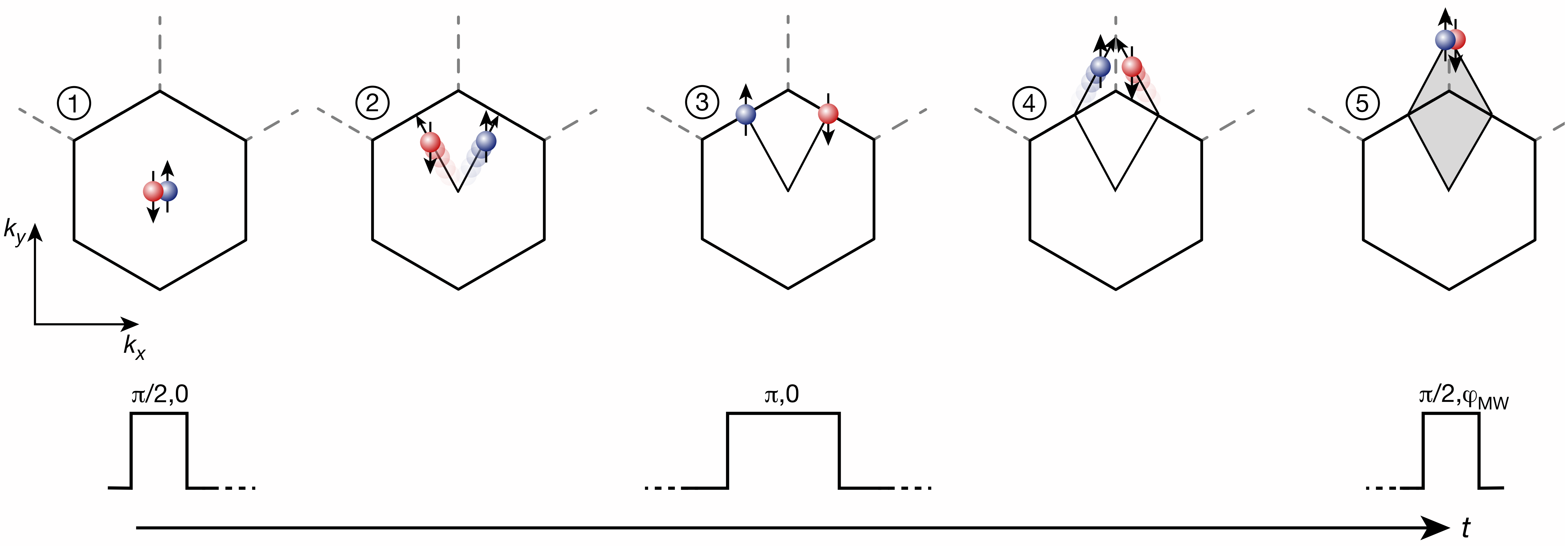


Forces applied by **lattice acceleration** and **magnetic gradients**!

# Stückelberg Interferometry

# Accelerating the Lattice

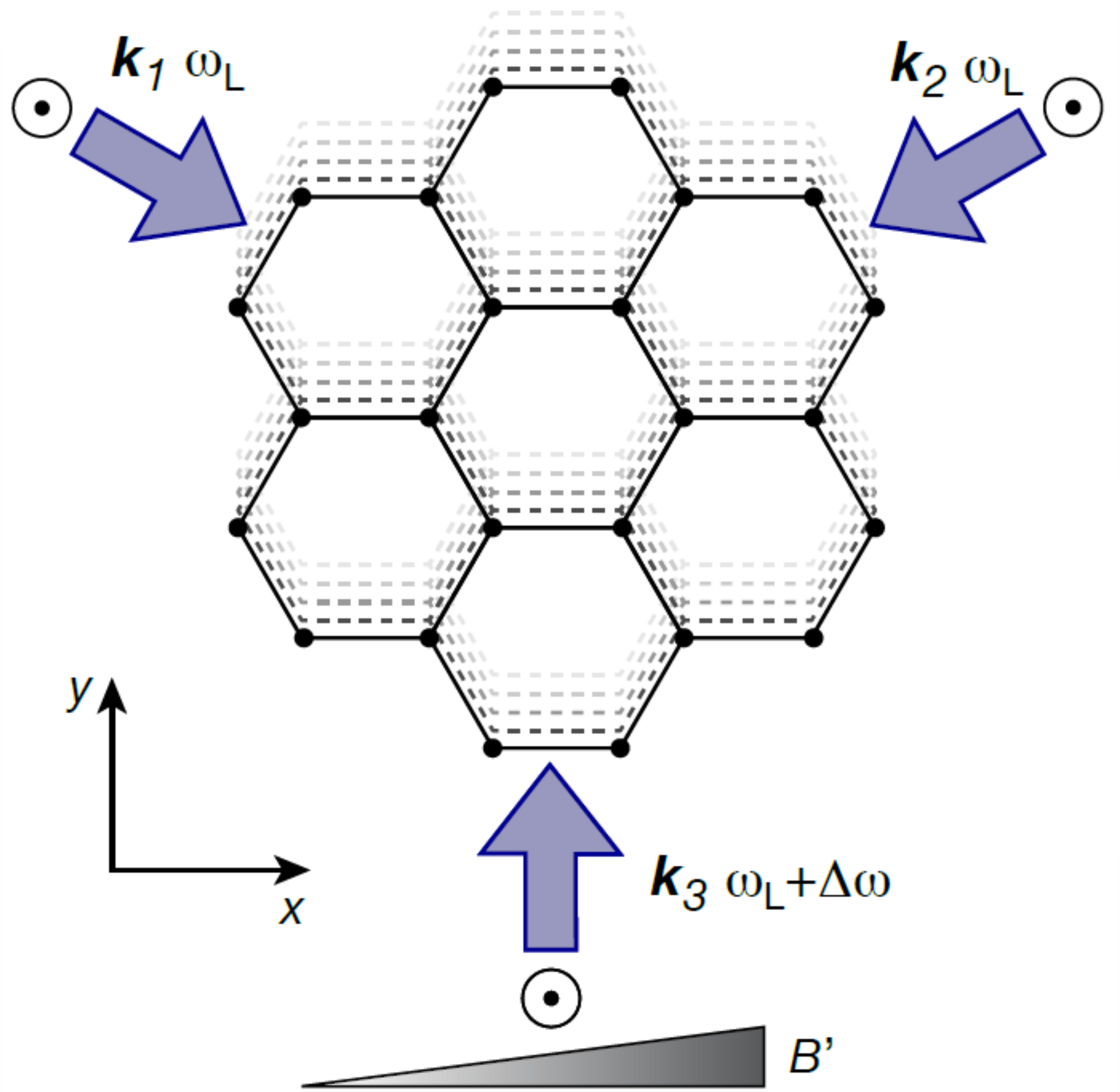


*Arbitrary accelerations in any direction can be applied!*

# Bloch Oscillations

Bloch oscillations induced by accelerating the lattice

**weaker force**

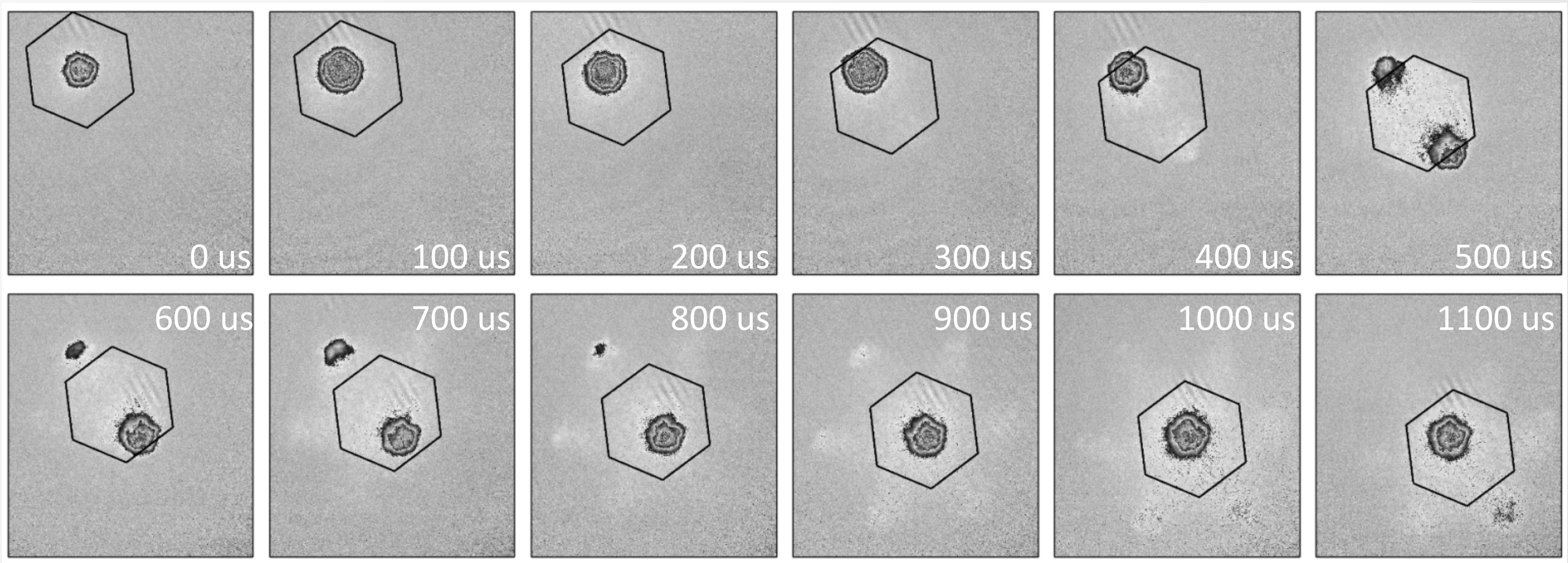


*quasi-momentum distribution*

**stronger force**

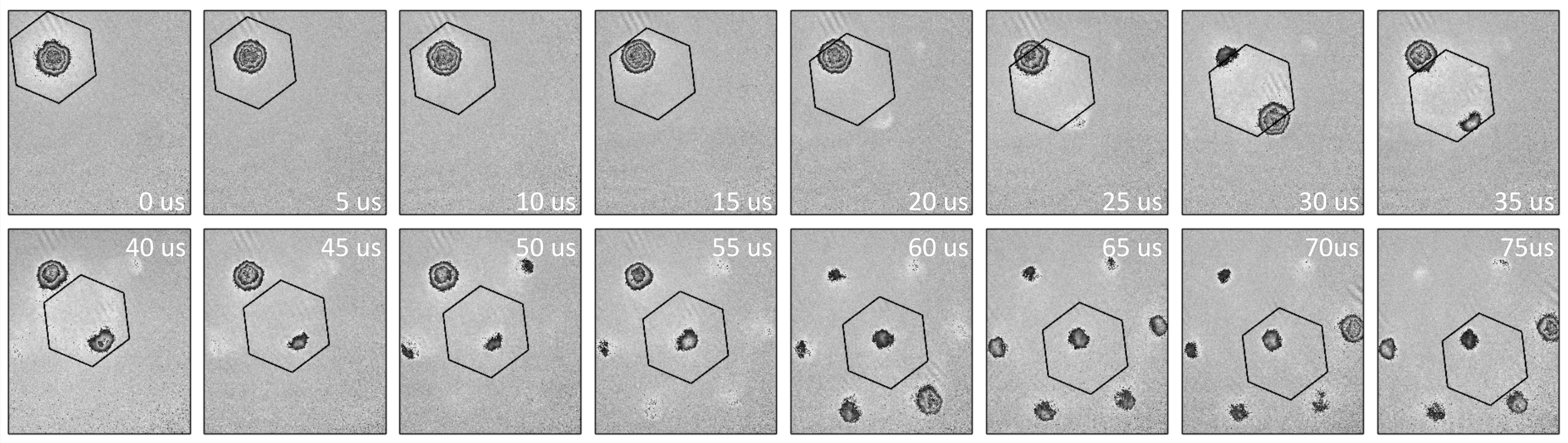

# Probing the Scalar Band Structure

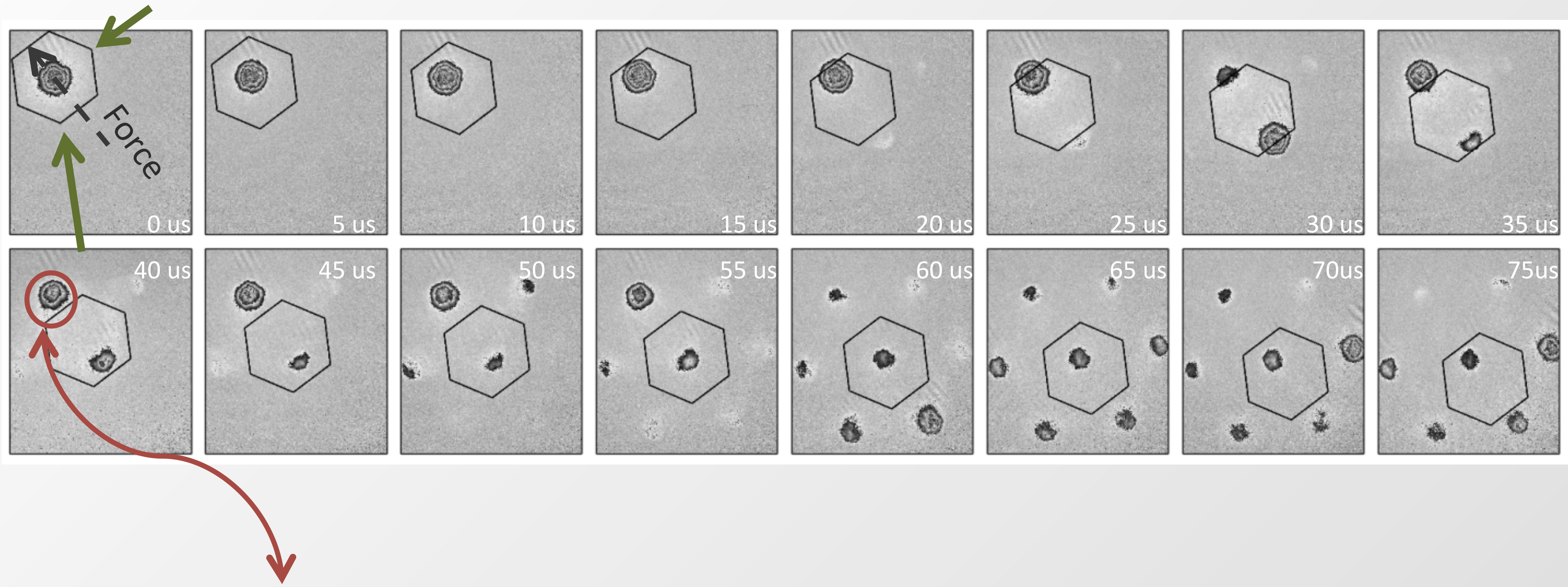


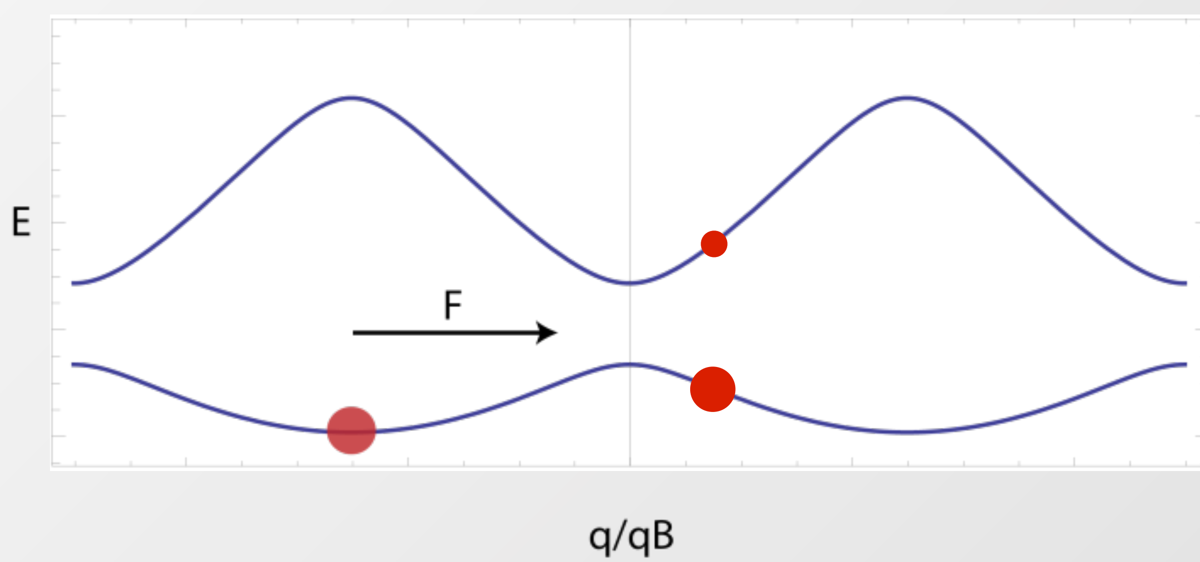


*Landau Zener acts as* ***beam splitter*** *between bands!*

*Interband transitions at edge*

# Stückelberg oscillations: Double Landau Zener

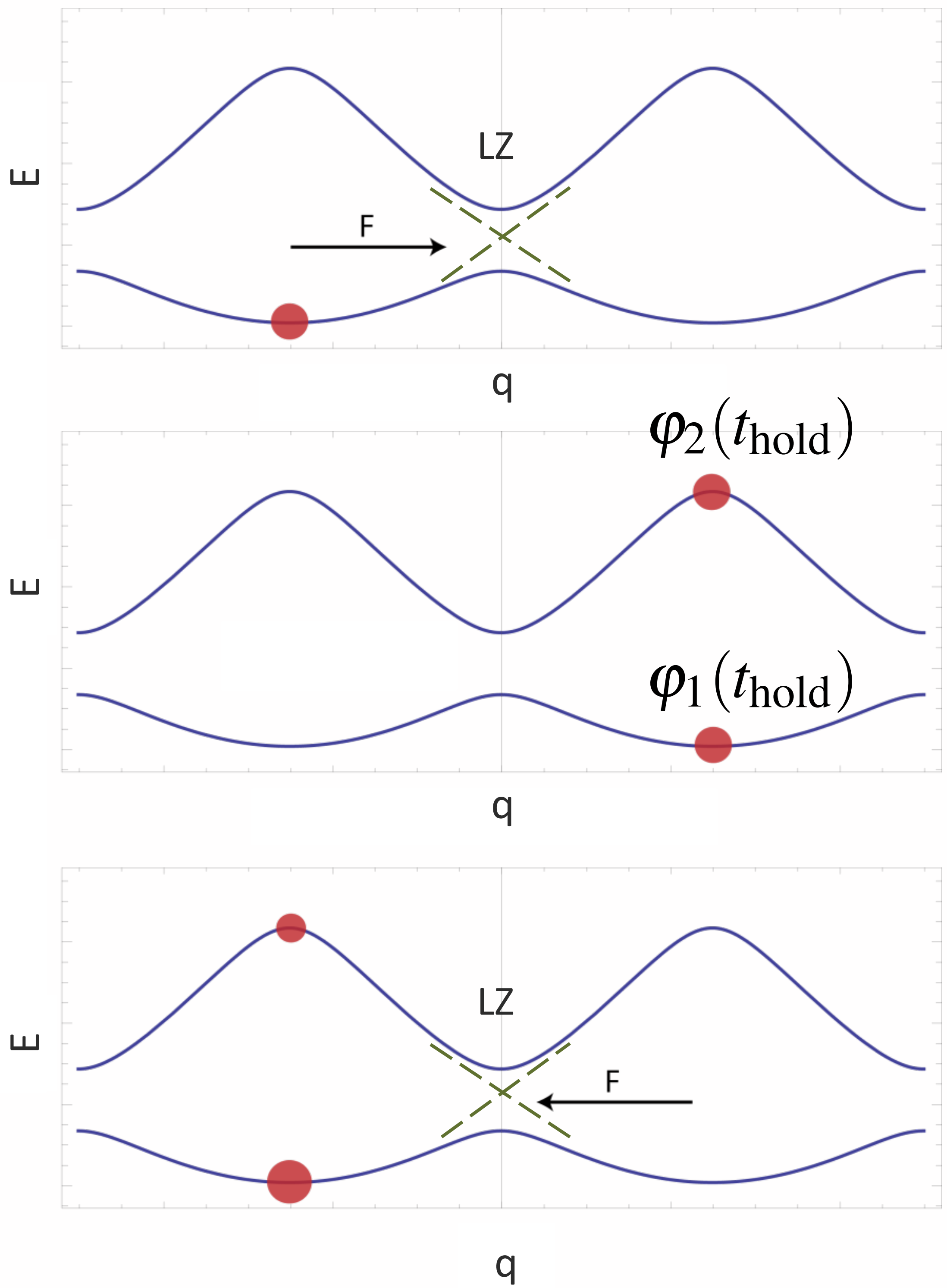


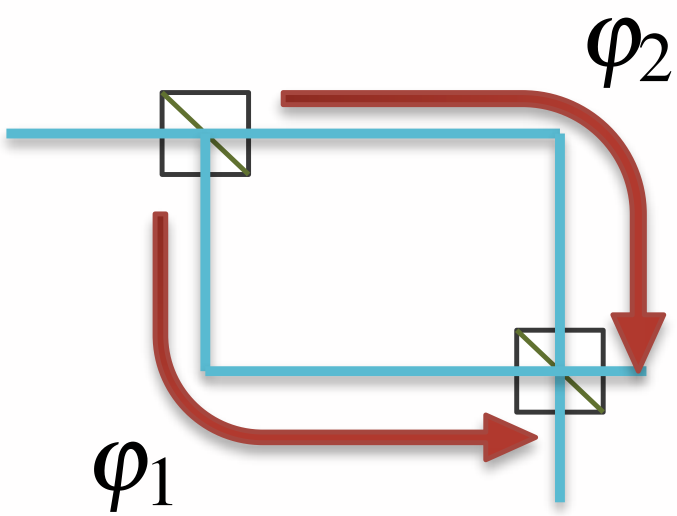


Final band populations encode

$$\varphi = \varphi_1 - \varphi_2$$

Stückelberg, Helv. Phys. Acta **5**, 369 (1932), Shevchenko et al., Phys. Rep. **492**, 1 (2010), Zanesini et al., PRA **82**, 065601, (2010), Weitz PRL **105**, 215301 (2010)

# Stückelberg oscillations: Double Landau Zener

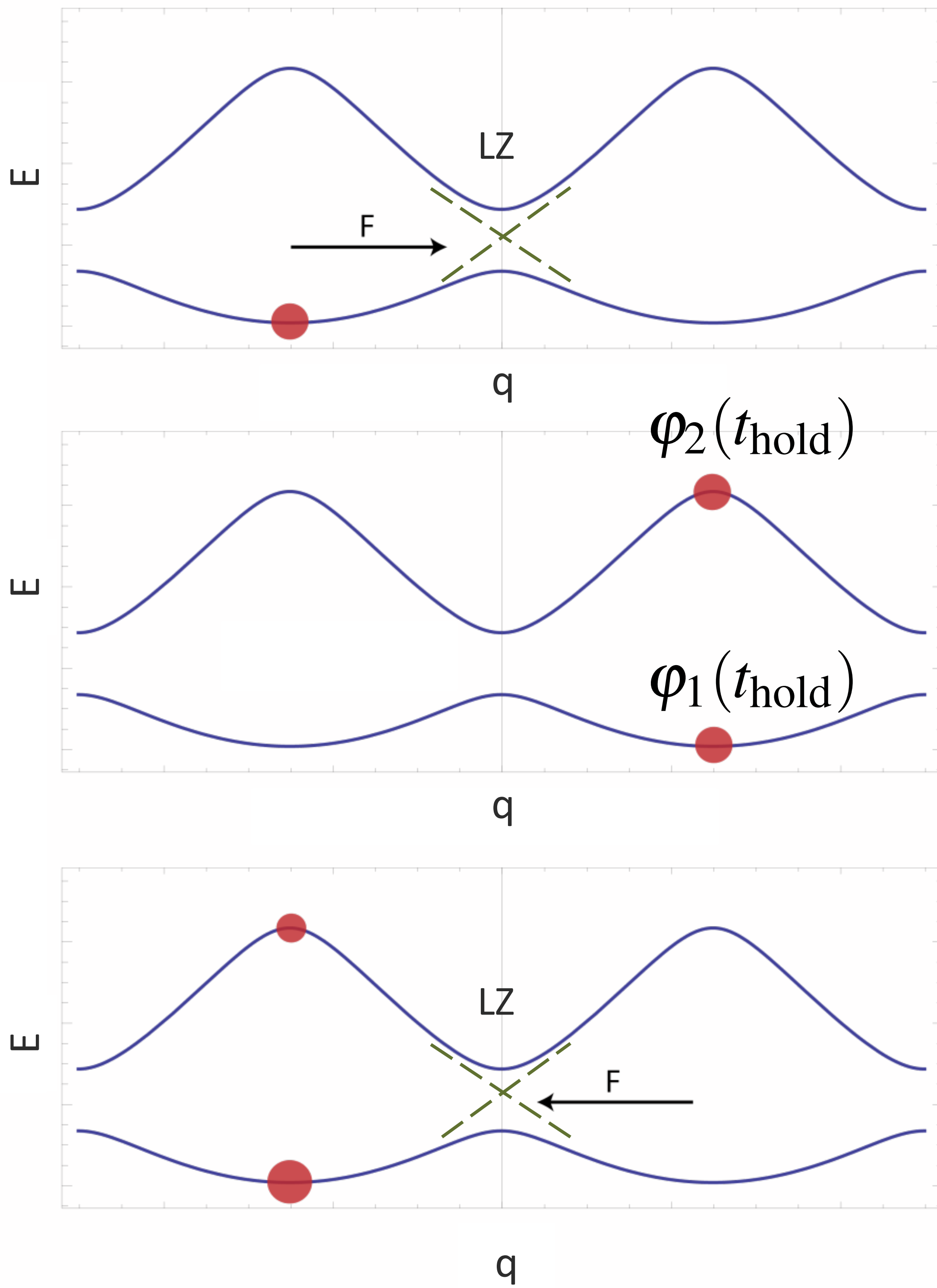


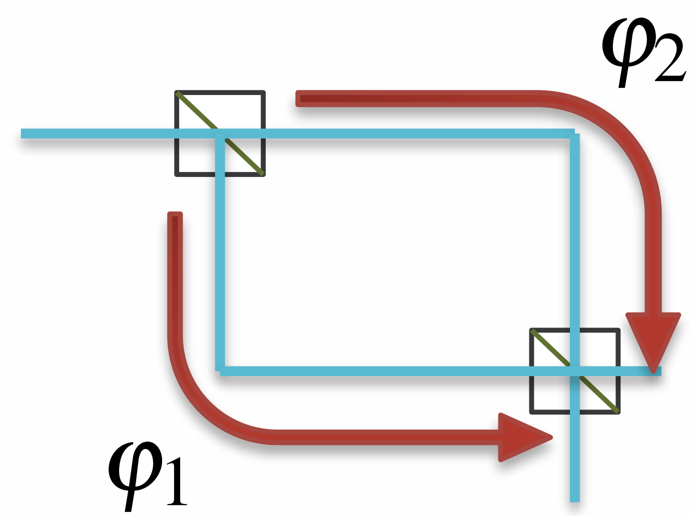


Final band populations encode

$$\varphi = \varphi_1 - \varphi_2$$

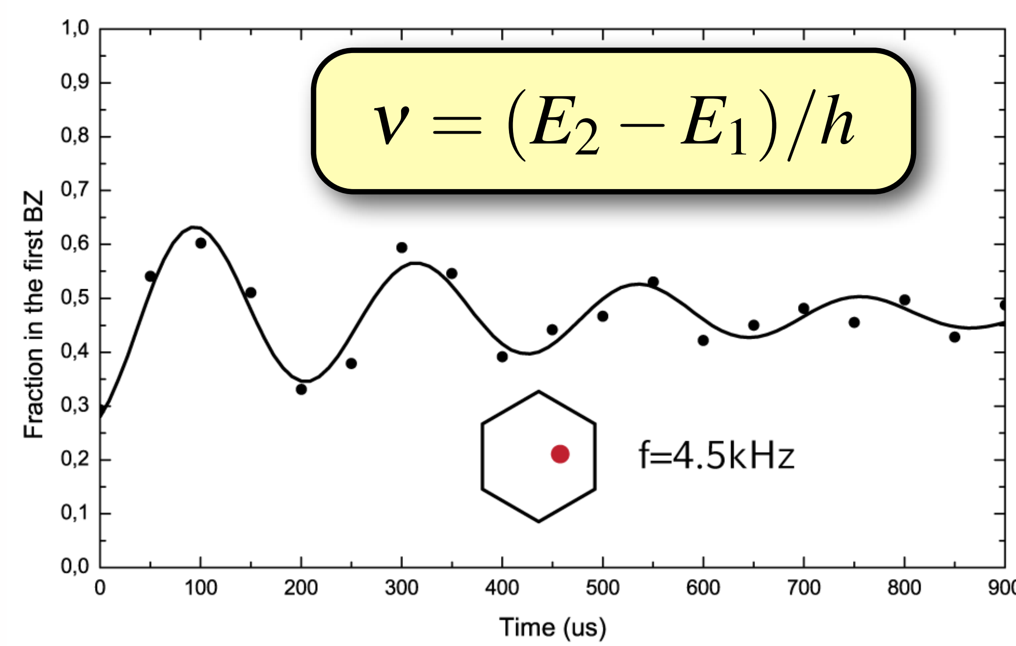


Stückelberg, Helv. Phys. Acta **5**, 369 (1932), Shevchenko et al., Phys. Rep. **492**, 1 (2010), Zanesini et al., PRA **82**, 065601, (2010), Weitz PRL **105**, 215301 (2010)

# Mapping the Dispersion Relation

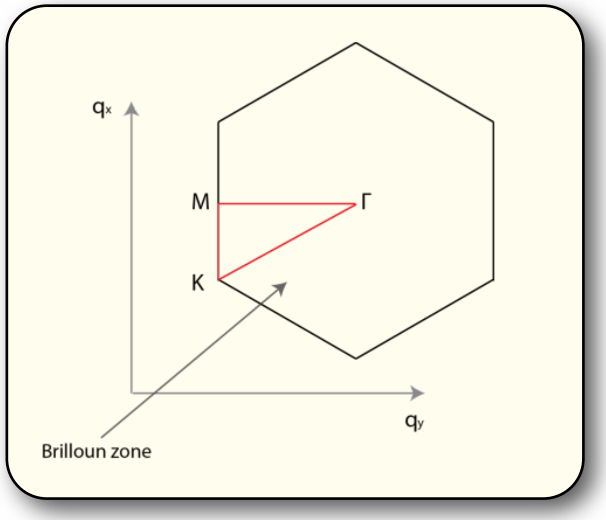


Frequency control on all three beams allows for **arbitrary accelerations!**

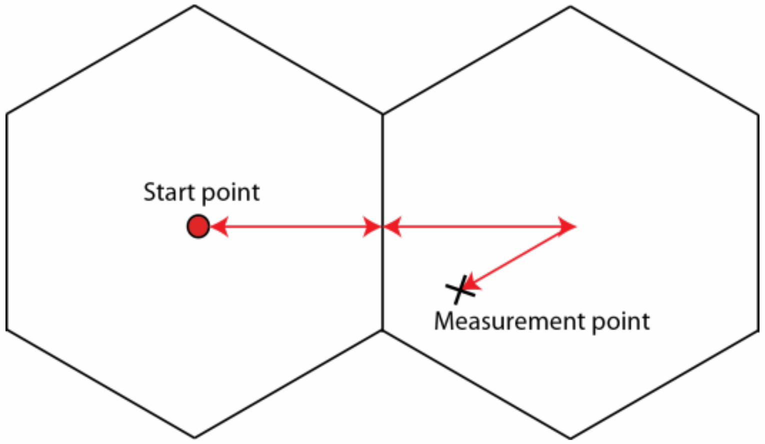


*Mapped path*

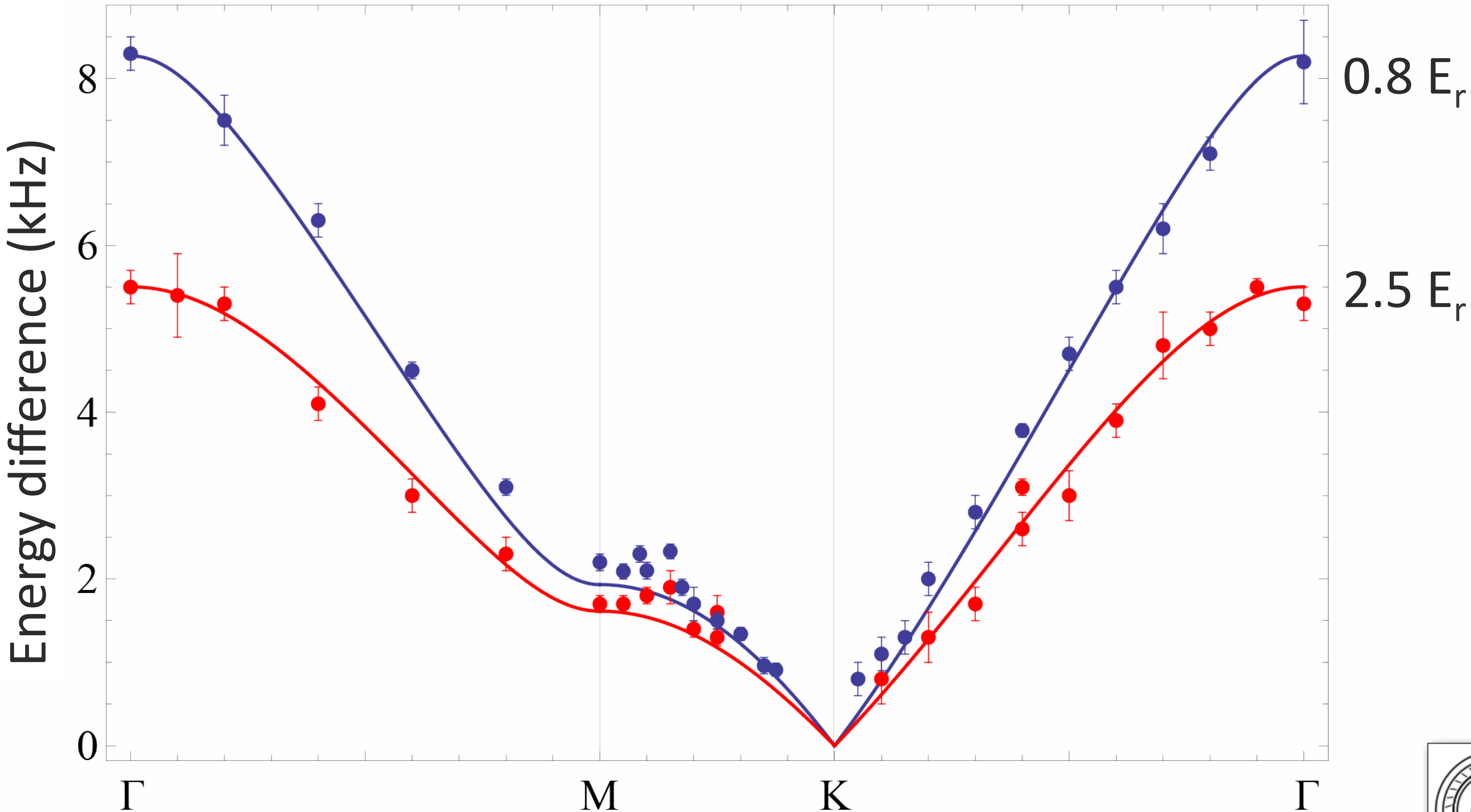

# Interferometer & Loops

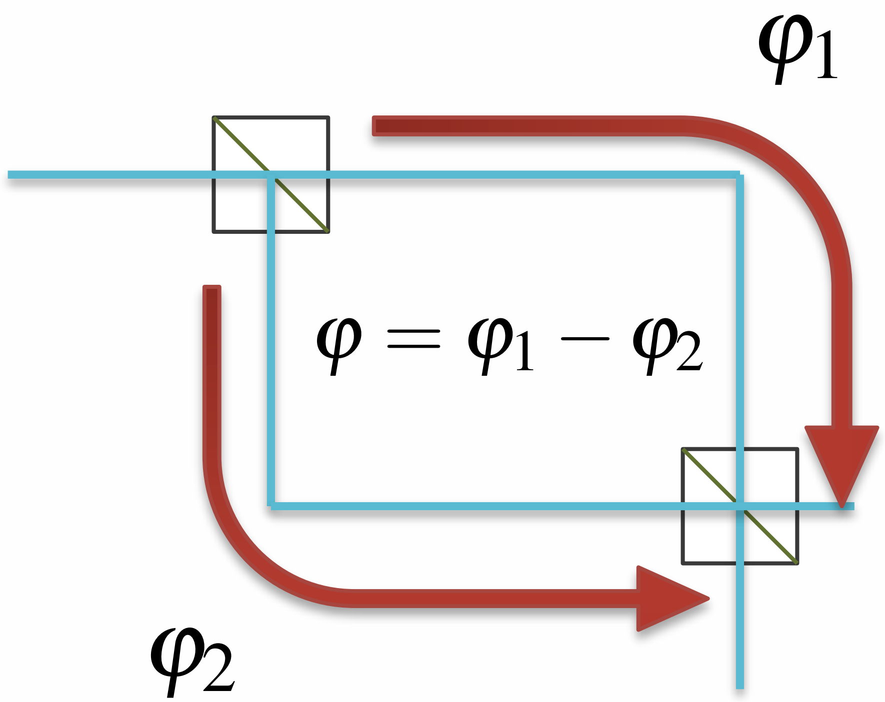


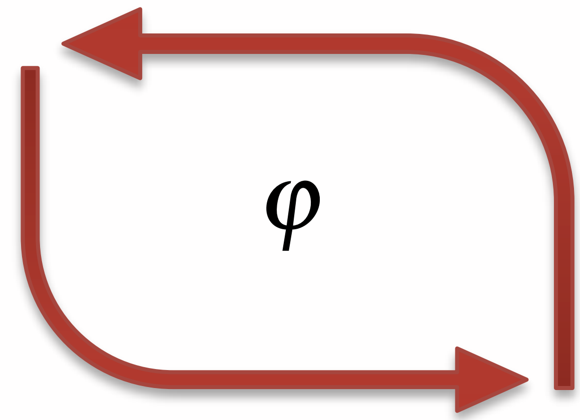


Interferometer Phase = Phase of closed loop

# Geometric Phases

## Berry's Phase

Cyclic adiabatic evolution in parameter space of $H(\mathbf{R})$

$$|\Phi(T)\rangle = e^{i(\varphi_{\text{dyn}}+\varphi_{\text{Berry}})}|\Phi(0)\rangle$$

$$\varphi_{\text{dyn}} = \frac{1}{\hbar}\int_0^T E(t)\,dt$$

$$\varphi_{\text{Berry}} = i\int_C \langle\Phi|\nabla_R|\Phi\rangle\,dR$$ *: geometric phase, independent of evolution speed*

## Aharonov-Anandan Phase

Assume evolution that is cyclic in **state**

$$|\Psi(T)\rangle = e^{i\varphi}|\Psi(0)\rangle$$

$$\varphi = \varphi_1(T) + \varphi_{AA}$$

$\varphi_{AA}$ *: geometric phase, independent of evolution speed*

Y. Aharonov & J. Anandan, Phys. Rev. Lett. **58**, 1593 (1987)

# Closed Loops

$|\Psi(q_x, q_y)\rangle$

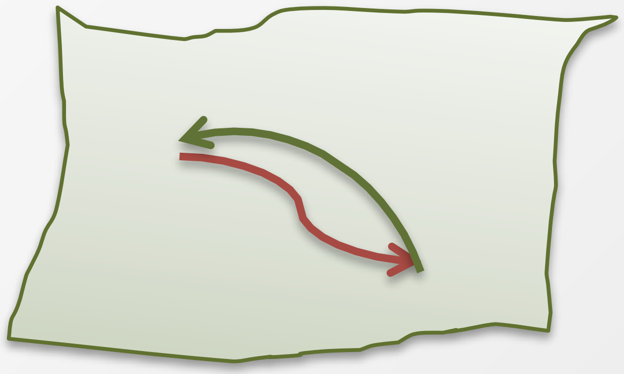

Closed loop **within band**

# Closed Loops

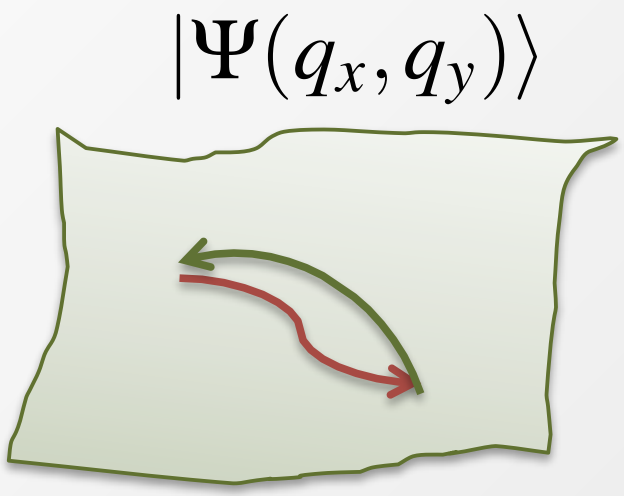


Closed loop **within band**

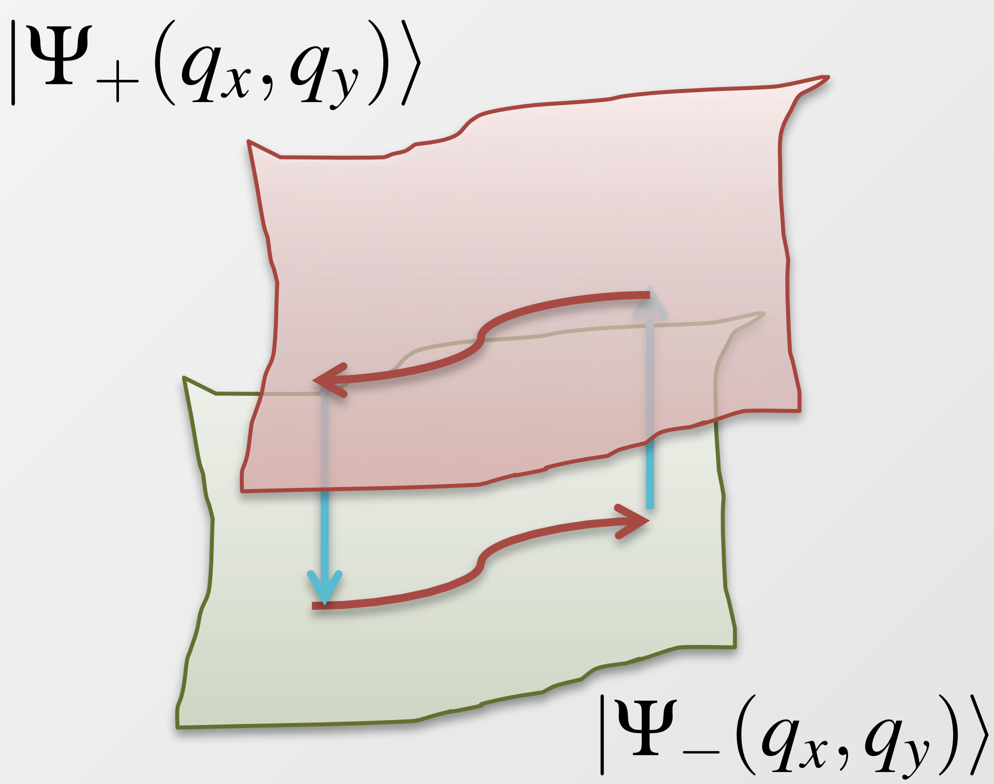


Closed loop **between bands**

# Geometric Phases in Stückelberg Interferometry

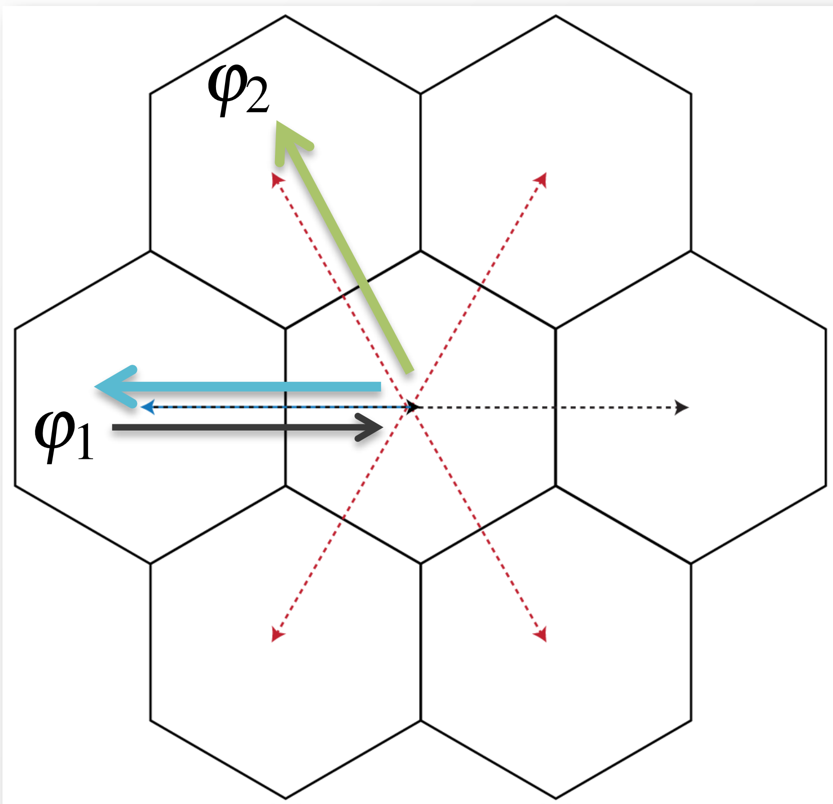


$$\boxed{\varphi = \varphi_i - \varphi_1 = \varphi_i^{AA} - \varphi_1^{AA}}$$

*purely geometrical!*

$$\varphi_i = \varphi_i^{dyn} + \varphi_i^{AA}$$

$$\varphi_i^{dyn} = \text{const.}$$

# Geometric Phases in Stückelberg Interferometry

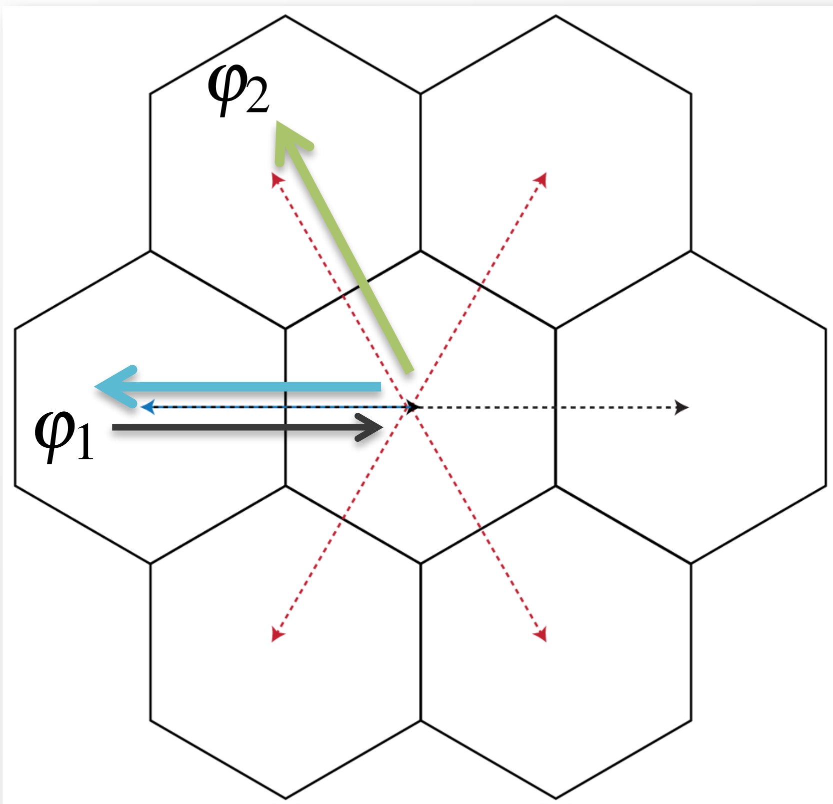


$$\varphi = \varphi_i - \varphi_1 = \varphi_i^{AA} - \varphi_1^{AA}$$

*purely geometrical!*

$$\varphi_i = \varphi_i^{dyn} + \varphi_i^{AA}$$

$$\varphi_i^{dyn} = \text{const.}$$

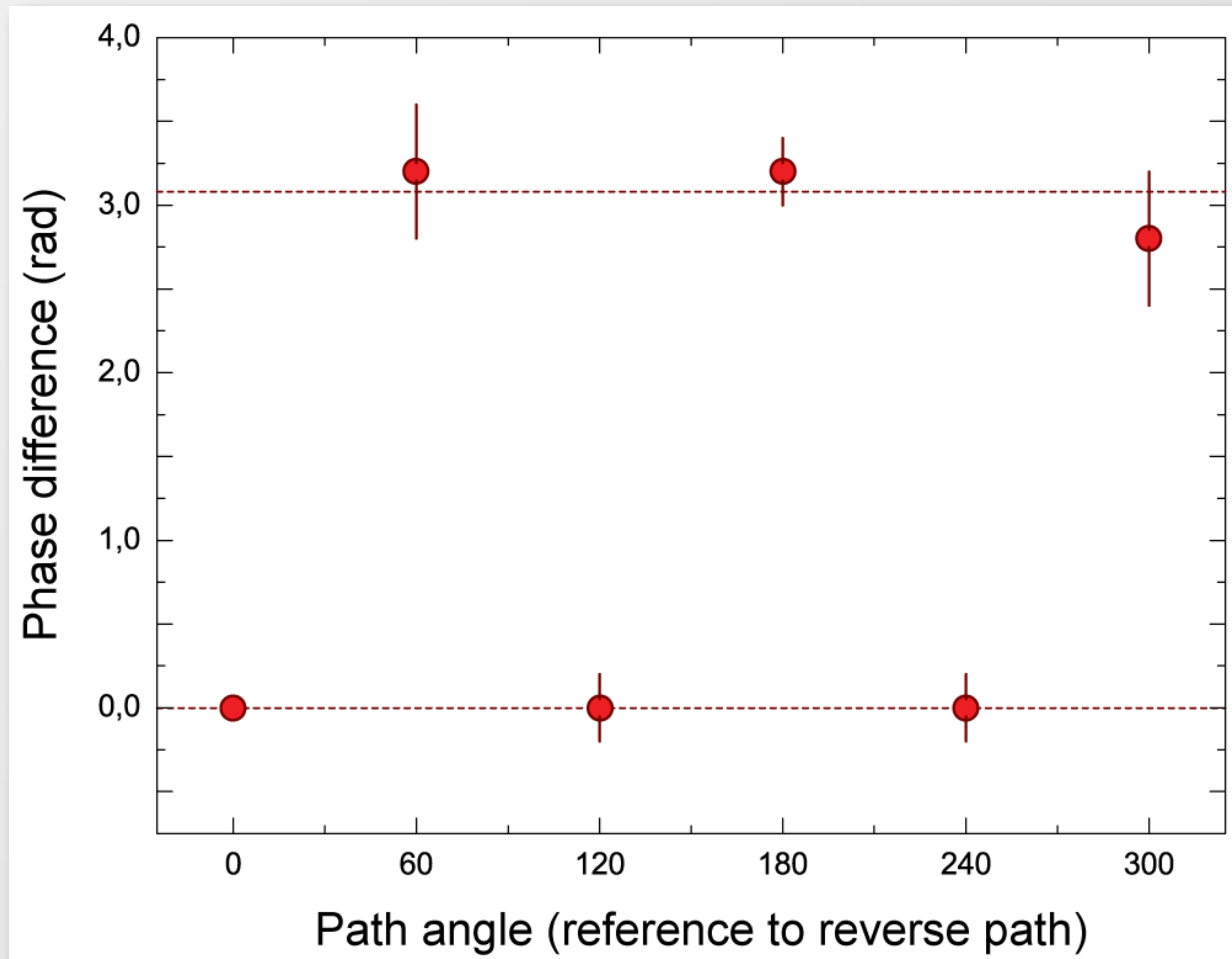

# Path without Dirac Cone

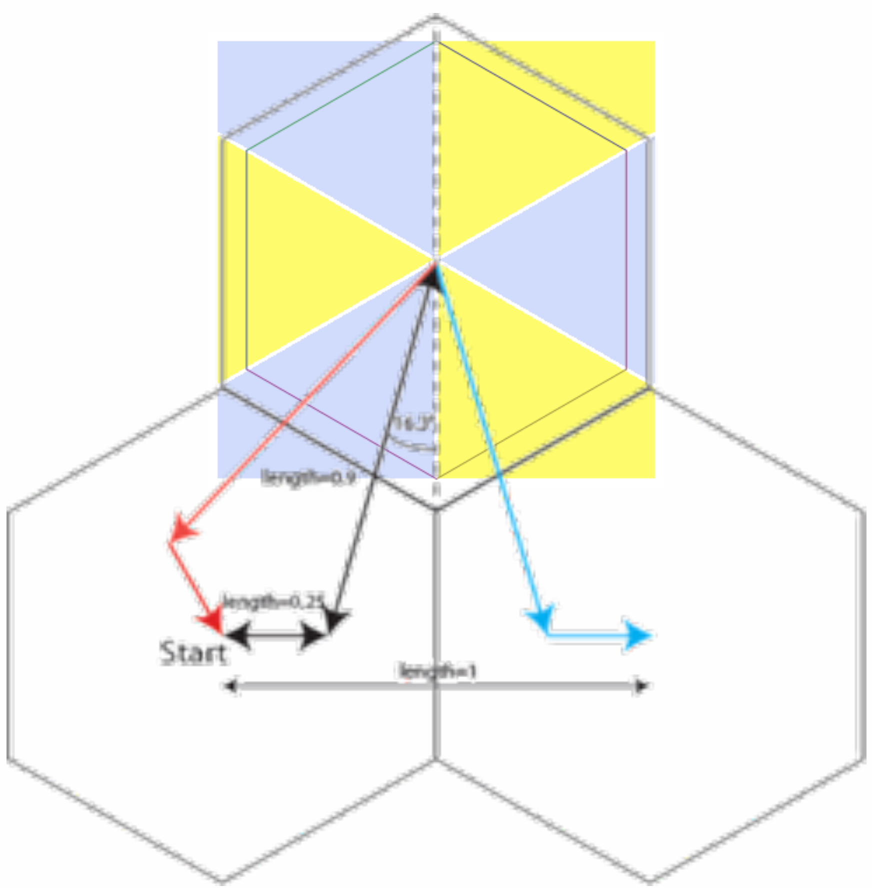


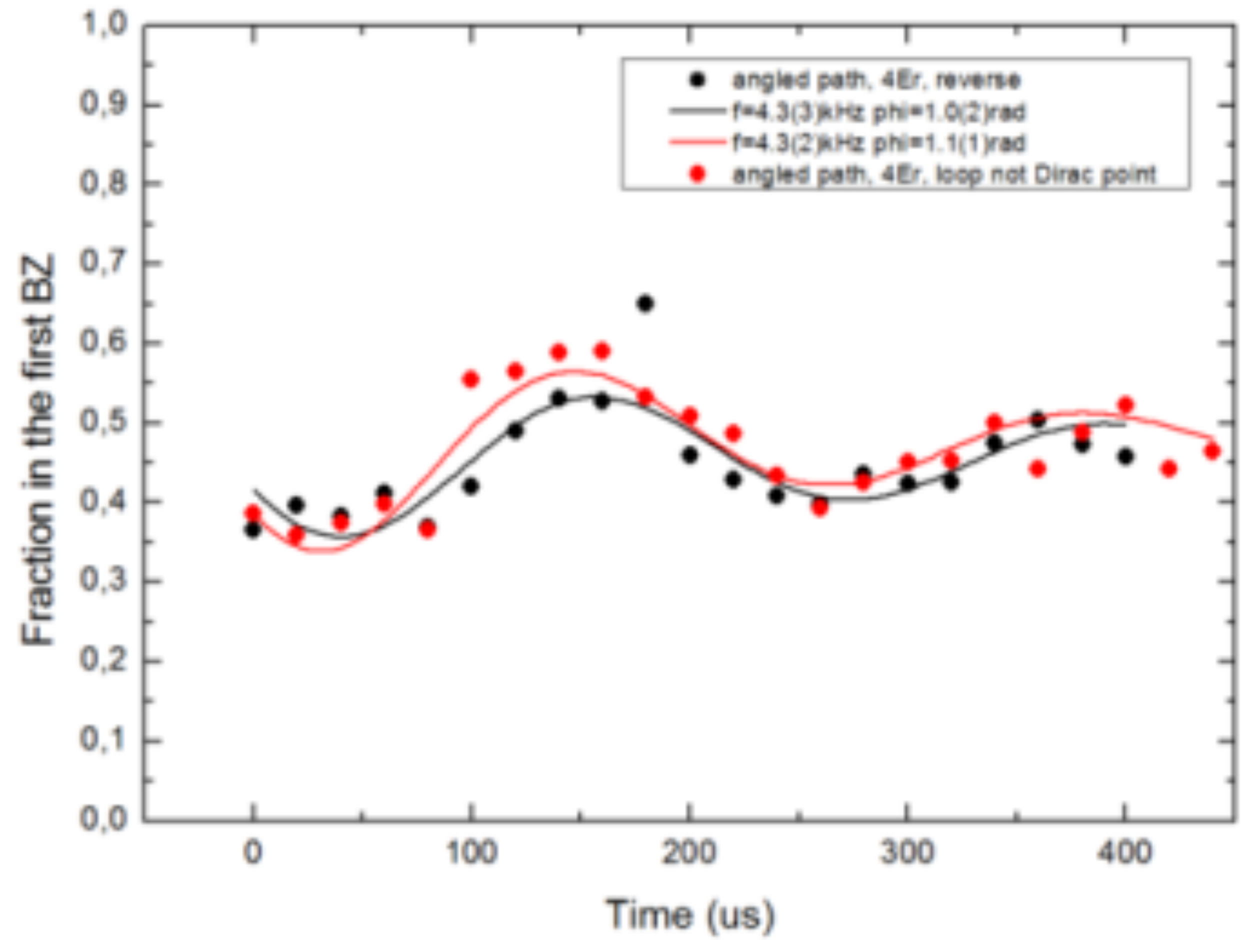

# Path without Dirac Cone

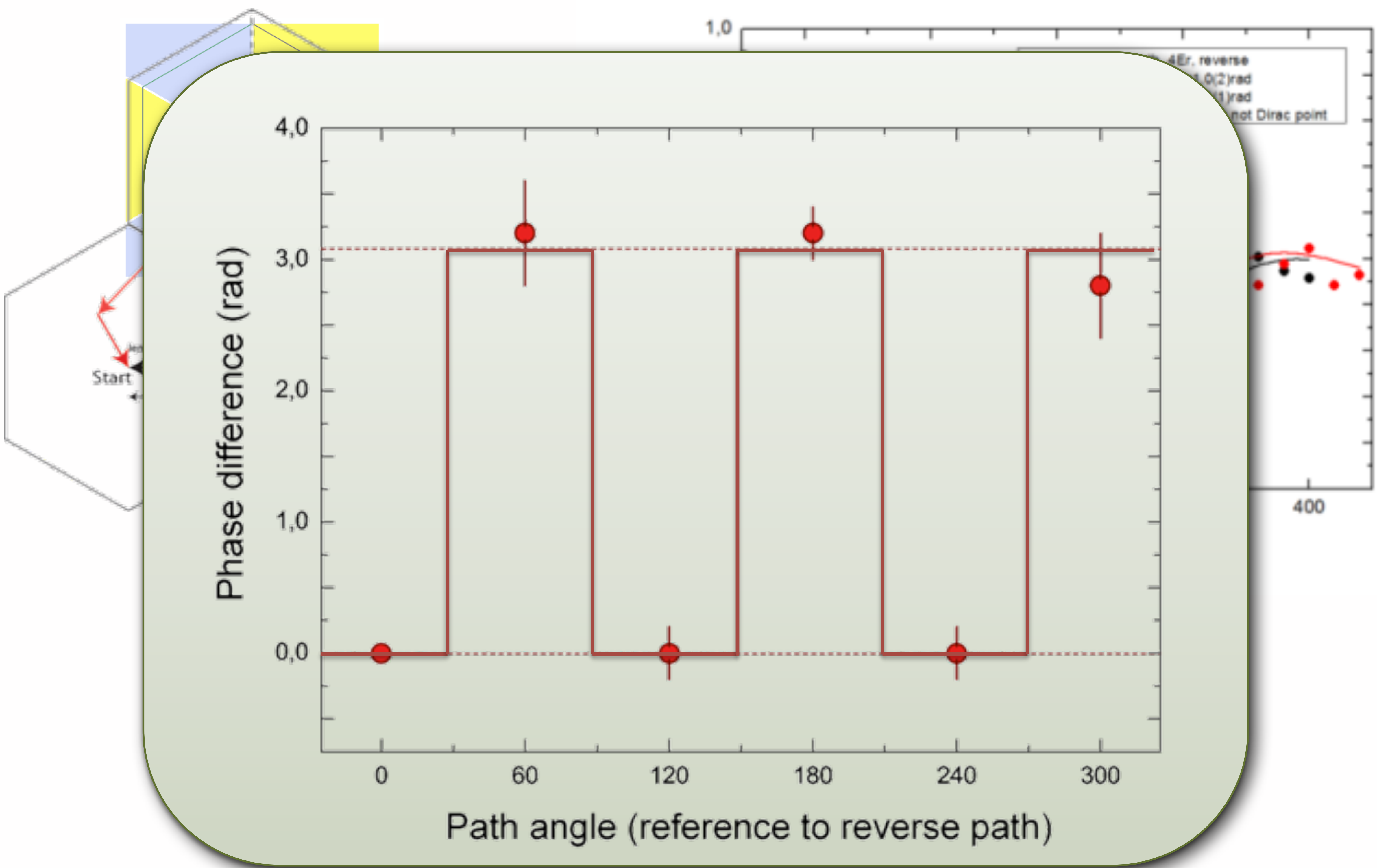

# Outlook

**ToDo:** Measure amplitude of off-diagonal Berry connection momentum resolved

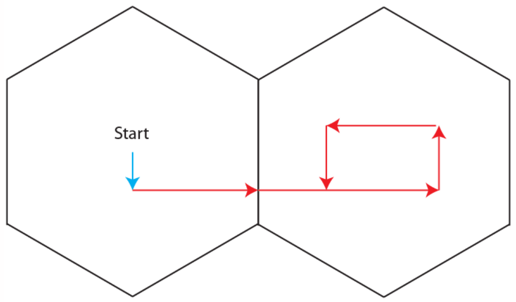


*Lattice acceleration allows for arbitrary path choice*

Ramsey & Stückelberg allow for a full determination of band structure
***Dispersion relation + full geometric tensor***

# Outlook

**ToDo:** Measure amplitude of off-diagonal Berry connection momentum resolved

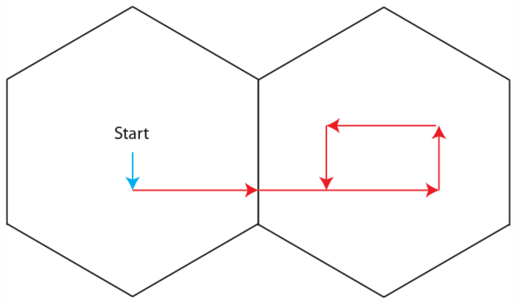


*Lattice acceleration allows for arbitrary path choice*

Ramsey & Stückelberg allow for a full determination of band structure
***Dispersion relation + full geometric tensor***

**Next:** Turn band topological! Turn on interactions!

Haldane PRL (1988)
Lindner et al. Nat. Phys. (2011)
Kitagawa et al. PRB (2011)
Rechtsman et al. Nature (2013)
Aidelsburger PRL (2013)
⋮

# Outlook

**ToDo:** Measure amplitude of off-diagonal Berry connection momentum resolved

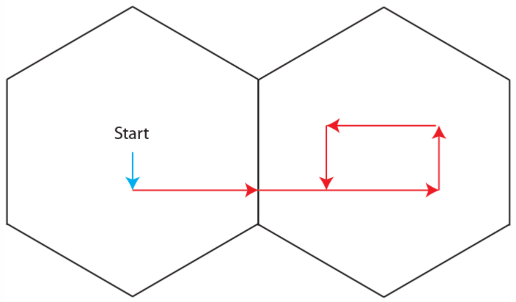


*Lattice acceleration allows for arbitrary path choice*

Ramsey & Stückelberg allow for a full determination of band structure
***Dispersion relation + full geometric tensor***

**Next:** Turn band topological! Turn on interactions!

Haldane PRL (1988)
Lindner et al. Nat. Phys. (2011)
Kitagawa et al. PRB (2011)
Rechtsman et al. Nature (2013)
Aidelsburger PRL (2013)
⋮

**Or:** Turn off interactions!

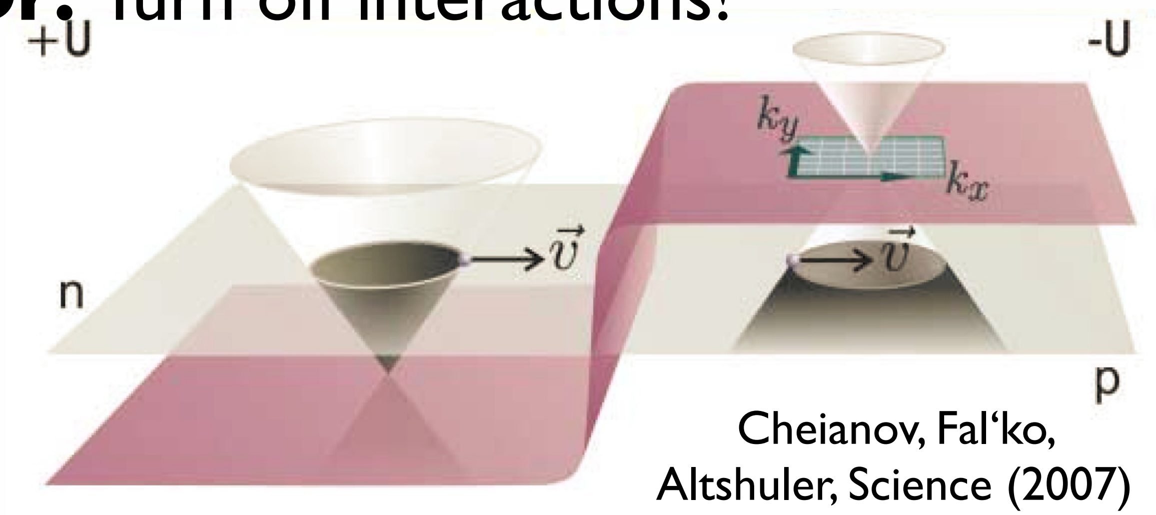


Cheianov, Fal'ko, Altshuler, Science (2007)

Veselago lens, Klein tunneling, ...

# Hall Response & Chern Number Measurement in Hofstadter Bands

N. Goldman

N. Cooper

M. Aidelsburger et al. (in preparation)

# Artificial B-Fields with Ultracold Atoms

Controlling atom tunneling along *x* with Raman lasers leads to effective tunnel coupling with spatially-dependent Peierls phase $\varphi(\mathbf{R})$

$$\hat{H} = -\sum_{\mathbf{R}} \left( K e^{i\varphi(\mathbf{R})}\, \hat{a}^\dagger_{\mathbf{R}} \hat{a}_{\mathbf{R}+\mathbf{d}_x} + J\, \hat{a}^\dagger_{\mathbf{R}} \hat{a}_{\mathbf{R}+\mathbf{d}_y} \right) + \text{h.c.}$$

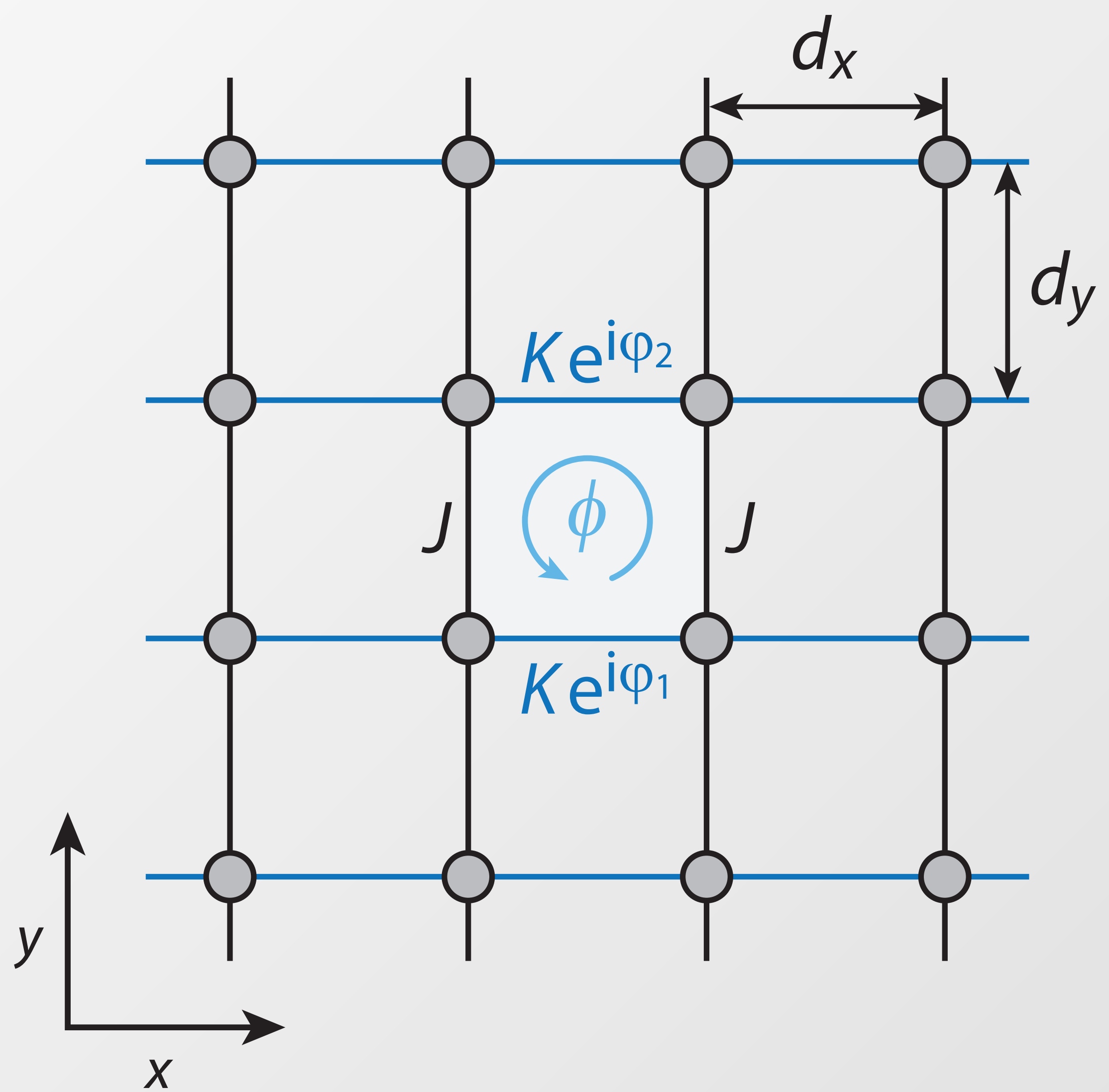


*Magnetic flux through a plaquette:*

$$\phi = \int_{\square} B\, \mathrm{d}S = \varphi_1 - \varphi_2$$

D. Jaksch & P. Zoller, New J. Phys. (2003)
F. Gerbier & J. Dalibard, New J. Phys. (2010)
N. Cooper, PRL (2011)
E. Mueller, Phys. Rev. A (2004)
L.-K. Lim et al. Phys. Rev. A (2010)
A. Kolovsky, Europhys. Lett. (2011)

**see also:** lattice shaking
E. Arimondo, PRL(2007) , K. Sengstock, Science (2011),
M. Rechtsman & M. Segev, Nature (2013)

# Artificial B-Fields with Ultracold Atoms

Controlling atom tunneling along *x* with Raman lasers leads to effective tunnel coupling with spatially-dependent Peierls phase $\varphi(\mathbf{R})$

$$\hat{H} = -\sum_{\mathbf{R}} \left( K e^{i\varphi(\mathbf{R})}\, \hat{a}^{\dagger}_{\mathbf{R}} \hat{a}_{\mathbf{R}+\mathbf{d}_x} + J\, \hat{a}^{\dagger}_{\mathbf{R}} \hat{a}_{\mathbf{R}+\mathbf{d}_y} \right) + \mathrm{h.c.}$$

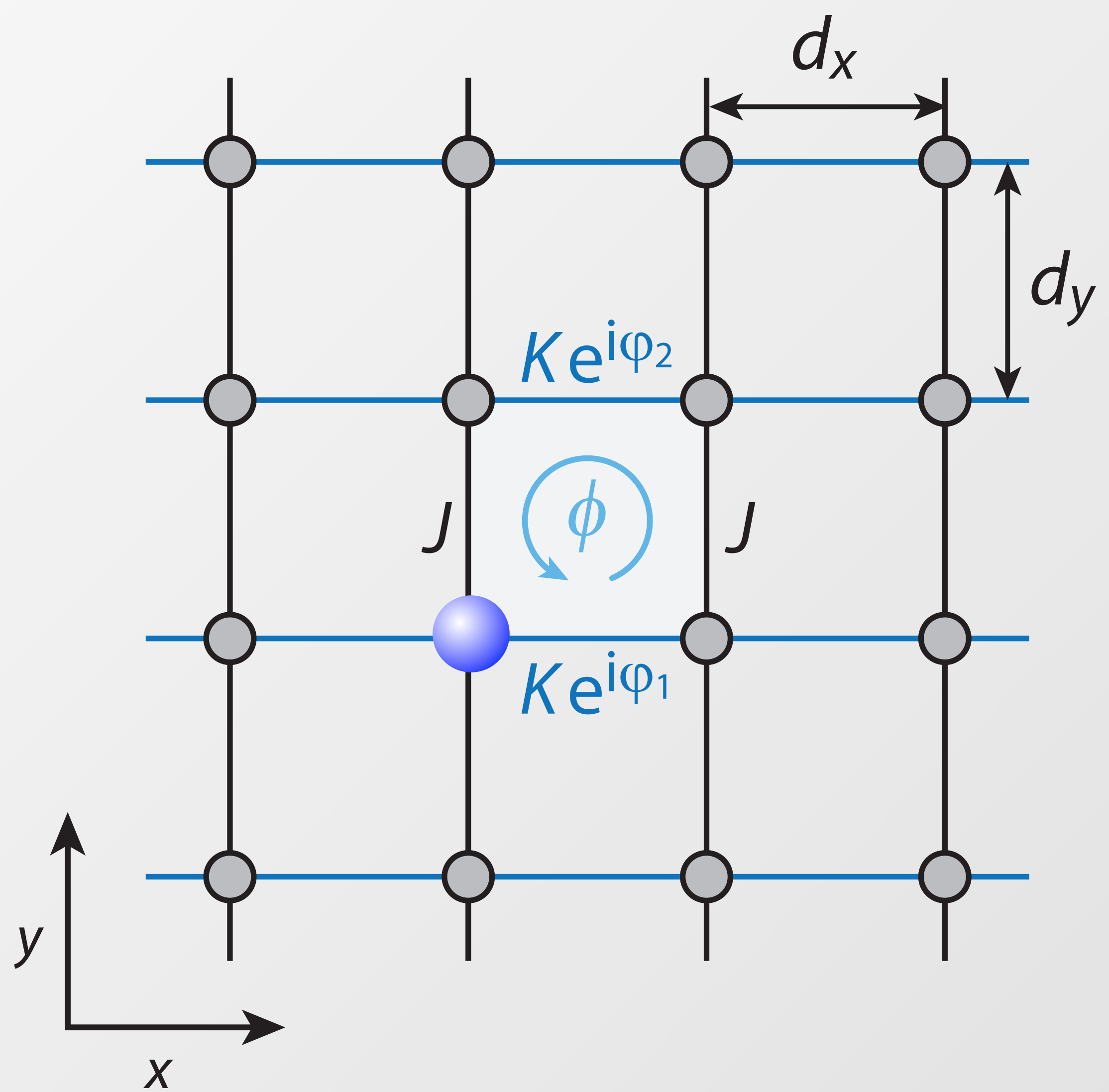


*Magnetic flux through a plaquette:*

$$\boxed{\phi = \int_{\blacksquare} B\, \mathrm{d}S = \varphi_1 - \varphi_2}$$

D. Jaksch & P. Zoller, New J. Phys. (2003)
F. Gerbier & J. Dalibard, New J. Phys. (2010)
N. Cooper, PRL (2011)
E. Mueller, Phys. Rev. A (2004)
L.-K. Lim et al. Phys. Rev. A (2010)
A. Kolovsky, Europhys. Lett. (2011)

**see also:** lattice shaking
E. Arimondo, PRL(2007) , K. Sengstock, Science (2011),
M. Rechtsman & M. Segev, Nature (2013)

# Artificial B-Fields with Ultracold Atoms

Controlling atom tunneling along $x$ with Raman lasers leads to effective tunnel coupling with spatially-dependent Peierls phase $\varphi(\mathbf{R})$

$$\hat{H} = -\sum_{\mathbf{R}} \left( K e^{i\varphi(\mathbf{R})}\, \hat{a}^{\dagger}_{\mathbf{R}} \hat{a}_{\mathbf{R}+\mathbf{d}_x} + J\, \hat{a}^{\dagger}_{\mathbf{R}} \hat{a}_{\mathbf{R}+\mathbf{d}_y} \right) + \text{h.c.}$$

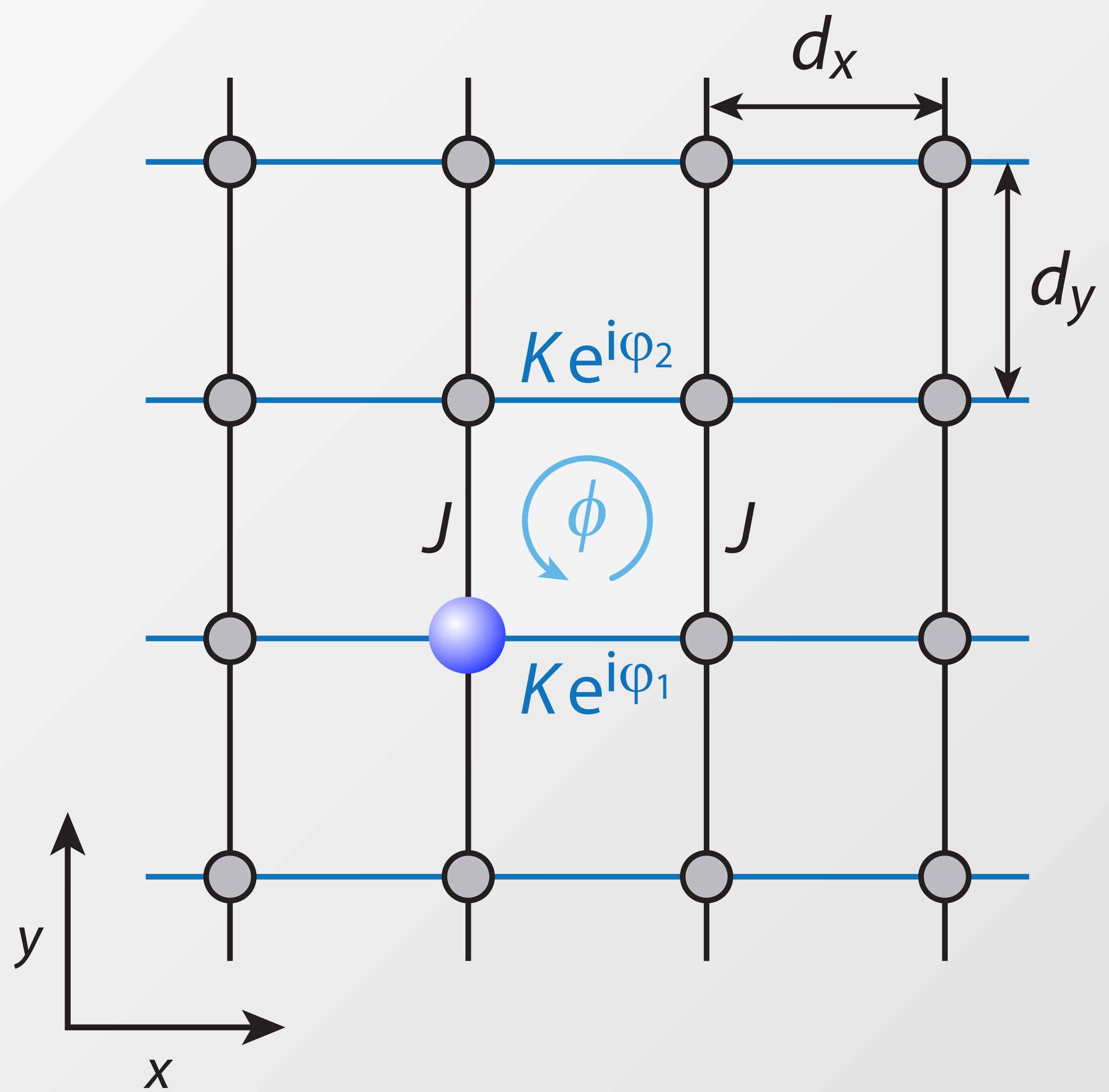


*Magnetic flux through a plaquette:*

$$\boxed{\phi = \int_{\blacksquare} B\, \mathrm{d}S = \varphi_1 - \varphi_2}$$

D. Jaksch & P. Zoller, New J. Phys. (2003)
F. Gerbier & J. Dalibard, New J. Phys. (2010)
N. Cooper, PRL (2011)
E. Mueller, Phys. Rev. A (2004)
L.-K. Lim et al. Phys. Rev. A (2010)
A. Kolovsky, Europhys. Lett. (2011)

**see also:** lattice shaking
E. Arimondo, PRL(2007) , K. Sengstock, Science (2011),
M. Rechtsman & M. Segev, Nature (2013)

# Artificial B-Fields with Ultracold Atoms

Controlling atom tunneling along *x* with Raman lasers leads to effective tunnel coupling with spatially-dependent Peierls phase $\varphi(\mathbf{R})$

$$\hat{H} = -\sum_{\mathbf{R}} \Big( \ldots \Big) + \text{h.c.}$$

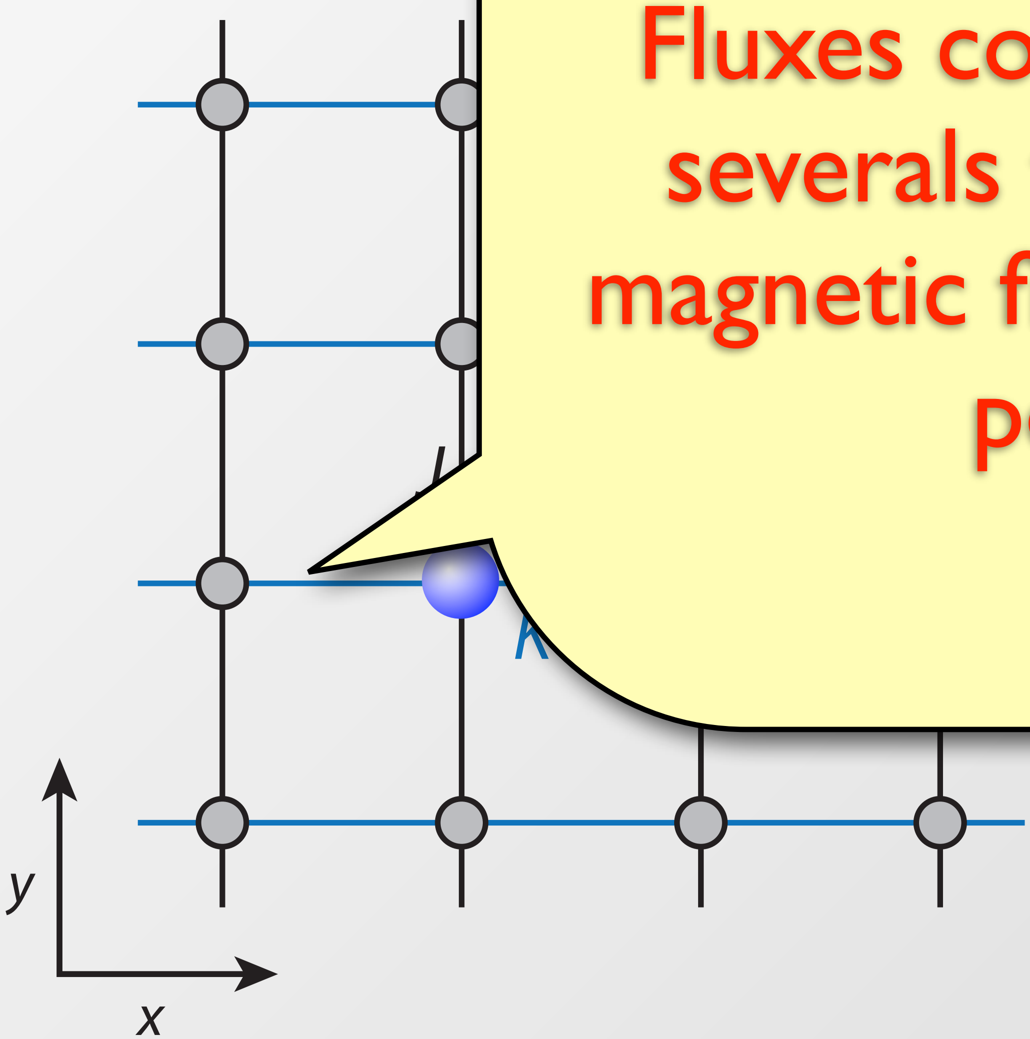


**Fluxes corresponding to severals thousand Tesla magnetic field strength are possible!**

*...rough a plaquette:*

$$\ldots S = \varphi_1 - \varphi_2$$

...ch & P. Zoller, New J. Phys. (2003)
... & J. Dalibard, New J. Phys. (2010)
N. Cooper, PRL (2011)
E. Mueller, Phys. Rev. A (2004)
L.-K. Lim et al. Phys. Rev. A (2010)
A. Kolovsky, Europhys. Lett. (2011)

**see also:** lattice shaking
E. Arimondo, PRL(2007), K. Sengstock, Science (2011), M. Rechtsman & M. Segev, Nature (2013)

# Harper Hamiltonian and Hofstadter Butterfly

Harper Hamiltonian: $J=K$ and $\phi$ uniform.

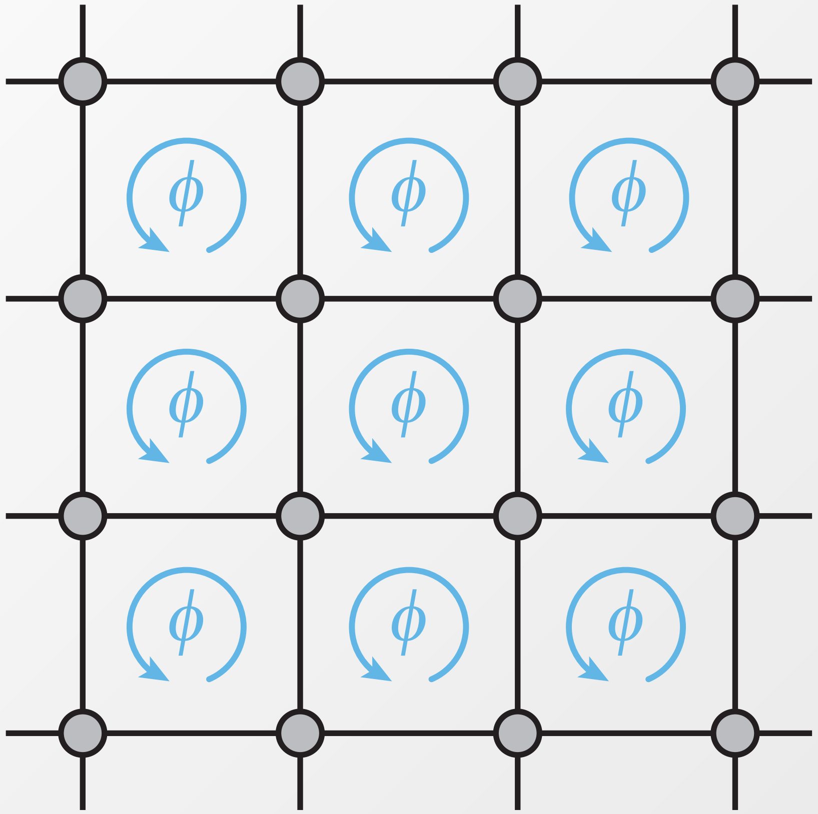


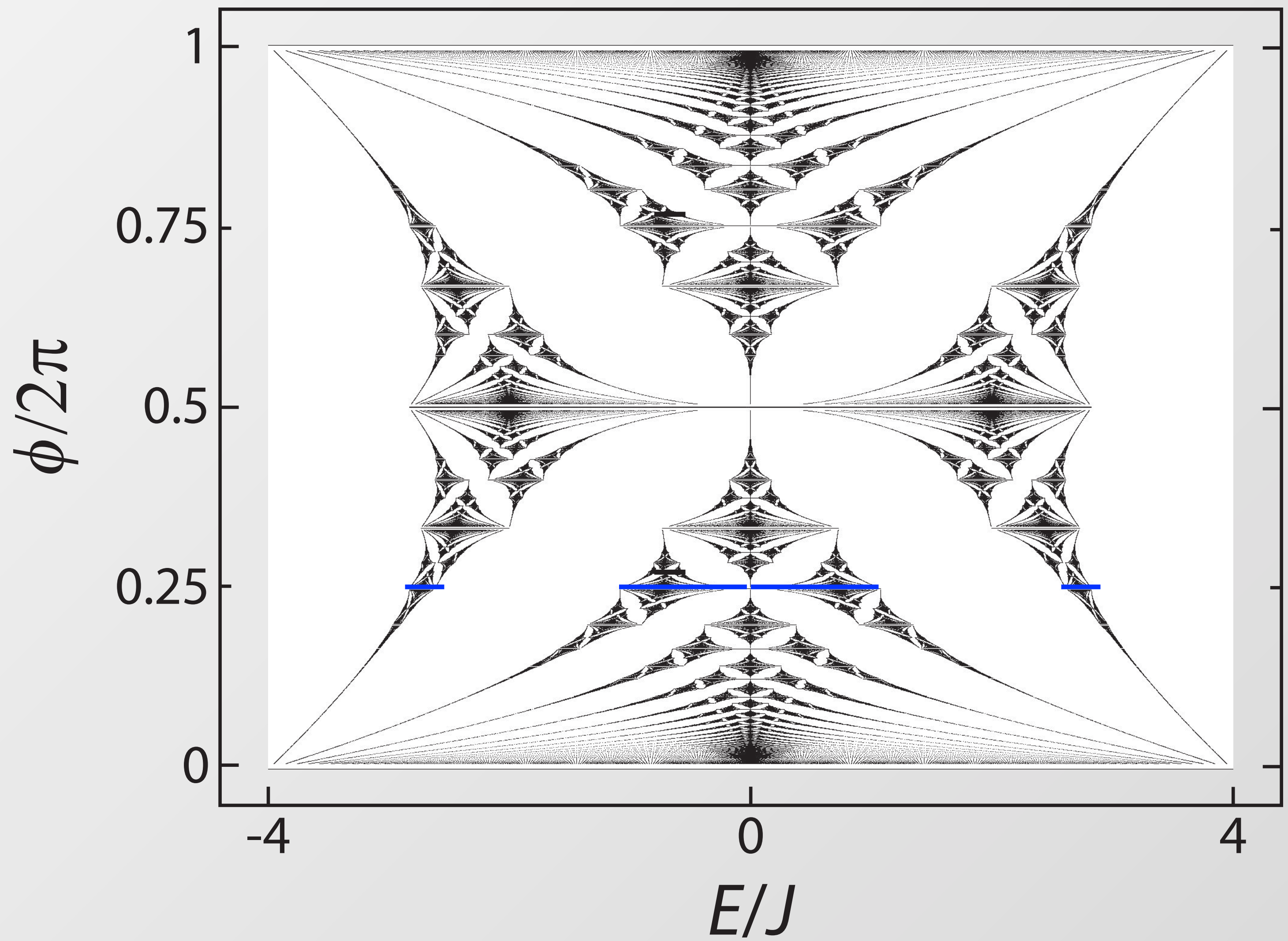


The lowest band is topologically equivalent to the lowest Landau level.

D.R. Hofstadter, Phys. Rev. B **14**, 2239 (1976)
see alo Y. Avron, D. Osadchy, R. Seiler, Physics Today 38, 2003

# Experimental method

- Atoms in a 2D lattice
- Tunneling inhibited along one direction using energy offsets

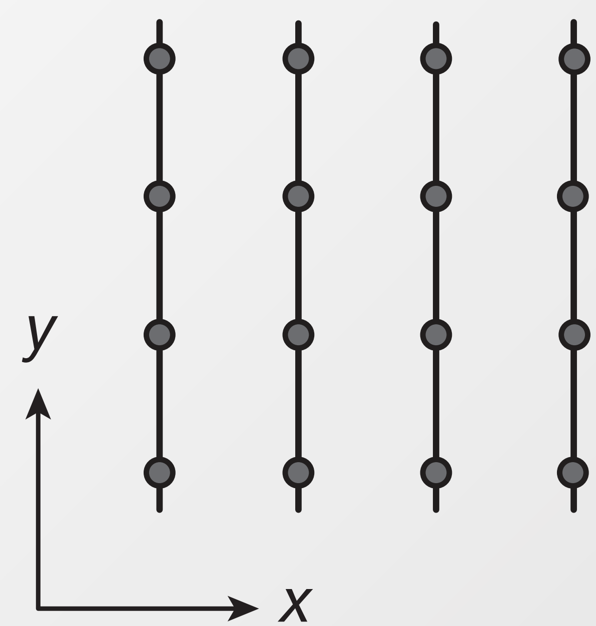


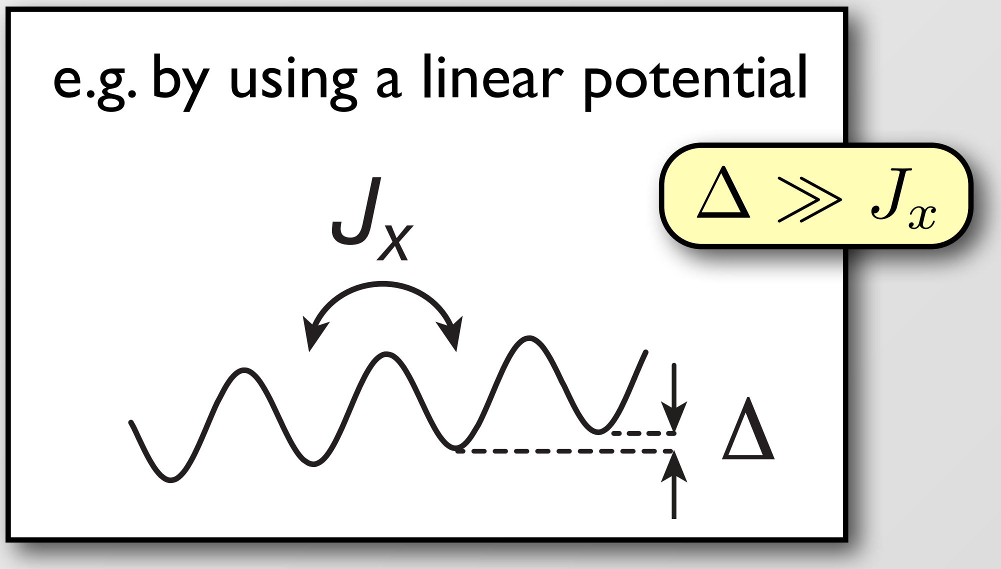

# Experimental method

- Atoms in a 2D lattice
- Tunneling inhibited along one direction using energy offsets

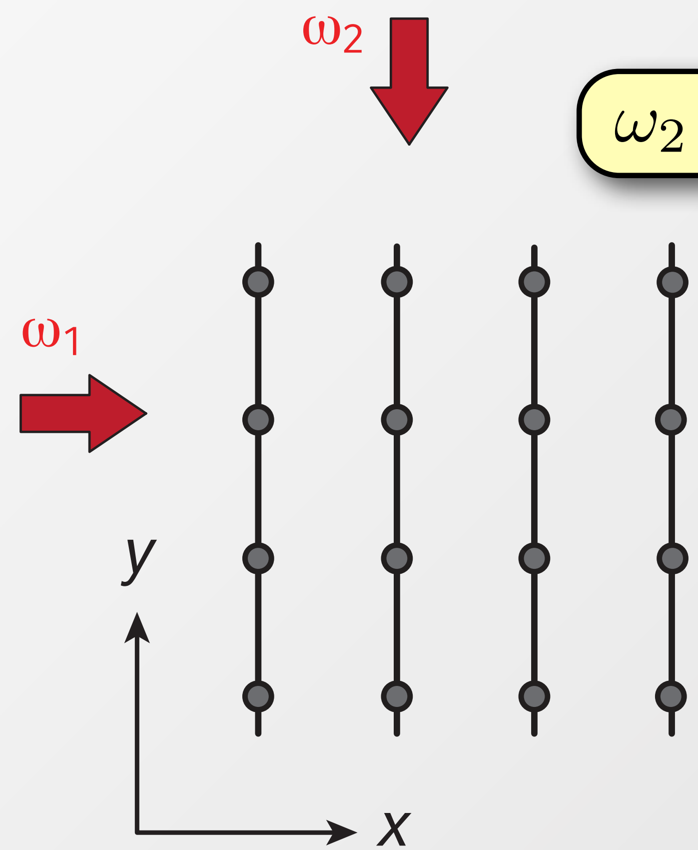


$$\omega_2 - \omega_1 = \Delta/\hbar$$

e.g. by using a linear potential

$$\Delta \gg J_x$$

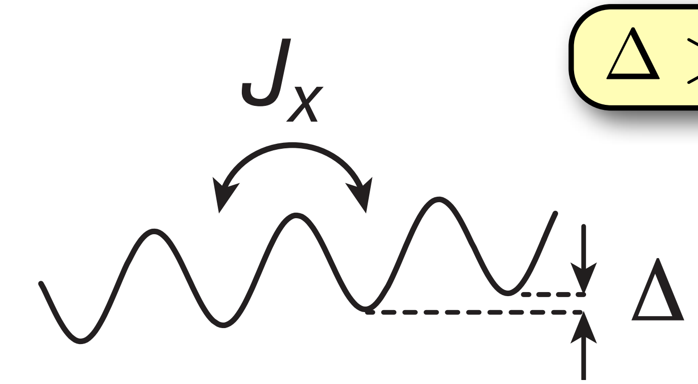


- Induce resonant tunneling with a pair of ***far-detuned*** running-wave beams
  - → ***Reduced heating*** due to spontaneous emission compared to Raman-assisted tunneling!
  - → ***Independent*** of the internal structure of the atom

# Experimental method

- Interference creates a running-wave that ***modulates*** the lattice
- The ***phase of the modulation*** depends on the position in the lattice

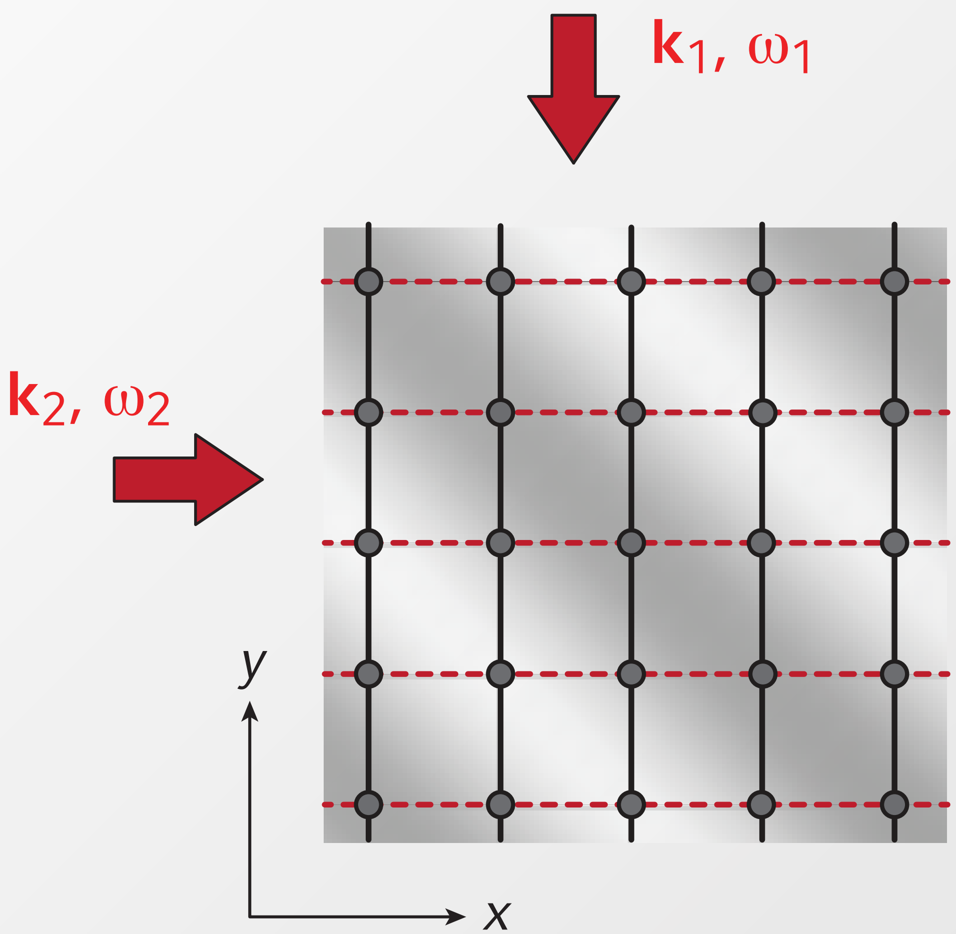


Lattice modulation:

$$V_K^0 \cos(\omega t + \phi(\mathbf{r}))$$

with ***spatial-dependent*** phase

$$\phi(\mathbf{r}) = \delta\mathbf{k} \cdot \mathbf{r}$$

$$\delta\mathbf{k} = \mathbf{k}_2 - \mathbf{k}_1$$

$$\omega = \omega_2 - \omega_1$$

- Realization of ***time-dependent*** Hamiltonian, where tunneling is restored
- Discretization of the phase due to underlying lattice → $\phi_{m,n}$

M. Aidelsburger *et al.*, PRL (2011); M. Aidelsburger *et al.*, Appl. Phys. B (2013)

# Experimental method

- Time-dependent Hamiltonian:

$$\hat{H}(t) = \sum_{m,n} \left( -J_x \ \hat{a}^\dagger_{m+1,n} \hat{a}_{m,n} - J_y \ \hat{a}^\dagger_{m,n+1} \hat{a}_{m,n} + \text{h.c.} \right)$$

$$+ \sum_{m,n} \left[ m\Delta + V_K^0 \cos(\omega t + \phi_{m,n}) \right] \hat{n}_{m,n}$$

# Experimental method

- Time-dependent Hamiltonian:

$$\hat{H}(t) = \sum_{m,n} \Big( -J_x\ \hat{a}^\dagger_{m+1,n}\hat{a}_{m,n} - J_y\ \hat{a}^\dagger_{m,n+1}\hat{a}_{m,n} + \text{h.c.} \Big)$$

$$+ \sum_{m,n} \left[ m\Delta + V_K^0 \cos(\omega t + \phi_{m,n}) \right] \hat{n}_{m,n}$$

- Can be mapped on an effective time-averaged time-independent Hamiltonian for $\hbar\omega \gg J_x, J_y, U$

$$\hat{H}_{eff} = \sum_{m,n} \Big( -K e^{i\phi_{m,n}}\ \hat{a}^\dagger_{m+1,n}\hat{a}_{m,n} - J\ \hat{a}^\dagger_{m,n+1}\hat{a}_{m,n} + \text{h.c.} \Big)$$

- To avoid excitations to higher bands $\hbar\omega$ has to be smaller than the band gap

F. Grossmann and P. Hänggi, EPL (1992)
M. Holthaus, PRL (1992)
A. Kolovsky, EPL (2011); A. Eckardt, PRL (2005)
A. Eckhardt, EPL (2007); P. Hauke, PRL (2012)
A. Bermudez, PRL (2011); A. Bermudez, NJP (2012)

# Experimental method

- Time-dependent Hamiltonian:

$$\hat{H}(t) = \sum_{m,n} \left( -J_x \ \hat{a}^{\dagger}_{m+1,n} \hat{a}_{m,n} - J_y \ \hat{a}^{\dagger}_{m,n+1} \hat{a}_{m,n} + \text{h.c.} \right)$$

$$+ \sum_{m,n} \left[ m\Delta + V_K^0 \cos(\omega t + \phi_{m,n}) \right] \hat{n}_{m,n}$$

**Note: Corrections could be important!**
see e.g. N. Goldman & J. Dalibard arXiv:1404.4373
& related work A. Polkovnikov

- Can be mapped on an e… …nian
  for $\hbar\omega \gg J_x, J_y, U$

$$\hat{H}_{eff} = \sum_{m,n} \left( -K e^{i\phi_{m,n}} \ \hat{a}^{\dagger}_{m+1,n} \hat{a}_{m,n} - J \ \hat{a}^{\dagger}_{m,n+1} \hat{a}_{m,n} + \text{h.c.} \right)$$

- To avoid excitations to higher bands
  $\hbar\omega$ has to be smaller than the band gap

F. Grossmann and P. Hänggi, EPL (1992)
M. Holthaus, PRL (1992)
A. Kolovsky, EPL (2011); A. Eckardt, PRL (2005)
A. Eckhardt, EPL (2007); P. Hauke, PRL (2012)
A. Bermudez, PRL (2011); A. Bermudez, NJP (2012)

# Hamiltonian

Realization of the Hofstadter-Harper Hamiltonian

$$\hat{H} = -\sum_{m,n} \left( K e^{i\phi_{m,n}} \hat{a}^\dagger_{m+1,n} \hat{a}_{m,n} + J \hat{a}^\dagger_{m,n+1} \hat{a}_{m,n} \right) + \text{h.c.}$$

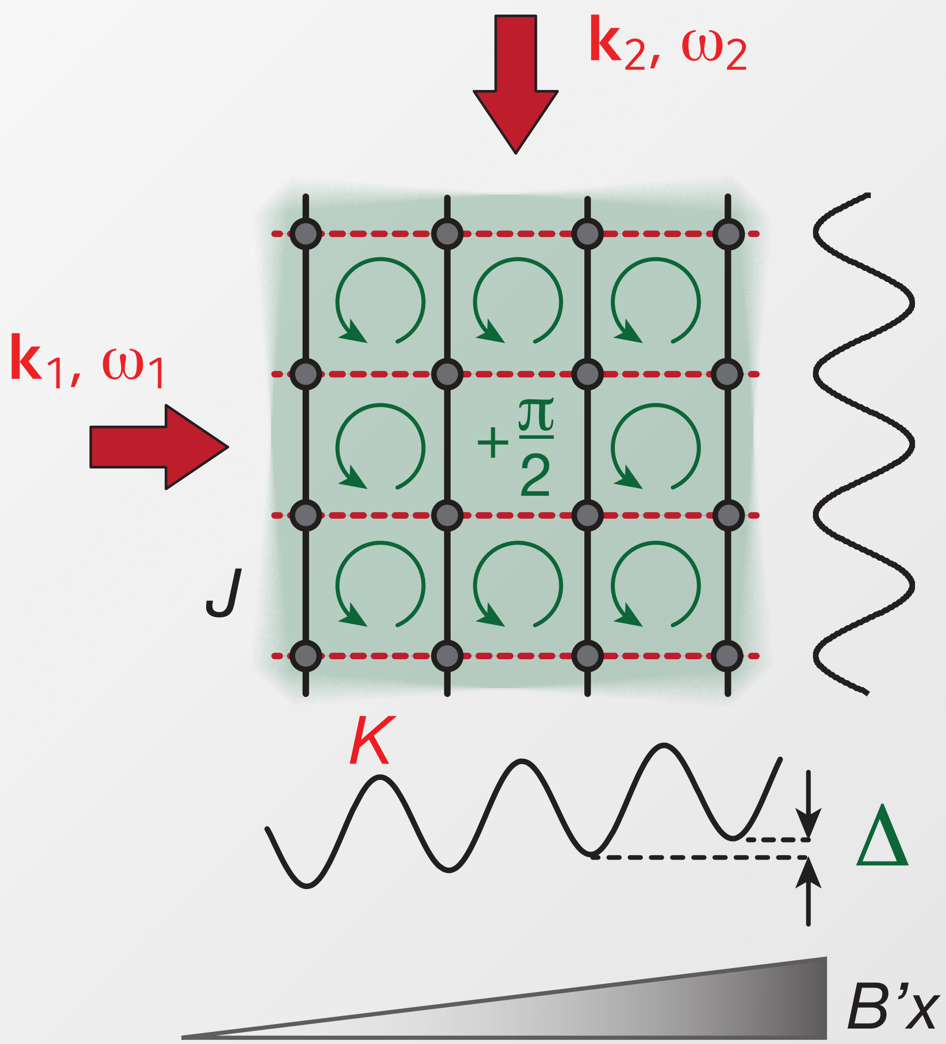


Scheme allows for the realization of an effective uniform flux of

$$\boxed{\Phi = \pi/2}$$

M. Aidelsburger *et al.*, PRL **111**, 185301 (2013)
H. Miyake *et al.*, PRL **111**, 185302 (2013)

# Local observable

- **Classical:**

  Charged particle in magnetic field

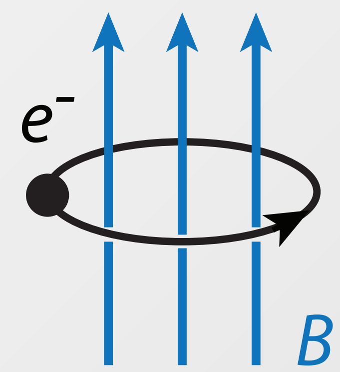

# Local observable

- **Classical:**

  Charged particle in magnetic field

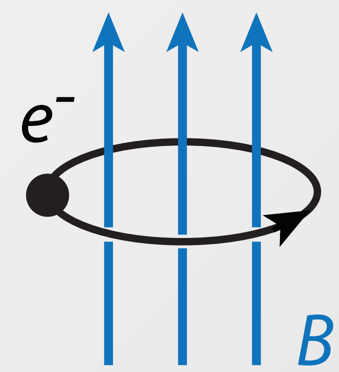


- **Quantum Analogue:**
  - Initial State:
  - Single Atom in the ground state of a tilted plaquette.

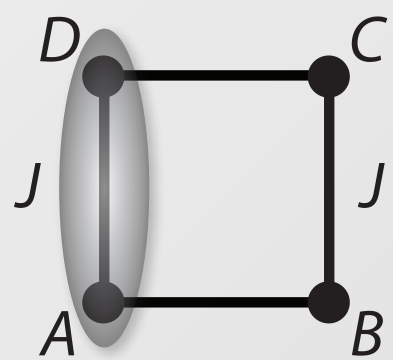


$$|\psi_0\rangle = \frac{|A\rangle + |D\rangle}{\sqrt{2}}$$

# Local observable

- **Classical:**

  Charged particle in magnetic field

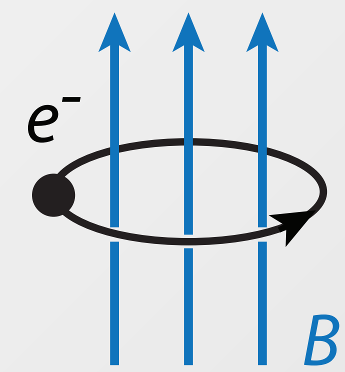


- **Quantum Analogue:**
  - Initial State:
  - Single Atom in the ground state of a tilted plaquette.

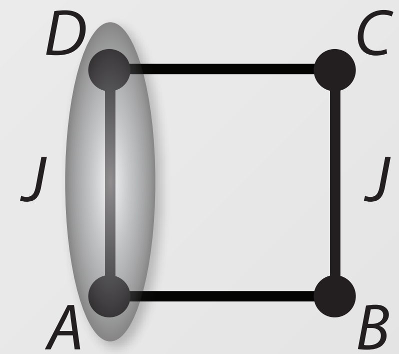


$$|\psi_0\rangle = \frac{|A\rangle + |D\rangle}{\sqrt{2}}$$

- Switch on running-wave to induce tunneling

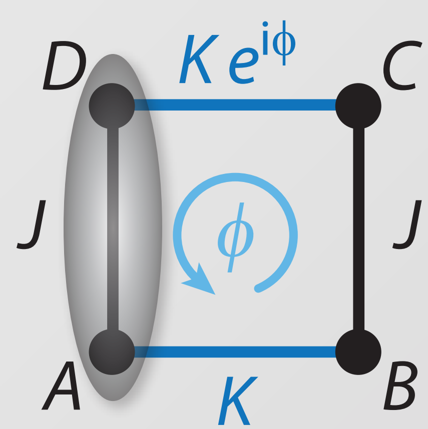

# A Lattice of Plaquettes

Using two superlattices, we realize a lattice whose elementary cell is a 4-site plaquette.

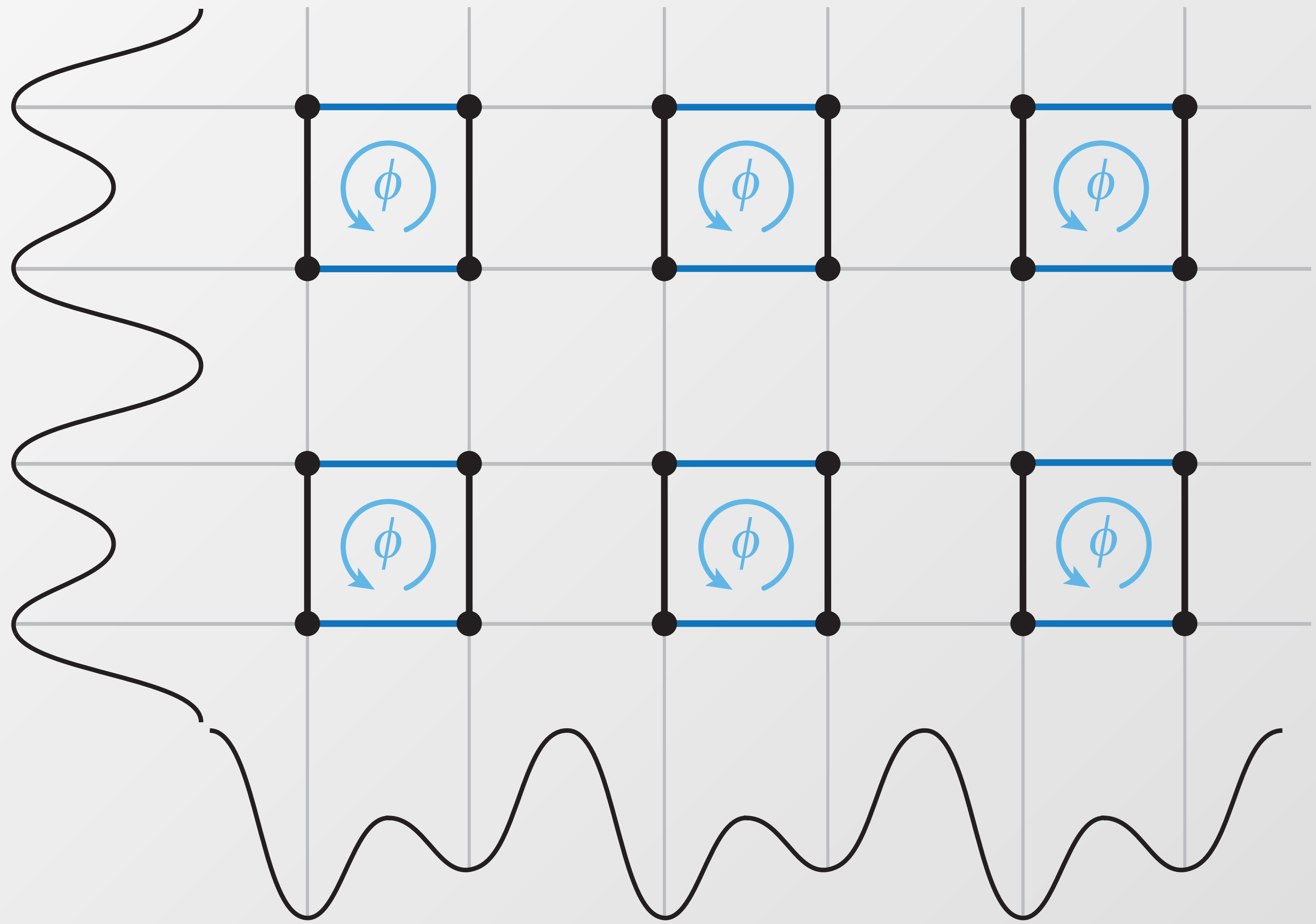

# Quantum Spin Hall Hamiltonian

Value of the flux depends on the internal state of the atom

- $|\uparrow\rangle = |F=1, m_F=-1\rangle$

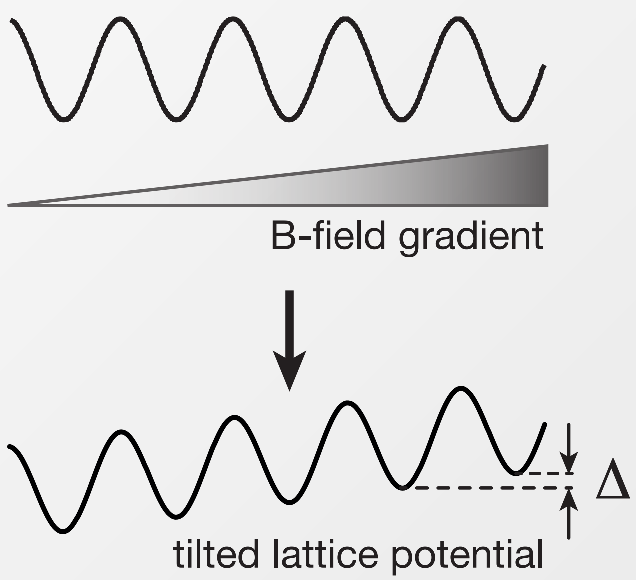

# Quantum Spin Hall Hamiltonian

Value of the flux depends on the internal state of the atom

- $|\uparrow\rangle = |F = 1, m_F = -1\rangle$

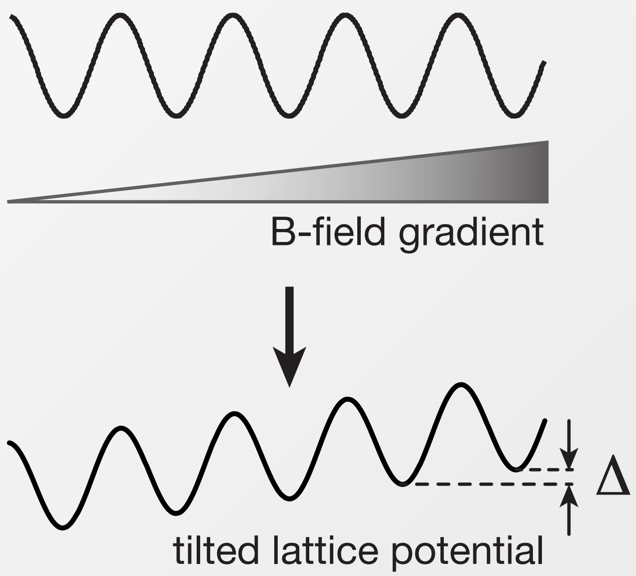


- $|\downarrow\rangle = |F = 2, m_F = -1\rangle$

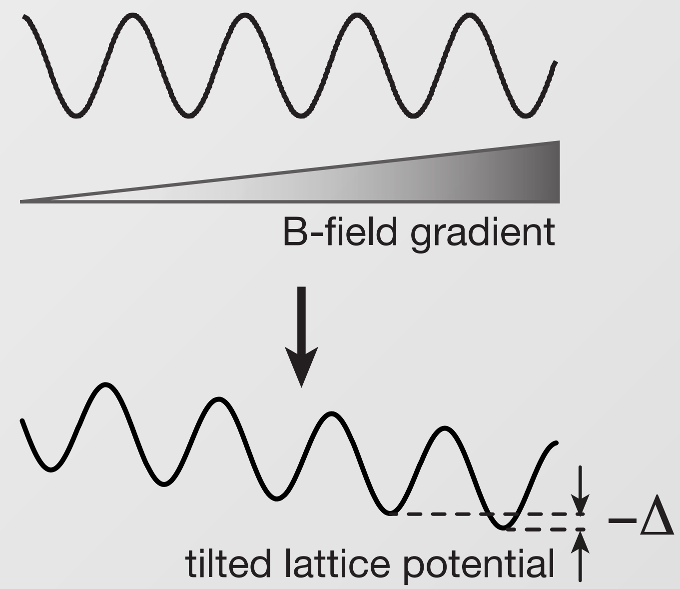

# Quantum Spin Hall Hamiltonian

Value of the flux depends on the internal state of the atom

- $|\uparrow\rangle = |F=1, m_F=-1\rangle$
- $|\downarrow\rangle = |F=2, m_F=-1\rangle$

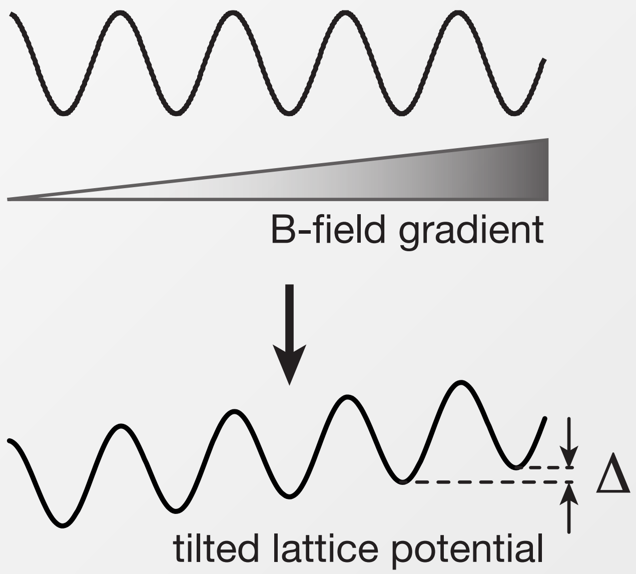


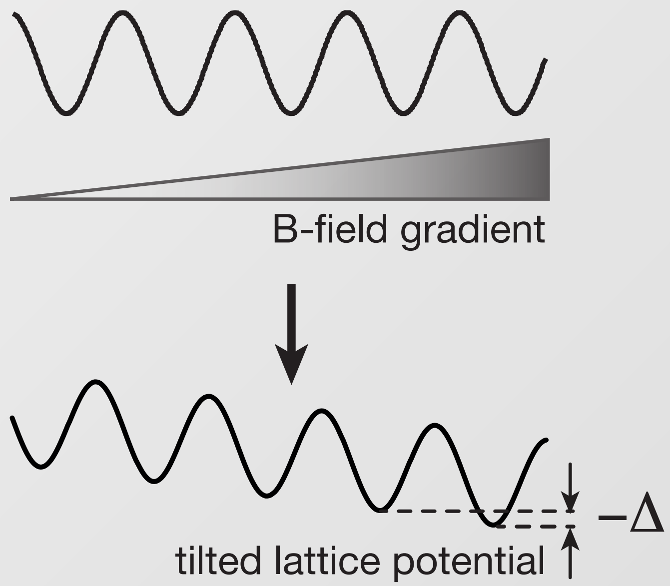


Spin-dependent optical potential: $\Delta \Longleftrightarrow -\Delta$

# Quantum Spin Hall Hamiltonian

Value of the flux depends on the internal state of the atom

- $|\uparrow\rangle = |F=1, m_F=-1\rangle$
- $|\downarrow\rangle = |F=2, m_F=-1\rangle$

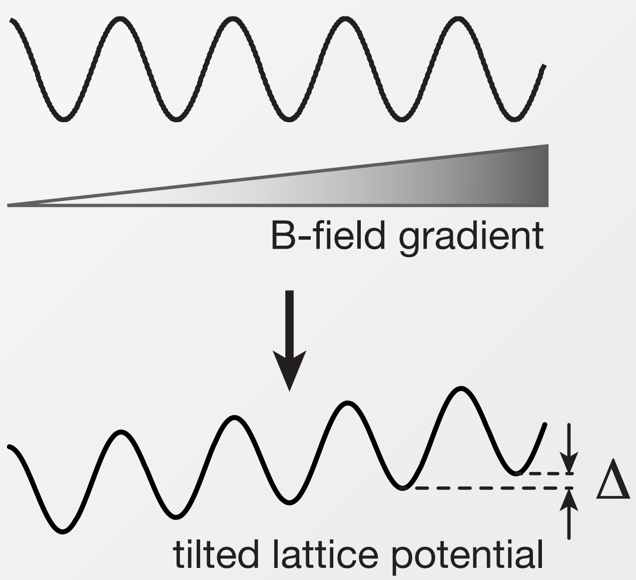


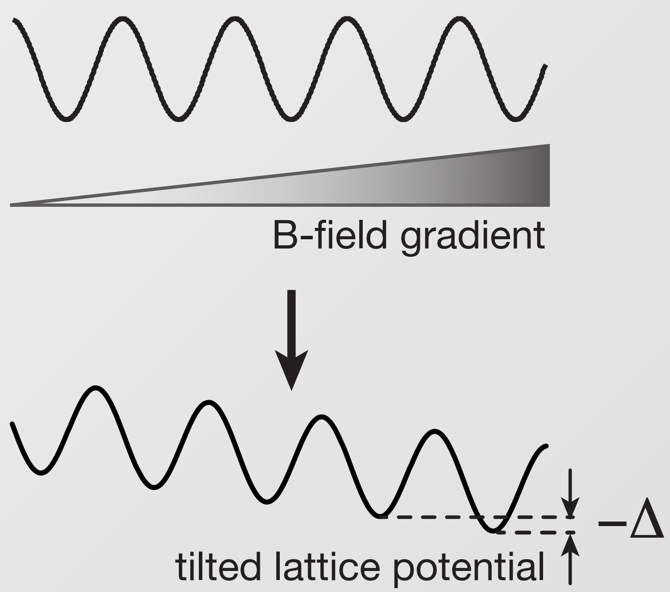


Spin-dependent optical potential: $\Delta \Longleftrightarrow -\Delta$

Spin-dependent complex tunneling amplitudes: $Ke^{i\phi_{mn}} \Longleftrightarrow Ke^{-i\phi_{mn}}$

# Quantum Spin Hall Hamiltonian

Value of the flux depends on the internal state of the atom

- $|\uparrow\rangle = |F=1, m_F=-1\rangle$
- $|\downarrow\rangle = |F=2, m_F=-1\rangle$

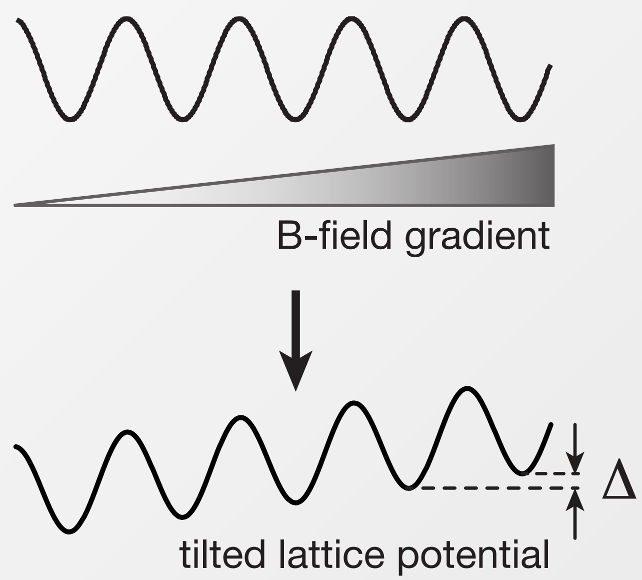


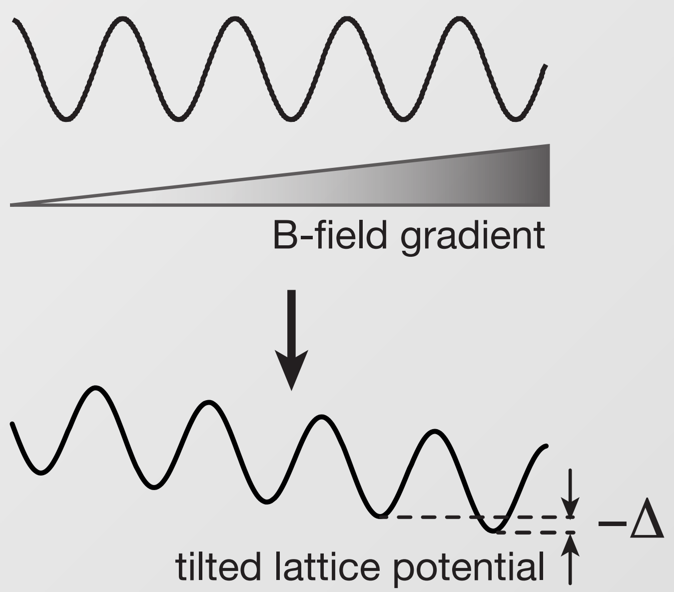


Spin-dependent optical potential: $\Delta \Longleftrightarrow -\Delta$

Spin-dependent complex tunneling amplitudes: $Ke^{i\phi_{mn}} \Longleftrightarrow Ke^{-i\phi_{mn}}$

Spin-dependent effective magnetic field: $\Phi = \pi/2 \Longleftrightarrow \Phi = -\pi/2$

# Quantum Spin Hall Hamiltonian

Time-reversal-symmetric quantum spin Hall Hamiltonian:

$$\hat{H}_{\uparrow,\downarrow} = -\sum_{m,n} \left( K \mathrm{e}^{\pm i\phi_{m,n}} \hat{a}^{\dagger}_{m+1,n} \hat{a}_{m,n} + J \hat{a}^{\dagger}_{m,n+1} \hat{a}_{m,n} \right) + \mathrm{h.c.}$$

Bernevig and Zhang, PRL **96**, 106802 (2006); N. Goldman *et al.*, PRL (2010)

# Quantum Spin Hall Hamiltonian

Time-reversal-symmetric quantum spin Hall Hamiltonian:

$$\hat{H}_{\uparrow,\downarrow} = -\sum_{m,n}\left(K\mathrm{e}^{\pm i\phi_{m,n}}\hat{a}^{\dagger}_{m+1,n}\hat{a}_{m,n} + J\hat{a}^{\dagger}_{m,n+1}\hat{a}_{m,n}\right) + \mathrm{h.c.}$$

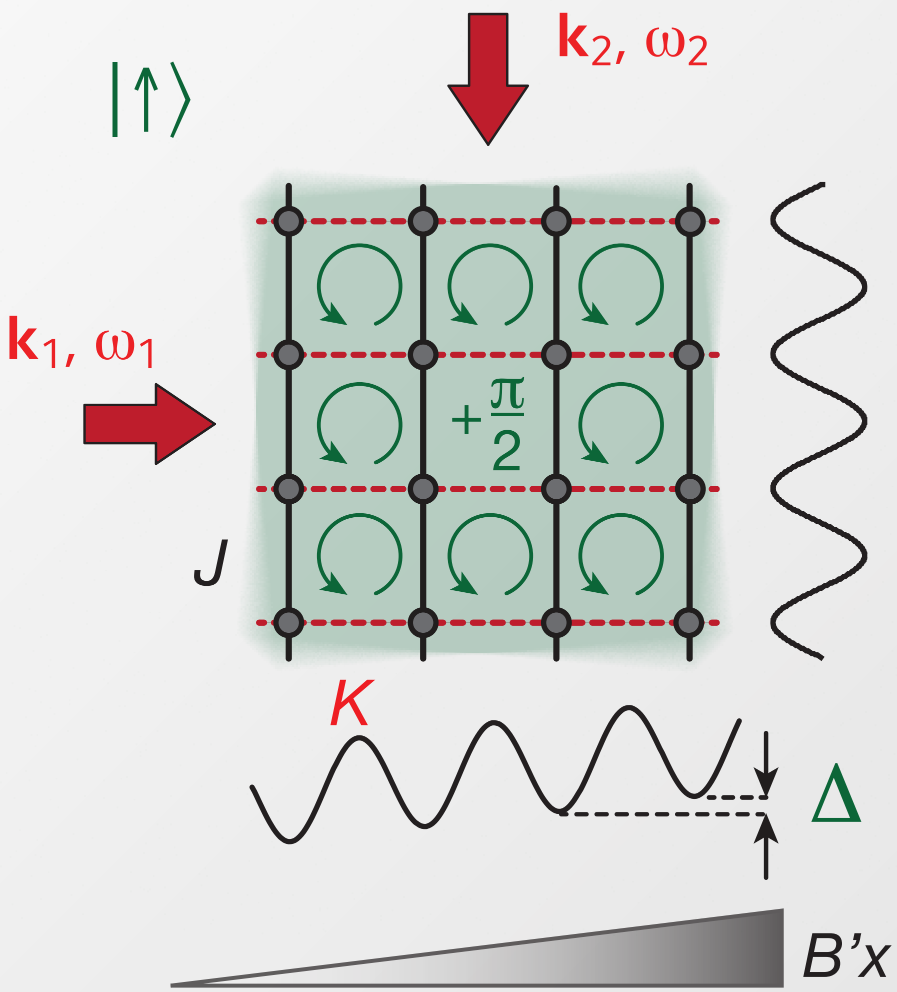


$$\boxed{\Phi_{\uparrow} = \pi/2}$$

Bernevig and Zhang, PRL **96**, 106802 (2006); N. Goldman *et al.*, PRL (2010)

# Quantum Spin Hall Hamiltonian

Time-reversal-symmetric quantum spin Hall Hamiltonian:

$$\hat{H}_{\uparrow,\downarrow} = -\sum_{m,n}\left(K\mathrm{e}^{\pm i\phi_{m,n}}\hat{a}^{\dagger}_{m+1,n}\hat{a}_{m,n} + J\hat{a}^{\dagger}_{m,n+1}\hat{a}_{m,n}\right) + \mathrm{h.c.}$$

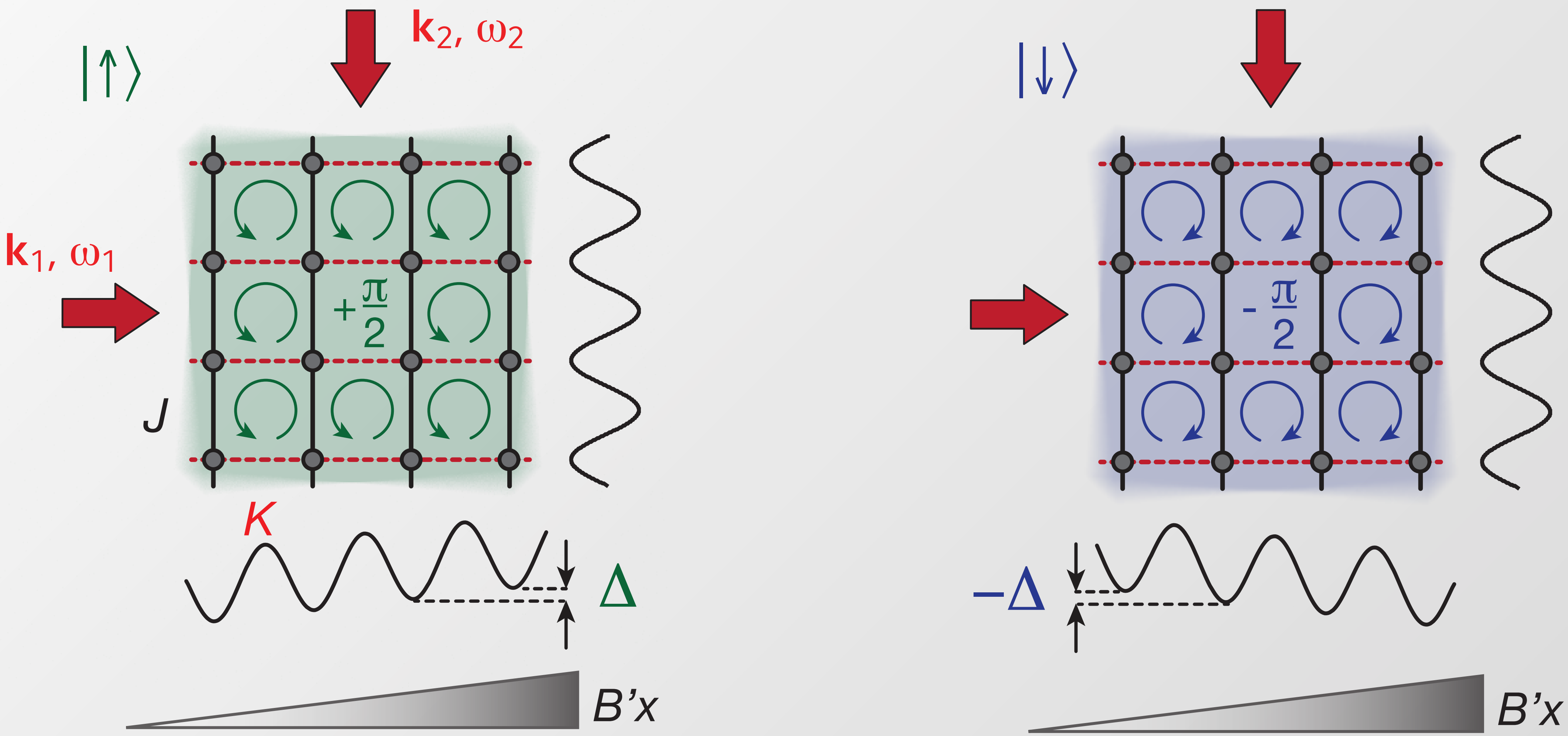


$$\boxed{\Phi_{\uparrow} = \pi/2}$$

$$\boxed{\Phi_{\downarrow} = -\pi/2}$$

Bernevig and Zhang, PRL **96**, 106802 (2006); N. Goldman *et al.*, PRL (2010)

# Spin-dependent cyclotron orbit

- Spin up:

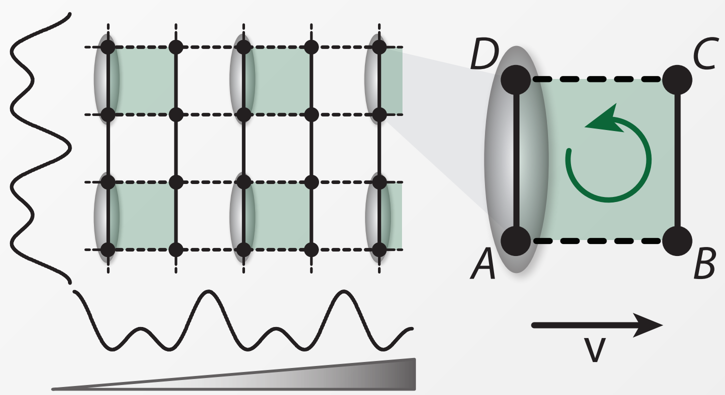


$$|\Psi_{\uparrow}\rangle = (|A\rangle + |D\rangle)/\sqrt{2}$$

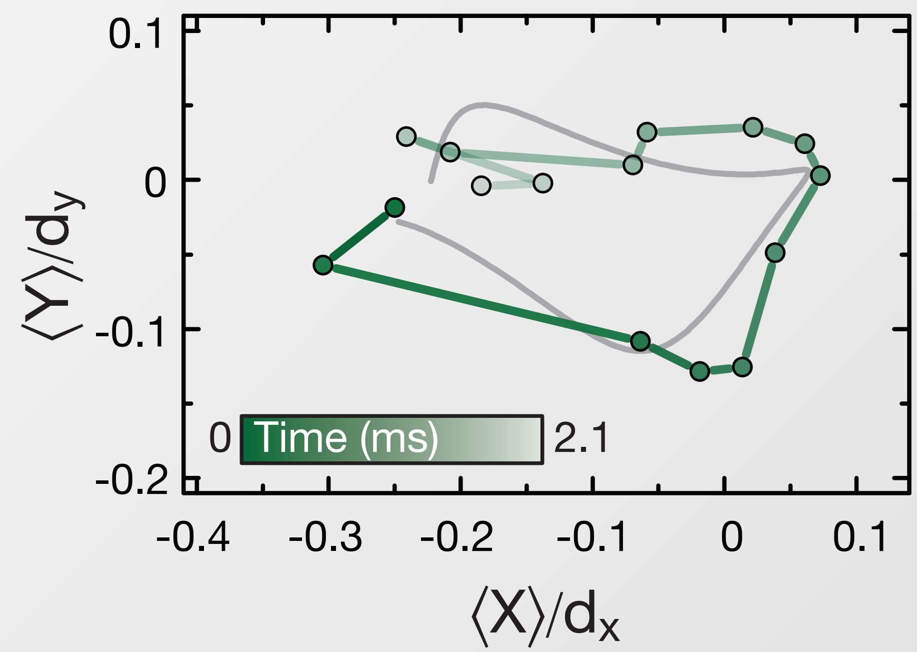


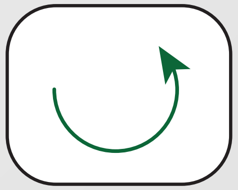

# Spin-dependent cyclotron orbit

- Spin up:

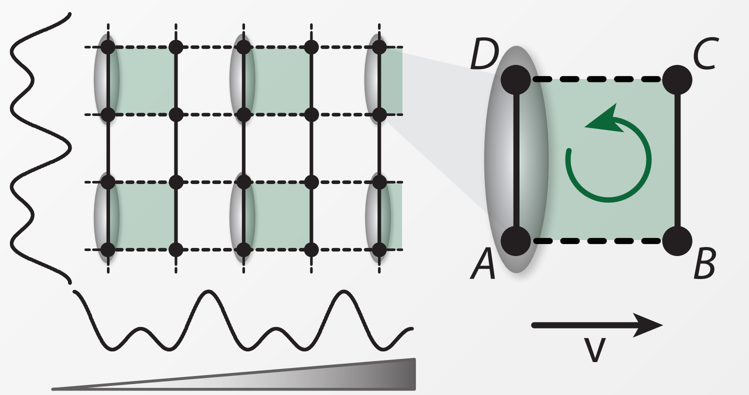


$$|\Psi_\uparrow\rangle = (|A\rangle + |D\rangle)/\sqrt{2}$$

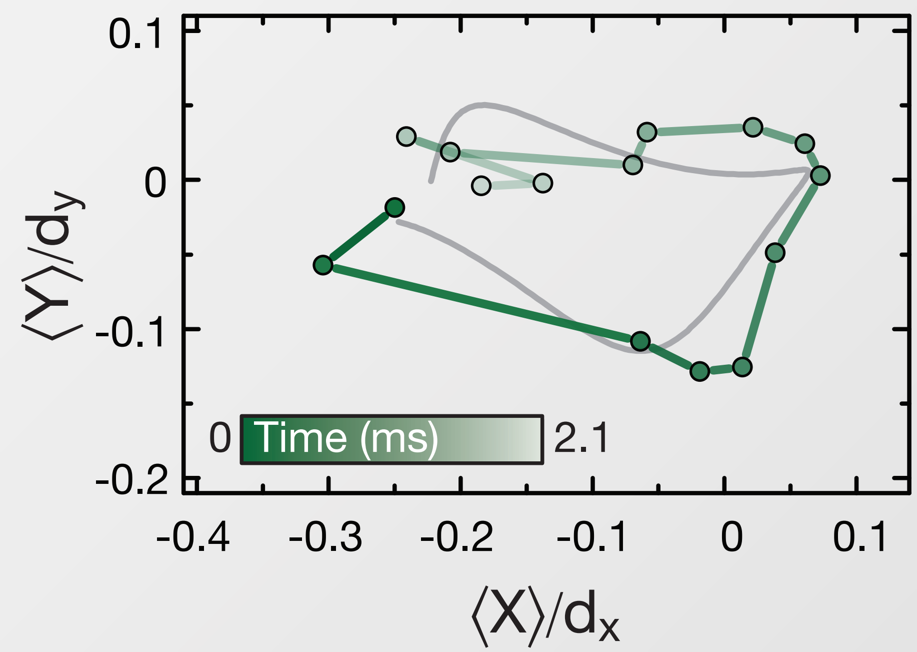


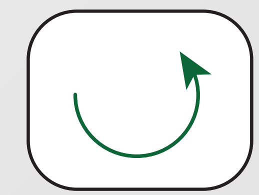

- Spin down:

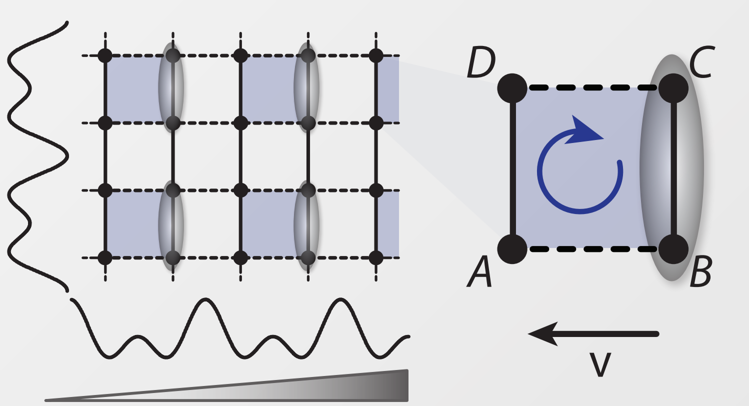


$$|\Psi_\downarrow\rangle = (|B\rangle + |C\rangle)/\sqrt{2}$$

# Spin-dependent cyclotron orbit

- Spin up:

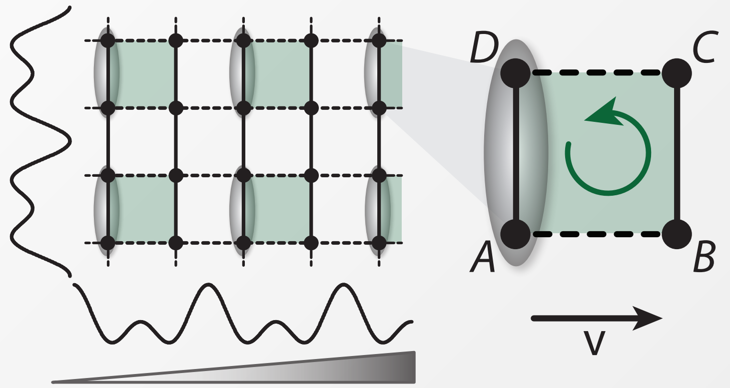


$$|\Psi_\uparrow\rangle = (|A\rangle + |D\rangle)/\sqrt{2}$$

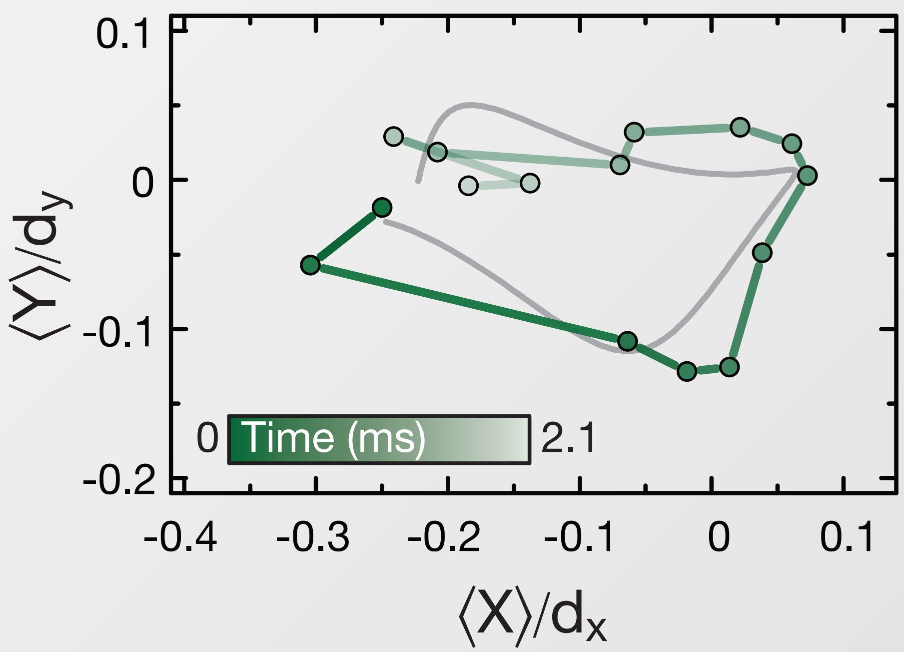


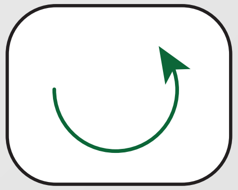

- Spin down:

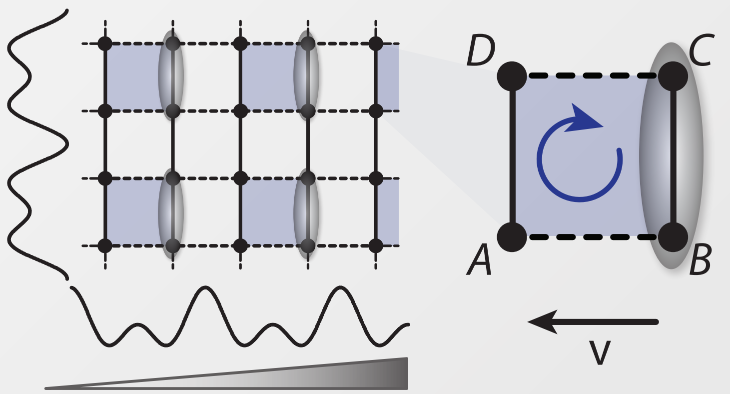


$$|\Psi_\downarrow\rangle = (|B\rangle + |C\rangle)/\sqrt{2}$$

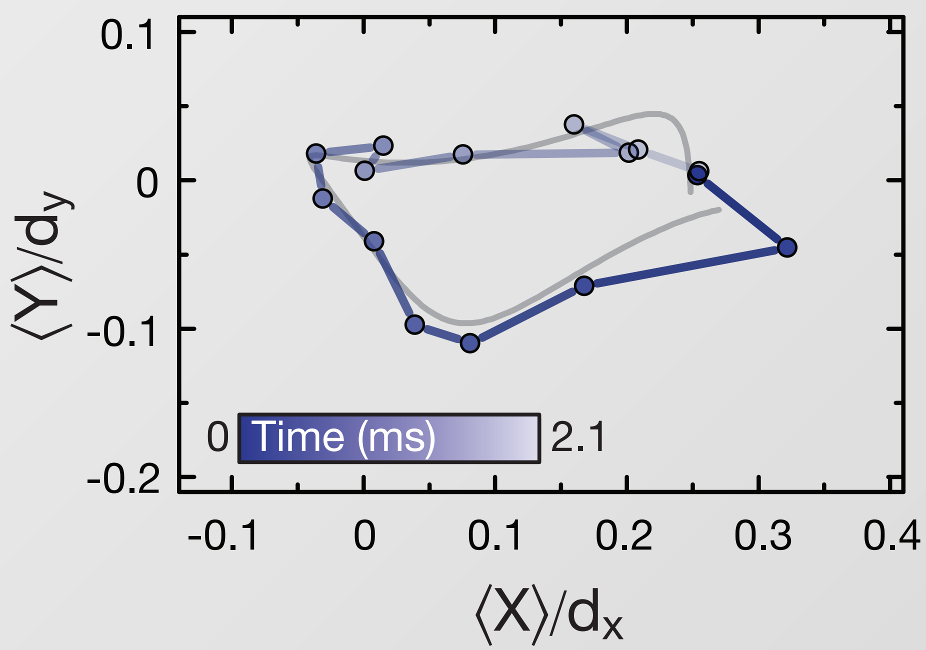


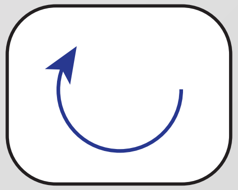

# Spin-dependent cyclotron orbit

- Spin up:

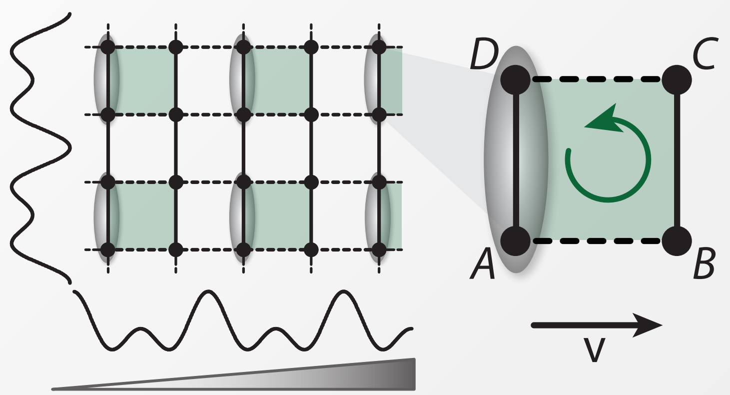


$$|\Psi_\uparrow\rangle = (|A\rangle + |D\rangle)/\sqrt{2}$$

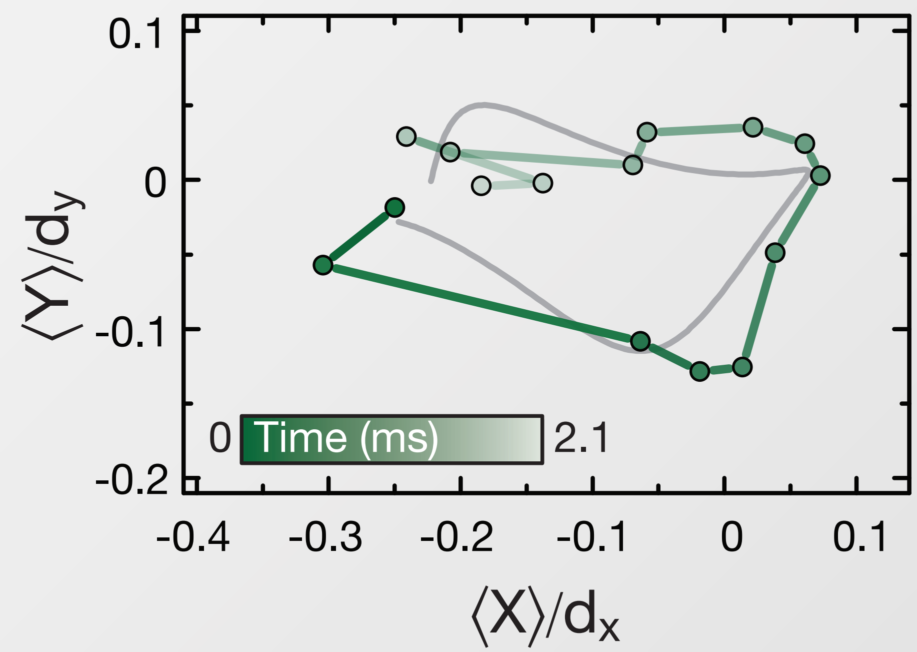


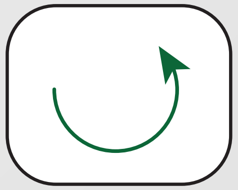

Opposite chirality!

- Spin down:

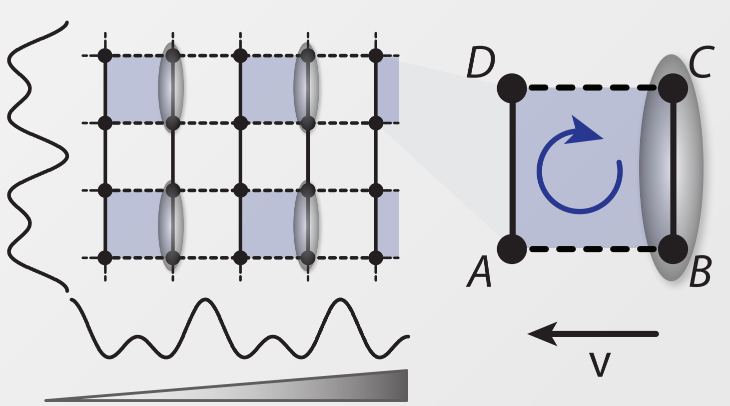


$$|\Psi_\downarrow\rangle = (|B\rangle + |C\rangle)/\sqrt{2}$$

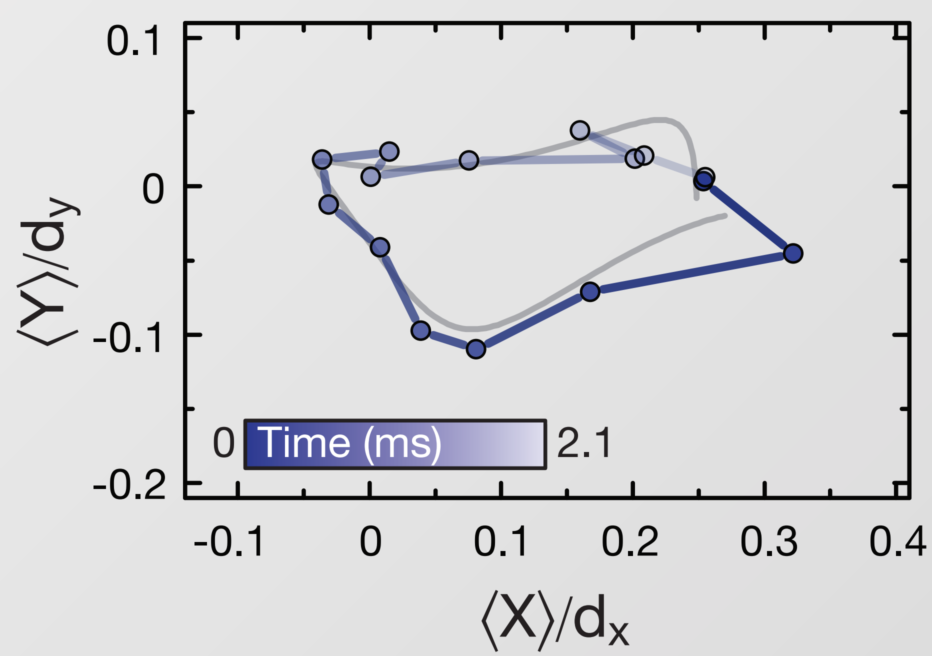


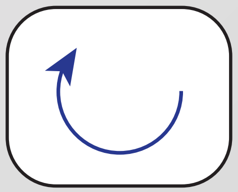

# New Flux Rectification Scheme

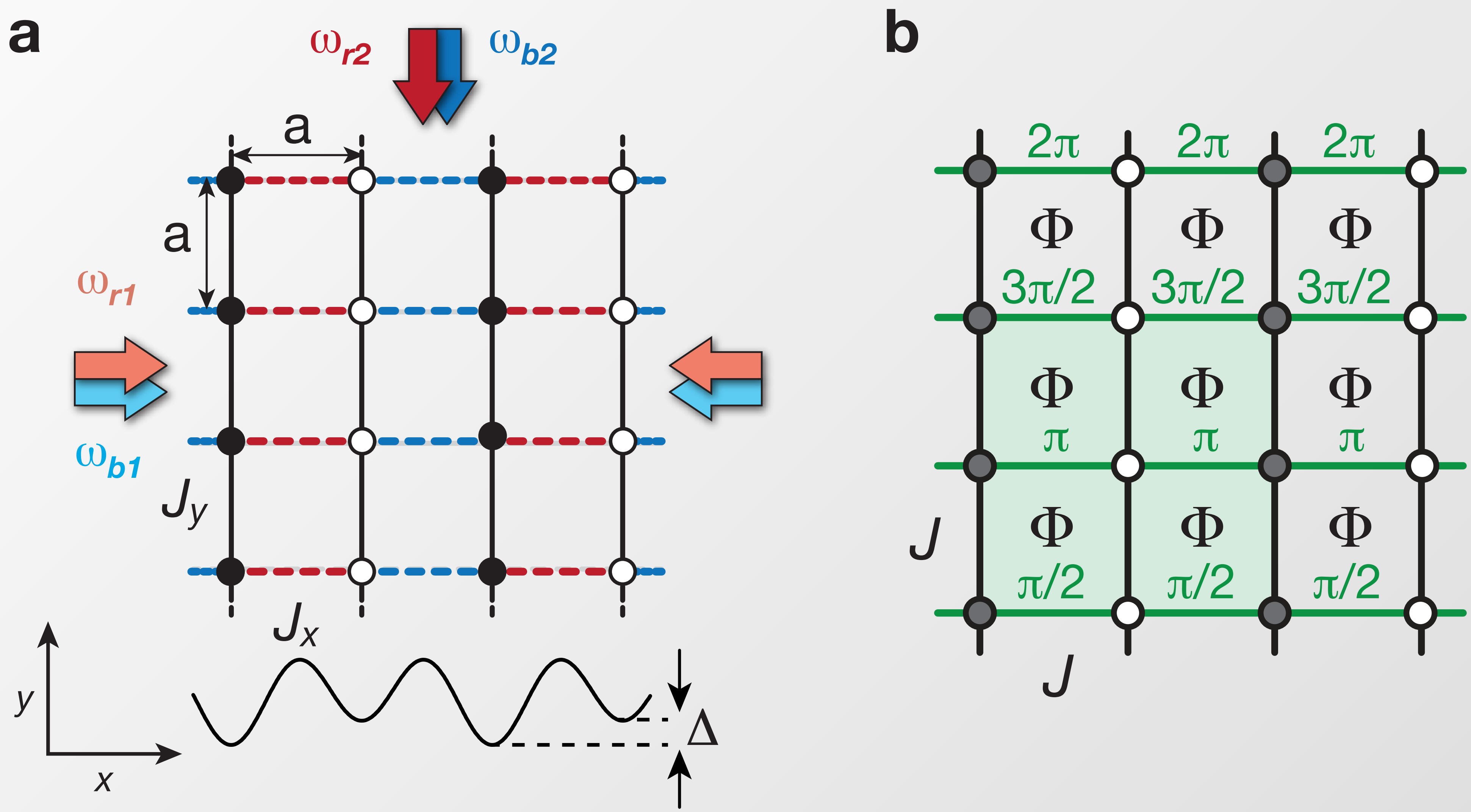


red & blue bonds can be modulated independently!

Flux rectification possible (related Gerbier & Dalibard NJP (2010))

# Uniform Flux

# Loading and Probing Hofstadter Bands

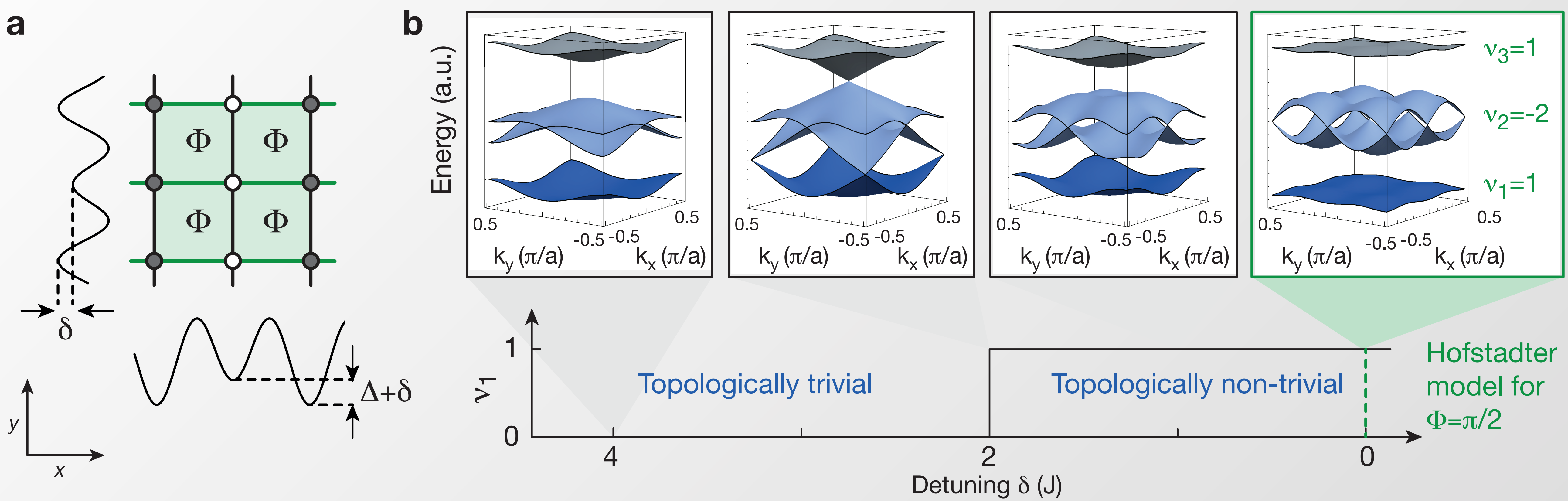


Key insight for adiabatic loading/probing:
***keep Brillouin zone***
***of topologically trivial & non-trivial phase matched!***

Flat bands realized! $E_{gap}/E_{bw} \simeq 8$

# Hall Response & Anomalous Velocity

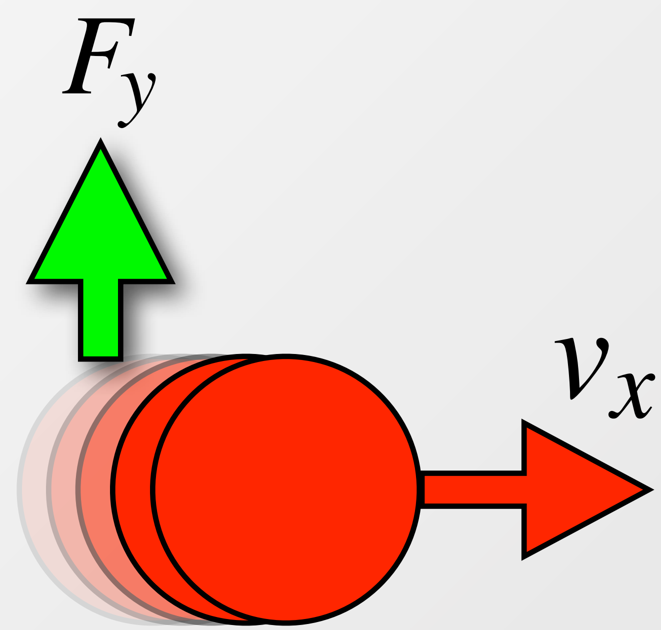


$$\hbar \frac{d\mathbf{k}_c}{dt} = -e\left(\nabla\phi(\mathbf{r}_c) + \frac{d\mathbf{r}_c}{dt} \times \mathbf{B}(\mathbf{r}_c)\right)$$

$$\frac{d\mathbf{r}_c}{dt} = \frac{1}{\hbar}\nabla_{k_c}\varepsilon_n(\mathbf{k_c}) - \frac{d\mathbf{k}_c}{dt} \times \Omega(\mathbf{k}_c)\hat{\mathbf{z}}$$

anomalous velocity

Karplus & Luttinger, Phys. Rev. (1954)
Sundaram & Niu, Phys. Rev. B (1999)

# Cloud Deflection & Chern Number

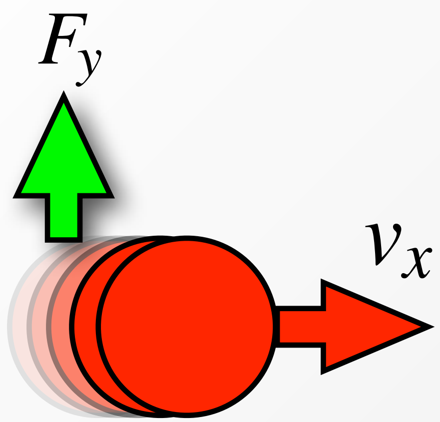


$$\mathbf{v}(\mathbf{k}_c) = \frac{d\mathbf{r}_c}{dt} = \frac{1}{\hbar}\nabla_{k_c}\varepsilon_n(\mathbf{k}_c) - \frac{d\mathbf{k}_c}{dt} \times \Omega(\mathbf{k}_c)\hat{\mathbf{z}}$$

# Cloud Deflection & Chern Number

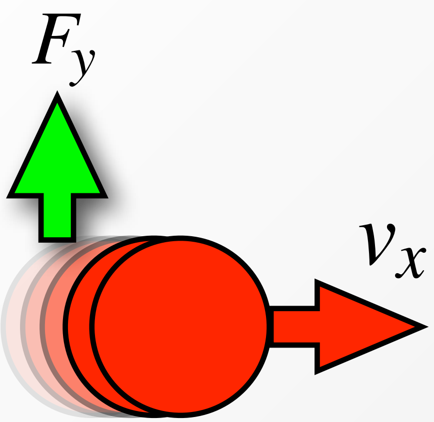


$$\boxed{\mathbf{v}(\mathbf{k}_c) = \frac{d\mathbf{r}_c}{dt} = \cancel{\frac{1}{\hbar}\nabla_k \epsilon_n(\mathbf{k}_c)} - \frac{d\mathbf{k}_c}{dt} \times \Omega(\mathbf{k}_c)\hat{\mathbf{z}}}$$

**Assume uniformly filled band and rational flux p/q:**

$$\begin{aligned}
\langle v_x \rangle &= \frac{1}{N_{at}} \int \rho(\mathbf{k}) v_x(\mathbf{k})\, d^2k \\
&= -\frac{1}{N_{at}} \cdot 2\pi \cdot \frac{N_{at}}{\delta k_x \delta k_y} \cdot \frac{F_y}{\hbar} \cdot \frac{1}{2\pi} \int \Omega(\mathbf{k})\, d^2k \\
&= -(2\pi)^2 \cdot \frac{1}{(2\pi/a)(2\pi/qa)} \cdot \frac{F_y}{h} \cdot \nu \\
&= -\frac{F_y q a^2}{h} \nu
\end{aligned}$$

H. Price & N. Cooper PRA (2012)
A. Dauphin & N. Goldman PRL (2013)

# Understanding the Displacement

**Only lowest band homogenously populated**

$$x(t) = -\frac{4a^2F}{h}\nu_1 t$$

**Higher bands also populated (short times)**

$$x(t) = -\frac{4a^2\gamma_0 F}{h}\nu_1 t, \text{ with } \gamma_0 = \eta_1^0 - \eta_2^0 + \eta_3^0$$

Filling factor

(make use of particle-hole symmetry in Hofstadter model & $\sum_\mu \nu_\mu = 0$

**Higher bands also populated (full time evolution)**

$$x(t) = -\nu_1 \frac{4a^2F}{h}\int_0^t \gamma(t')\mathrm{d}t'$$

*But how to measure band-population???*

# Conclusions

- First realization of topological Bloch bands in 1d & 2d (SSH, Hoftstadter, Quantum Spin Hall)
- First direct measurements of topological invariants in 1d & 2d
- Aharonov-Bohm interferometric determination of band topology
- Stückelberg Interferometry for dispersion relation
- Extensions to non-Abelian Berry connection (Wilson loops)

Framework for **full determination of band geometry** and experimental implementation!

**Questions:** interactions, heating, adiabatic loading, ......

# Outlook

- Rectified Flux, Hofstadter Butterfly
- Novel Correlated Phases in Strong Fields,
  Transport Measurements
- Adiabatic loading schemes
- Spectroscopy of Hoftstadter bands
- Novel Topological Insulators
- Image Edge States - directly/spectroscopically
- Measure spatially resolved full current distribution
- Non-equilibrium dynamics in gauge fields
- Thermalization?

⋮

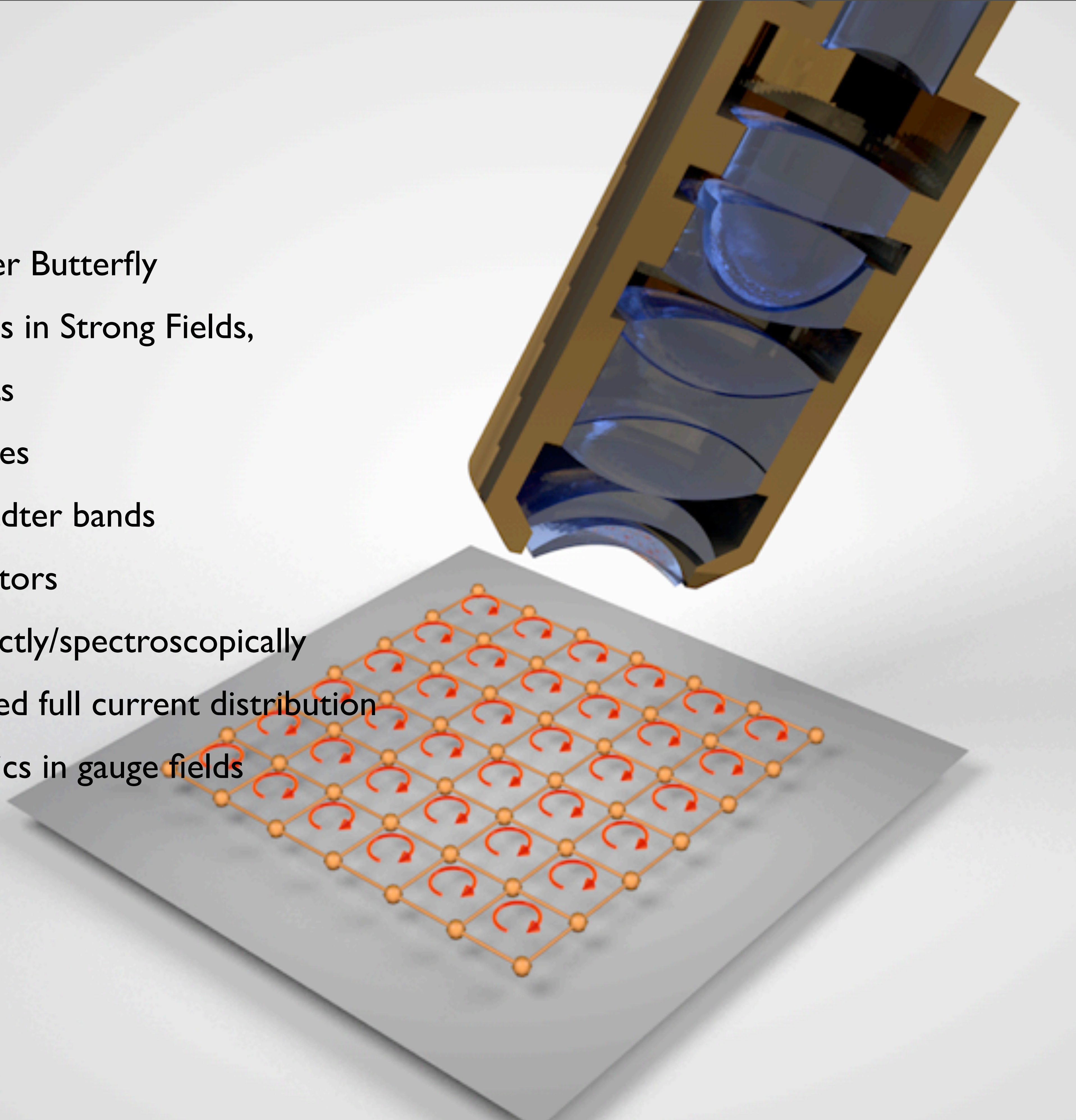

# Gauge Field Team

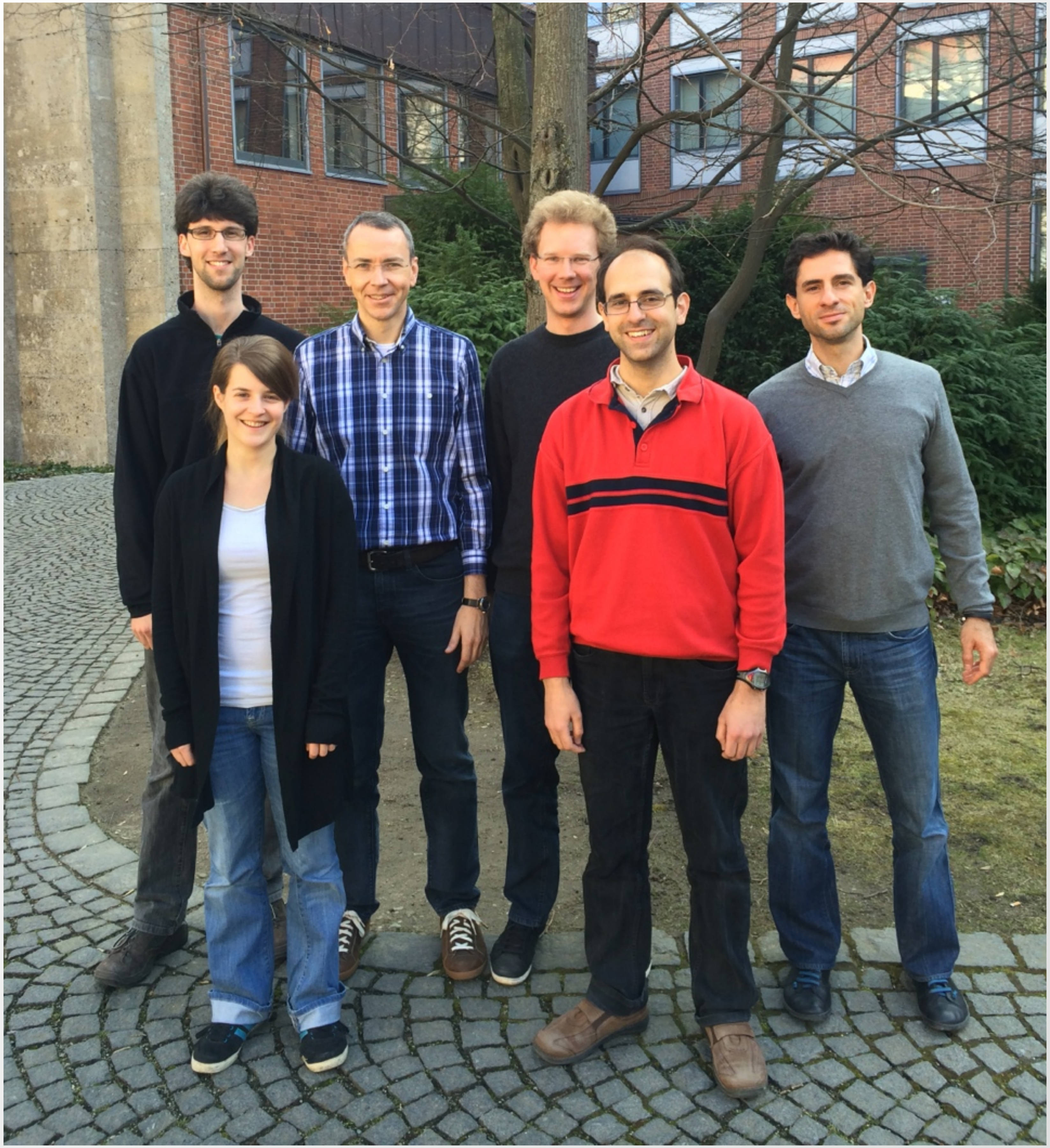

From left to right:

Christian Schweizer

Monika Aidelsburger

I.B.

Michael Lohse

Marcos Atala

Julio Barreiro

# 2D Berry Curvature Interferometer Team

Lucia Duca

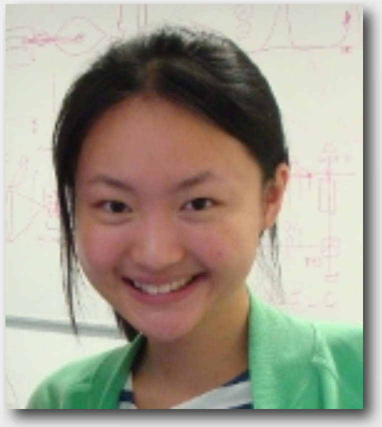

Tracy Li

Martin Reitter

Monika Schleier-Smith

IB

Ulrich Schneider

# Single Atom Team

Sebastian Christian Peter Johannes Takeshi

Marc

Tommaso

Thomas


isola di
san se
BENVE
WELC
erc
synergy
www.uquam.eu
Venice VIU 2014


www.quantum-munich.de